

# **Dispersion Management of Optical Transmission Systems**

Lee John Barker

Master of Philosophy

Aston University

August 2011

Lee John Barker asserts his moral right to be identified as the author of this thesis  
This copy of the thesis has been supplied on condition that anyone who consults it is  
understood to recognise that its copyright rests with its author and that no quotation  
from the thesis and no information derived from it may be published without proper  
acknowledgement.

Aston University

## Dispersion Management of Optical Transmission Systems

Lee Barker  
Master of Philosophy

June 2011

### Summary

This thesis consists of experimental demonstration of different forms of dispersion management of optically transmitted signals. The thesis investigates how these different forms can be modified and then used to improve an optical transmission system. The results in this thesis have been separated and presented in four different sections:

The use of present technology and using this to aid the demodulation of the signal is explored in the first part. The use of wave division multiplexers, that are already commonly used at the receive end of transmission spans, is shown in experimental results to provide a novel but simple unique method to provide a shift from the phase domain to the amplitude keyed communication system.

The second area of investigation is in to a tunable dispersion device. The device was place under laboratory conditions that represented real life situations. The measurements gained show how a device can be used for a more versatile and adaptive communication system.

Thirdly an investigation into a novel application to optical transmission system, Quasi-lossless amplification. The method uses broaden Raman pumped light to amplify an optical transmitted signal. The experimental results show how this transmission system can provide a more improved amplified scheme compared to that of the more commonly used amplified systems.

Finally there is an investigation into another novel amplification scheme for optical communications, Optical Phase Conjugation. This scheme, which are reverses the dispersive effects at a mid point, is reviewed and then experimental compared to the amplification scheme of Quasi-lossless.

**Keywords:** Quasi-lossless, Optical Phase Conjugation, Nonlinear Optics, Dispersion Compensation, Demodulation.

## Acknowledgements

This thesis would not have been produced if not for the input and continued help of other members of the photonic research teams at Aston University in Birmingham.

My greatest thanks and appreciation goes to my supervisor Dr Paul Harper. His vast knowledge on the subject of optical communications kept me pointed in the correct direction throughout the whole of my research life at Aston University. If ever there was a point during the research that I felt lost or began to feel a little despondent about the subject, the enthusiasm Paul showed always gave me a lift and a reassured feeling.

I would also like to say thank you to Dr Juan-Diego Ania-Castañón, who provided simulation work that I could compare to my experimental work to produce more in depth research work.

My research at Aston University led to me working with many different people from different backgrounds from around the world, and all these people I would like to thank. Dr Nigel Johnson and Dr James Harrison were two well established research members of the Photonic group that I would like to say thank you to for the help they gave me in my early stages of my research work. Dr Atalla E. El-Taher, Mercedes Alcon and Hua Wang, who were my fellow lab colleagues for the final year of my research, I would also like to say a big thank you to for their constant encouragement. I'd also like to thank Mr Sadiq Jaffer who I started my research life with, who has now become a very good friend.

I would also like to say a thank you to Dr Pablo Minzioni and Vince Pusino visitors to the research department from the University of Pavia in Italy who I worked with for a short time and helped me get an understanding of subject in this thesis.

A big thank you has to be given to Professor Keith Blow who offered me the position on the research team and whose lectures on the subject of communications first got me interested in photonics. And a big thanks to all the team from AZEA who funded me in the position available.

My mother and Fred have been a constant help and source of encouragement and to them I thank you. Finally but not least a very large and loving thank you to my partner Jo, she has always been there for me through the good times and the bad and I appreciate her companionship more than any others.

## Contents

	Page
<b>Chapter 1 Introduction</b> .....	13
1.1 Introduction .....	13
1.2 Historic View .....	13
1.3 Thesis Outline .....	14
<b>Chapter 2 Fibre Optic Systems</b> .....	17
2.1 Introduction .....	17
2.2 Optical Transmitter .....	17
2.2.1 Mach-Zender Modulator .....	18
2.3 Fibre Design .....	28
2.3.1 Fibre Losses .....	29
2.4 Dispersion .....	30
2.5 Bit Error Rate and Q .....	32
2.5 Optical Receiver .....	32
2.6 Optical Amplifiers .....	33
2.6.1 Stimulated Emission .....	34
2.6.2 Erbium-doped Fibre Amplifiers .....	35
2.6.3 Amplifier Noise .....	36
2.6.4 Raman Amplifiers .....	36
2.7 Multiplexing .....	37
2.8 Conclusions .....	38
<b>Chapter 3 Fibre Optic Systems</b> .....	40
3.1 Introduction .....	40
3.2 Modulation Formats .....	40
3.2.1 Amplitude Shift Keying .....	42
3.2.2 Phase shift Keying .....	43
3.3 Differential Encoding .....	43
3.3.1 Demodulation .....	44
3.4 Delay Line Interferometer .....	45
3.4.1 Delay Line Interferometer Experimental results .....	47
3.5 DPSK Filter Measurements .....	48
3.6 Delay Line Interferometer and filter Demodulation .....	51
3.7 Filter Receiver Penalty Measurements .....	52

3.7.1	Filter Detuning Measurements .....	53
3.8	Conclusions .....	54
<b>Chapter 4</b>	<b>Optical Tuneable Dispersion Compensator</b> .....	<b>56</b>
4.1	Introduction .....	56
4.2	Chromatic Dispersion and Group Delay .....	56
4.2.1	Dispersion Techniques .....	57
4.3	Tuneable Dispersion Compensators .....	59
4.3.1	Three Distributed Gires –Tournois Etalon TDC .....	60
4.4	TDC Experimental Setup .....	61
4.4.1	Transmission Measurements .....	62
4.4.2	Change in Transmission Wavelength .....	64
4.4.2	Wave-Sweep Measurements .....	65
4.4.3	Signal Sensitivity .....	68
4.4.4	TDC Profile .....	70
4.5	DPSK Compensation .....	72
4.5.1	Multiplexed DPSK .....	73
4.6	Adaptive Control .....	75
4.7	Conclusions .....	75
<b>Chapter 5</b>	<b>Ultra-long Raman Fibre Laser</b> .....	<b>77</b>
5.1	Introduction .....	77
5.2	Nonlinear Effects .....	77
5.2.1	Stimulated Light Scattering .....	78
5.2.1.1	Stimulated Brillouin Scattering .....	79
5.2.1.2	Stimulated Raman Scattering .....	80
5.2.2	Self-Phase Modulation .....	82
5.2.3	Four-Wave Mixing .....	83
5.3	Generating Quasi-lossless Conditions .....	84
5.4	Quasi-lossless Single Channel Transmission .....	87
5.4.1	Quasi-lossless Transmission Launch Powers .....	89
5.4.2	Quasi-lossless Transmission Distances .....	92
5.4.3	Transmission OSNR .....	95
5.5	Quasi-lossless Multi-Channel Transmission .....	99
5.5.1	Bandwidth .....	99
5.5.2	Transmission .....	102

5.6	Conclusions .....	103
<b>Chapter 6</b>	<b>Optical Phase Conjugation .....</b>	<b>106</b>
6.1	Introduction .....	106
6.2	The OPC Device .....	106
6.3	OPC in a Lossless Transmission Span.....	107
6.3.1	Compensation of Optimum Launch Powers .....	107
6.3.2	Transmission Distances .....	110
<b>Chapter 7</b>	<b>Conclusions .....</b>	<b>111</b>
<b>Chapter 8</b>	<b>Publications .....</b>	<b>115</b>
<b>Chapter 9</b>	<b>Bibliography .....</b>	<b>116</b>

## List of Figures

Figure 1.1	Increase in bit rate –distance product BL from 1850 to 2000 . . . . .	14
Figure 2.1	Optical transmission communication systems . . . . .	17
Figure 2.2	Basic Mach-Zender modulator design . . . . .	18
Figure 2.3	Basic diagram of a Mach-Zender modulator . . . . .	23
Figure 2.4	Basic diagram of a Mach-Zender modulator . . . . .	24
Figure 2.5	Core and cladding of the optical fibre . . . . .	28
Figure 2.6	Fundamental three processes occurring between two energy state of an Atom . . . . .	34
Figure 2.7	An EDFA . . . . .	35
Figure 3.1	Modulated signals (a) return-to-zero and (b) non-return-to-zero . . .	41
Figure 3.2	The (a) data input and the corresponding modulating formats of (b) amplitude shift keyed and (c) phase shift keyed . . . . .	42
Figure 3.3	The Delay Line Interferometer with a modulated PSK signal input. One arm introducing a one bit period delay and the combination of the phase difference producing a ASK signal . . . . .	45
Figure 3.4	The Delay Line Interferometer with a modulated PSK signal input, and the constructive and destructive ASK outputs . . . . .	46
Figure 3.5	DLI with a NRZ-DPSK 42.6 Gb/s data input with eye shown. Output on one arm of the DLI showing the eye and data output . . . .	47
Figure 3.6	The output on both arms of the DLI showing the constructive and destructive data outputs . . . . .	48
Figure 3.7	Filter experiment setup. . . . .	49
Figure 3.8	The spectrum of the (a) carrier wavelength and filter, with (b) data pattern after the filter . . . . .	49
Figure 3.9	The spectrum of the (a) carrier wavelength and filter, with (b) data pattern after the filter . . . . .	50
Figure 3.10	(a) DLI (i) Constructive port, (ii) Destructive port, (b) 0.25nm filter, (c) 0.35nm filter, (d) 0.45nm filter. For filters column (i) shows filter & carrier frequency aligned, column (ii) show filter offset 42.7GHz from carrier frequency. For reference the binary bit sequences are also shown . . . . .	51

Figure 3.11	The output on both arms of the DLI showing the constructive and destructive data outputs . . . . .	52
Figure 3.12	Receiver Sensitivity Measurements . . . . .	53
Figure 3.13	Detuning Penalty . . . . .	54
Figure 4.1	Dispersion in SMF . . . . .	57
Figure 4.2	Dispersion in DCF . . . . .	58
Figure 4.3	Combination of SMF and DCF . . . . .	58
Figure 4.4	The configuration of the TDC based upon three DGTEs . . . . .	61
Figure 4.5	The configuration for the experimental results . . . . .	61
Figure 4.6	Transmitted eye (a) and the received eyes for 80km SMF (b) and 60km DCF (c) . . . . .	62
Figure 4.7	Received eye after 60km DCF at 1554.74nm . . . . .	64
Figure 4.8	Received eye after 60km DCF at 1554.22nm . . . . .	65
Figure 4.9	Received eyes after 60km DCF . . . . .	66
Figure 4.10	Received eyes after 60km DCF . . . . .	67
Figure 4.11	Received eyes after 60km DCF . . . . .	68
Figure 4.12	Circuit diagram with noise floor injected . . . . .	69
Figure 4.13	Sensitivity measurements . . . . .	69
Figure 4.14	Sensitivity measurements . . . . .	70
Figure 4.15	Group delay TDC measurement setup . . . . .	71
Figure 4.16	TDC Group Delay profile of device compensating for 60km DCF @ 1554.22nm (a), 1554.54nm (b) and 1554.74nm . . . . .	71
Figure 4.17	TDC dispersion profile of device compensating for 60km DCF @ 1554.22nm (a), 1554.54nm (b) and 1554.74nm . . . . .	72
Figure 4.18	DPSK eyes, input (a) and output (b) @ 1554.54nm . . . . .	72
Figure 4.19	DPSK outputs for 1554.13nm (a), 1554.94nm (b) and 1555.34nm. . . . .	73
Figure 4.20	Multi-channel transmission setup with DPSK data . . . . .	73
Figure 4.21	The DPSK multiplexed received eyes @ 1554.13nm (a), 1554.54nm (b), 1554.94nm (c) and 1555.34nm . . . . .	74
Figure 4.22	1554.54nm output wavelength DPSK eyes for the combination of wavelengths of 1554.54nm and 1554.22nm (a) and 1554.54nm and 1554.74nm (b) . . . . .	74
Figure 5.1	The effect of SRS. Power from the lower wavelengths being transferred to the higher wavelengths . . . . .	80

Figure 5.2	Participating energy levels pump frequency $\omega_p$ and Stoke Frequency $\omega_s$ . . . . .	81
Figure 5.3	Ultra-long Raman Fibre Laser with pumping configuration to produce quasi-lossless conditions . . . . .	84
Figure 5.4	OTDR trace of 82km SMF with and without QLL conditions . . . . .	85
Figure 5.5	OTDR trace of 82km SMF with QLL conditions . . . . .	86
Figure 5.6	Optical transmission loop with URFL . . . . .	87
Figure 5.7	Optical transmission loop with EDFA scheme . . . . .	88
Figure 5.8	Input and output eyes for one loop re-circulation . . . . .	89
Figure 5.9	Optimum launch power measurements for QLL and EDFA amplification schemes at a data rate of 10.6Gb/s . . . . .	90
Figure 5.10	Optimum launch power measurements for QLL and EDFA amplification schemes at a data rate of 42.6Gb/s. . . . .	91
Figure 5.11	Transmission distances for the QLL and EDFA schemes at a data rate of 10.6Gb/s . . . . .	92
Figure 5.12	Transmission distances for the QLL and EDFA schemes at a data rate of 42.6Gb/s . . . . .	93
Figure 5.13	Eye diagrams for EDFA transmission system at 42.6Gb/s . . . . .	94
Figure 5.14	Eye diagrams for QLL transmission system at 42.6Gb/s . . . . .	94
Figure 5.15	Modelled performances of OSNR through the EDFA scheme . . . . .	95
Figure 5.16	Modelled performance of OSNR through the QLL scheme . . . . .	96
Figure 5.17	Transmission performance of OSNR through the QLL and EDFA scheme . . . . .	97
Figure 5.18	Losses through the QLL and EDFA scheme . . . . .	97
Figure 5.19	Equal losses through the QLL and EDFA scheme . . . . .	98
Figure 5.20	Transmission performance of OSNR through the QLL and EDFA scheme with equal losses . . . . .	98
Figure 5.21	Lower wavelengths spectrum of 21 channel input (a) and EDFA amplification (b) URFL (c) amplification schemes outputs . . . . .	100
Figure 5.22	Higher wavelengths spectrum of 21 channel input (a) and EDFA amplification (b) URFL (c) amplification schemes outputs . . . . .	101
Figure 5.23	Transmission results for EDFA and URFL WDM schemes . . . . .	102
Figure 5.24	Launch powers for EDFA and URFL WDM schemes . . . . .	103

Figure 6.1	The reflective effect of (a) a Conventional mirror and a (b) phase conjugated mirror. ....	105
Figure 6.2	Recirculating loop configuration and OPC set-up .....	107
Figure 6.3	Q-penalty as a function of optical launch power, comparing the difference between a EDFA and QL link. Dispersion compensation obtained with DCF. ....	108
Figure 6.4	A comparison between EDFA and QL link with dispersion compensation is obtained by OPC. ....	109
Figure 6.5	Comparison of launch power tolerance between QL link using DCF and OPC using DCF. ....	109
Figure 6.6	BER curve as a function of the system length comparing the QL with DCF and QL with OPC system configurations. ....	110

## List of Tables

Table 3.1	Encoding and decoding using differential encoding . . . . .	43
Table 3.2	The phase combination of the two PSK transmitted data patterns where one pattern is delayed by one bit and the resulting ASK bit pattern generated . . . . .	46
Table 4.1	Previous TEC Settings . . . . .	63
Table 4.2	New TEC Settings . . . . .	63

## Abbreviations

ASE	Amplified Emission
ASK	Amplitude Shift Keyed
BER	Bit Error Rate
DCF	Dispersion Compensating Fibre
DGTE	Distributed Gires-Tournois Etalons
DLI	Delay Line Interferometer
DWDM	Dense Wavelength Division Multiplexing
EDFA	Erbium Doped Fibre Amplifier
FBG	Fibre Bragg Grating
FEC	Forward Error Correction
FWM	Four Wave Mixing
LED	Light Emitting Diode
NRZ	Non Return-to-Zero
OPC	Optical Phase Conjugation
OSA	Optical Spectrum Analyser
OSNR	Optical Signal-to-Noise Ratio
PRBS	Pseudo Random Bit Sequence
PSK	Phase Shifted Keyed
QLL	Quasi-Lossless
ROADM	Reconfigurable Optical Add/Drop Multiplexer
RZ	Return-to-Zero
SBS	Stimulated Brillouin Scattering
SMF	Single Mode Fibre
SPM	Self Phase Modulation
SRS	Stimulated Raman Scattering
TDC	Tunable Dispersion Compensator
URFL	Ultra-long Raman Fibre Laser
WDM	Wave Division Multiplexer
ZMD	Zero Material Dispersion

## Chapter 1

# Optical Communications

### 1.1 Introduction

Optical communication is a medium that can be used for short or long-haul transmitted information. It is now a well established world wide method and, whether it is through making a phone call or watching the television, the majority of people on planet earth are dependent on fibre optic communication technology.

### 1.2 Historic View

Using light as a form of communication can be traced back through history. Civilizations around the world have been using different forms of optical communication, to transmit single bit of information be it with a mirror or, as the English did when the Spanish Armada approached, with fire beacons. [1] In 1792 Claude Chappe suggested a mechanical way of transmitting coded messages over long distances with the use of relay stations. [2] This first optical telegraph was put in place between Paris and Lille in July 1794 and then over the next 30 years the service expanded throughout Europe. [1]

The optical telegraph system was a slow one, with the system working at what could be considered as less than one bit per second. Throughout time however with the introduction of new technologies this bit rate was to increase and the transfer speed of information would increase.

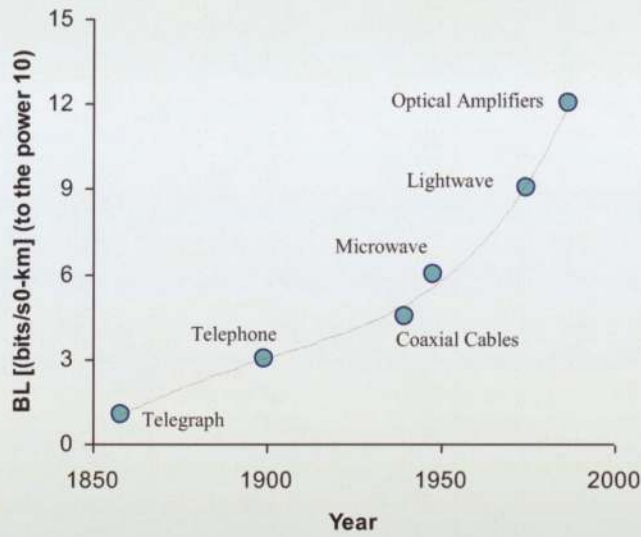


Figure 1.1: Increase in bit rate –distance product BL from 1850 to 2000. [3]

Figure 1.1 shows the increase in data rate capabilities over distance over 150 years due to new technologies. The introduction of the telegraph started the electrical communications era, where the bit rate increased to approximately 10 bits/s. The telephone brought analogue electrical techniques which dominated communication systems for more than a century. [3] The introduction of coaxial cables increased system capacities, but the bandwidth for these systems is limited by the frequency-dependent cable losses. These losses led to microwave technology with frequencies in the range of 1-10 GHz that was suitable for modulation for transmission. [3]

The problem with coaxial and microwave systems were that the coaxial system needed short repeater spacing which was costly and the microwave carrier frequency was limited. The invention of the laser in the 1960's and research into applications for communication began to resolve the problems that occurred in the established transmission systems. In the late 1960's optical fibre was suggested as a medium to transmit optically modulated information and optical transmission system came into being.

### 1.3 Thesis Outline

When optical transmission systems were first introduced several problems had to be overcome and the solving of these problems gave this type of communication a rapid progression in development. In recent years there has been a rapid increase in data rates and data capacity of transmission systems and with this rapid increase new problems and challenges are born. In this thesis I have looked at the development and redeployment old technology and establishing new methods for optical communication to explore different avenues of improvement for optical communication systems.

The thesis consists of:

- Chapter 1 gives a brief history of fibre optic history and a thesis outline.
- Chapter 2 gives an explanation about optical transmission techniques and what components are required to build an optical transmission system. The chapter looks at what impairments have to be overcome to ensure that the system will perform at the required levels.
- Chapter 3 looks at a method of demodulating a received transmitted signal from the phase to amplitude domain. The research takes technology already in use and applies it a different way to produce demodulation results.
- Chapter 4 shows research work that has been performed using a dispersion compensating device. Its characteristics are explored and the positive properties that the device can provide are examined as well as its usefulness to optical transmission systems.
- Chapter 5 compares the long-haul transmission of an amplified system with Erbium-Doped Fibre Amplifier which is a commonly used in transmission systems, with that of a new method of amplified transmission system using a Quasi-Lossless amplifier scheme which uses the properties of Raman amplification.

- Chapter 6 compares and uses the transmission of the Quasi-Lossless scheme to that of an Optical Phase Conjugation system. Both the methods are also used together and transmission performance compared.
- Chapter 7 reflects on all the experiments and the measurements results achieved.

## Chapter 2

# Fibre Optic Systems

### 2.1 Introduction

A fibre optic system consists of three basic stages; a method to transmit the signal, a method to carry the signal and a method to receive the signal as shown in Figure 2.1. Each stage of the communication setup must be established and functioning correctly for the complete communication system to work.

The optical transmitter provides the carrier frequency and data format that the communication system will be operating with, which the communication channel and optical receiver have to be compatible. The optical receiver is an important part of the communication setup that has to interpret the signal that has been transmitted, so it is important that the signal received is one that is error-free as possible. For optical communications the communication channel will consist of different components that ensure that the transmitted signal does not suffer and under perform. These components may include multiplexers, couplers and amplifiers. To get an understanding of how these three basic stages are applied and what basic principles each stage of the communication setup must follow is what this chapter will explore.

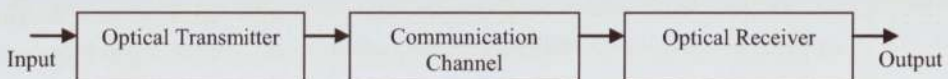


Figure 2.1: Optical transmission communication system [1]

### 2.2 Optical Transmitter

The optical transmitter has the role of converting electrical input signal to an optical signal and then launching this signal down the optical fibre. One of the components of an optical transmitter is the optical source. Fibre optical communications systems mainly use semiconductor optical sources such as light emitting diodes (LEDs) and semiconductor lasers

because of several inherent advantages such as compact size, narrow line-width, high efficiency and right wavelength range and direct modulation at relatively high frequencies. As bit rates have increased to 10Gb/s and higher the frequency chirp imposed by direct modulation to semiconductor lasers has now become so large that direct modulation of such devices is now rarely done. Optical modulators are now used along side a CW laser output, with the modulator converting the CW light into a data-coded pulse with the right modulation format. [4] One form of optical modulator is the Mach-Zehnder (MZ) interferometer.

### 2.2.1 Mach-Zehnder Modulator

The Mach Zehnder modulator is an important device for high Q bit rate light systems as these devices are of great use when a laser has to be modulated at high speeds. The device uses phase changes within its design and external applied voltages to perform the modulation of optical signals. In Figure 2.2 the modulator is represented by different points 1 through to 8 and point 1 is the input of the device and point 8 representing of the output. The phase changes within the device occur when the signal is split between the positions 1 to 4 and the recombined positions of 6 to 7 and 5 to 8. These phase interactions have to occur for the input and output powers to balance.

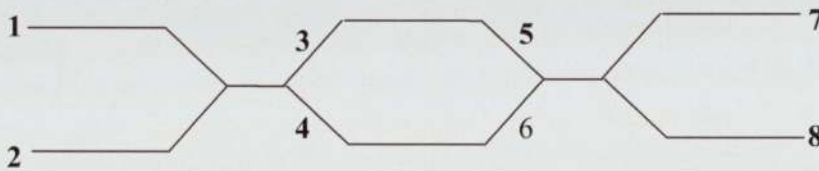


Figure 2.2: Basic Mach-Zehnder modulator design

This balance can be found and checked by working through the interactions that happen through stage of the device. We can first look at what happens when we introduce no phase change at the positions of signal interference in the device and see the resulting output. If we take an input represented as  $e^{i\omega t}$  at position 1 with as a power level of 1 (there is no input on

the branch arm 2) and then split this signal onto the two arms of the modulator which takes us to points 3 and 4, the equally split signal gives us:

$$E_3 = \frac{1}{\sqrt{2}} e^{i\omega t} \quad E_4 = \frac{1}{\sqrt{2}} e^{i\omega t} \quad (2.1)$$

At points 5 and 6 we have the same equations for what we have at points 3 and 4 respectively.

These two signals will now recombine to give us the outputs at position 7 and 8:

$$\begin{aligned} E_7 &= \frac{1}{\sqrt{2}} \left( \frac{1}{\sqrt{2}} e^{i\omega t} \right) + \frac{1}{\sqrt{2}} \left( \frac{1}{\sqrt{2}} e^{i\omega t} \right) \\ &= \frac{1}{2} e^{i\omega t} + \frac{1}{2} e^{i\omega t} \\ &= e^{i\omega t} \end{aligned} \quad (2.2)$$

$$\begin{aligned} E_8 &= \frac{1}{\sqrt{2}} \left( \frac{1}{\sqrt{2}} e^{i\omega t} \right) + \frac{1}{\sqrt{2}} \left( \frac{1}{\sqrt{2}} e^{i\omega t} \right) \\ &= \frac{1}{2} e^{i\omega t} + \frac{1}{2} e^{i\omega t} \\ &= e^{i\omega t} \end{aligned} \quad (2.3)$$

These resulting power levels at the outputs at positions 7 and 8 tell us that the power out on each arm is equal to 1, giving a total output of 2 for an input of 1, which of course is not possible and goes against the conservation of energy. This means that an interaction inside the modulator is required to occur, and this is where a phase shift comes in.

When the signal in a modulator is being split or recombined a phase shift difference of  $90^\circ$  ( $e^{i(\pi/2)}$ ) occurs to one of the signals. We can find this by taking the previous example where we have the input at 1 of  $e^{i\omega t}$  where we again have:

$$E_3 = \frac{1}{\sqrt{2}} e^{i\omega t} \quad (2.4)$$

But this time due to the phase change at position 4 we get:

$$E_4 = \frac{1}{\sqrt{2}} e^{i\omega t} \bullet e^{i\frac{2}{\pi}} \quad (2.5)$$

$$= \frac{i}{\sqrt{2}} e^{i\left(\omega t + \frac{\pi}{2}\right)}$$

$$= \frac{i}{\sqrt{2}} e^{i\omega t} \quad (2.6)$$

Once again at points 5 and 6 we have the same as what we have at 3 and 4. So to find the outputs at 7 and 8 the signals are again recombined with position 7 giving:

$$\begin{aligned} E_7 &= \frac{1}{\sqrt{2}} \left( \frac{1}{\sqrt{2}} e^{i\omega t} \right) + \frac{i}{\sqrt{2}} \left( \frac{i}{\sqrt{2}} e^{i\omega t} \right) \\ &= \frac{1}{2} e^{i\omega t} + \frac{-1}{2} e^{i\omega t} \\ &= \mathbf{0} \end{aligned} \quad (2.7)$$

(It has to be noted that the -1 from equation 2.7 is achieved due to the trigonometry term:

$$i \cdot i = -1)$$

And position 8 giving:

$$\begin{aligned} E_8 &= \frac{i}{\sqrt{2}} \left( \frac{1}{\sqrt{2}} e^{i\omega t} \right) + \frac{1}{\sqrt{2}} \left( \frac{i}{\sqrt{2}} e^{i\omega t} \right) \\ &= \frac{i}{2} e^{i\omega t} + \frac{i}{2} e^{i\omega t} \\ &= i e^{i\omega t} \end{aligned} \quad (2.8)$$

Using the trigonometry term  $i = e^{j(\pi/2)}$  we now have:

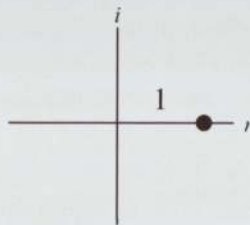
$$\begin{aligned}
 &= e^{j\frac{\pi}{2}} \bullet e^{j\omega t} \\
 &= e^{j\left(\frac{\pi}{2} + \omega t\right)} \\
 &= e^{j\left(\omega t + \frac{\pi}{2}\right)} \tag{2.9}
 \end{aligned}$$

Where  $e^{j0} = \text{Cos } 0$ , and so:

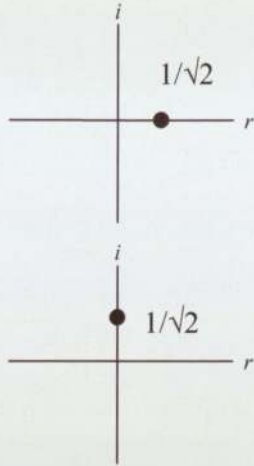
$$\begin{aligned}
 &= \text{COS}\left(\omega t + \frac{\pi}{2}\right) \\
 &= 1 \tag{2.10}
 \end{aligned}$$

For the input of a power of 1 we have out on 7 a power of zero and on 8 a power of 1, an equal power in-to-out ratio.

Another way to view this interaction within the device is to use constellation diagrams where an  $i$  represents the imaginary and  $r$  is representing the real. This form of diagram gives you a visual representation of what is occurring due the different stages within the modulator. If again we use the modulator and the numbered position points represented in Figure 2.2 we have:



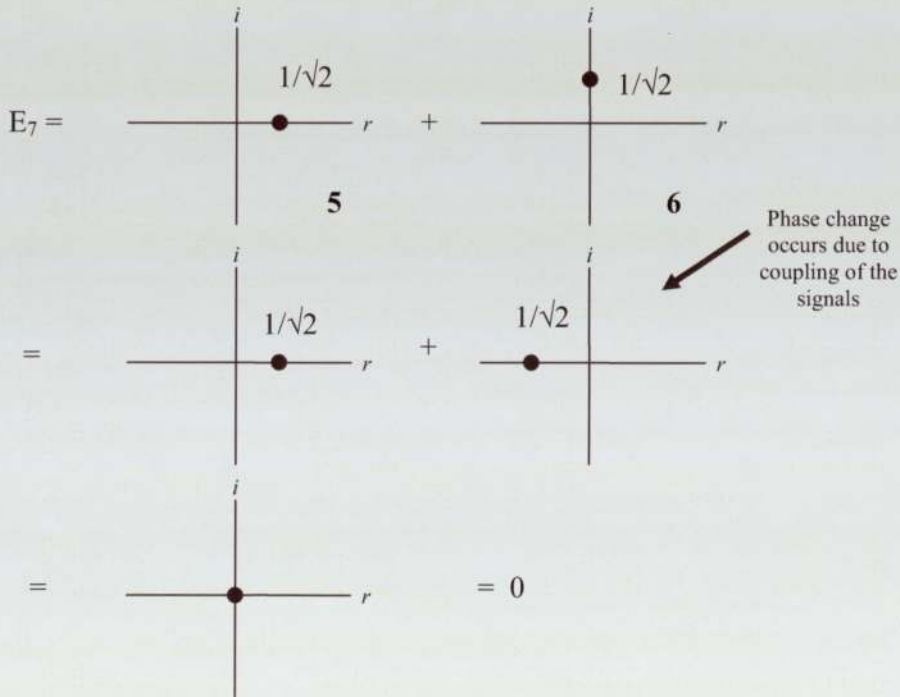
This shows the input into the modulator at position 1 from Figure 2.2 with an input power at the level of 1. If we now look at the power and phase representation at positions 3 and 4 we have:



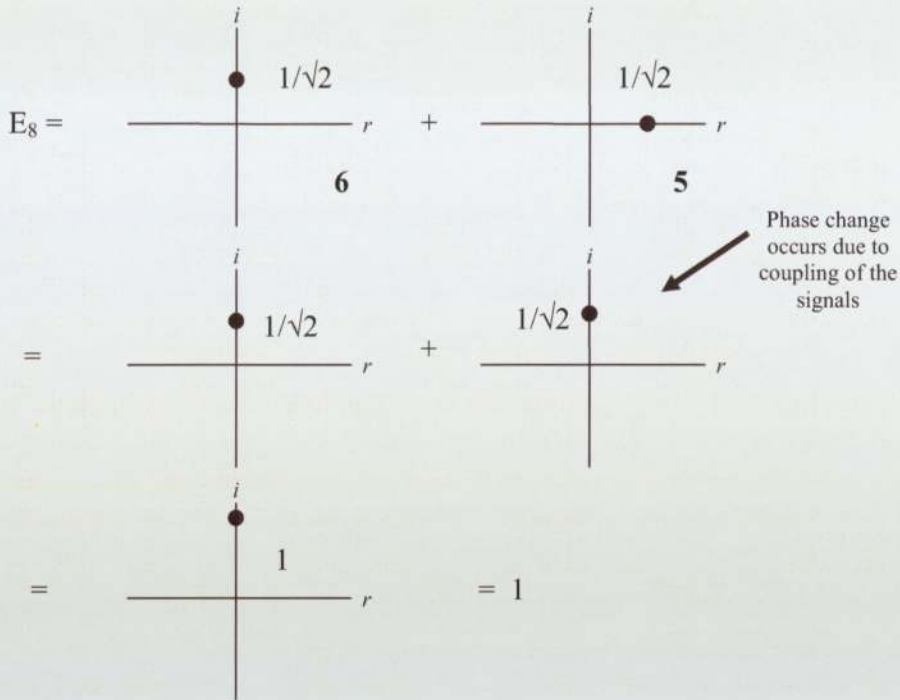
For position 3, where there has been no phase change but the power has been halved.

For position 4, where there has been a phase change and the power has been halved.

There is no change at points 5 and 6 with respect to 3 and 4, so the combination of the signals for the outputs at position 7 and 8 is:



And if we look at what happens at position 8:



We can see is that from the resulting equations and constellation diagrams that a change in phase inside the modulator occurs when there is a combination of two signals. The change in phase has to occur to ensure that the correct levels of energy are transferred through the device. The phase change becomes useful in other devices within transmission system and one of the devices, the interferometer, is looked at in a later chapter.

To provide different modulation formats and give a form of control over the output signal external voltages are applied to the device. This external voltage is applied by two phase modulators, as shown in Figure 2.3 and these alter the phase of the fields of the signals that travel down there individual arms.

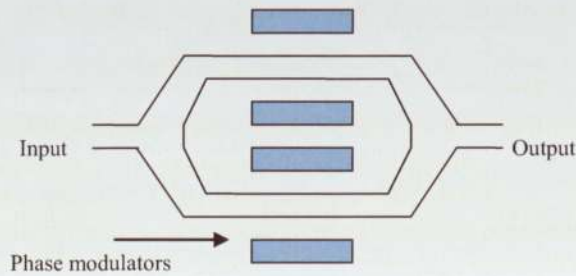


Figure 2.3: Basic diagram of a Mach-Zender modulator.

To understand how this can affect the signal through the device we can take the same approach as previously seen and using the modulation representation and numbered positions in Figure 2.4 we can produce constellation diagrams for the expected outputs.

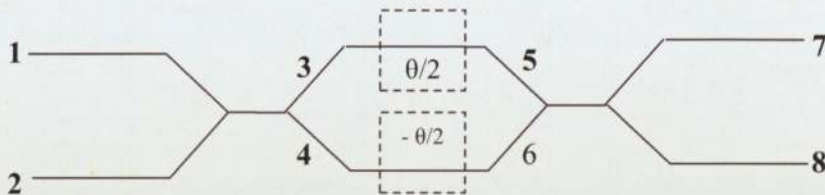
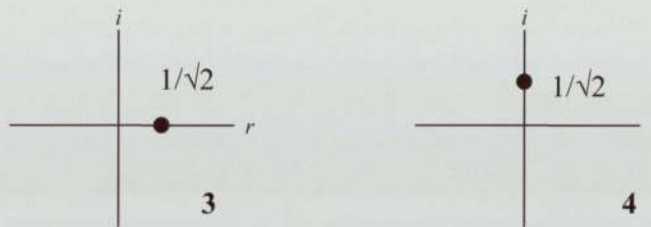
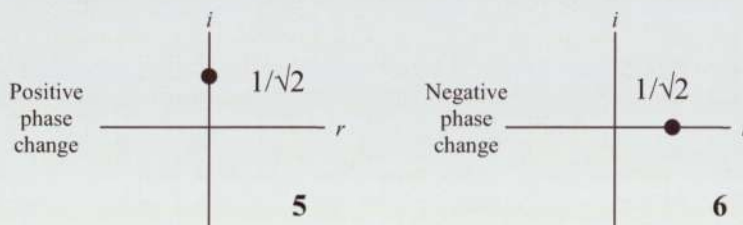


Figure 2.4: Basic diagram of a Mach-Zender modulator.

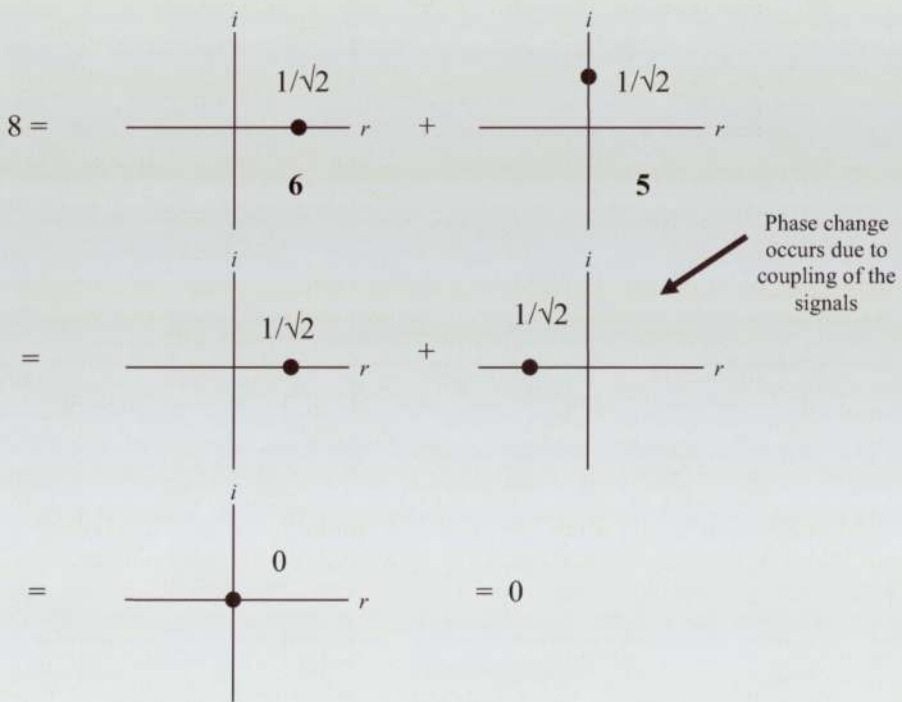
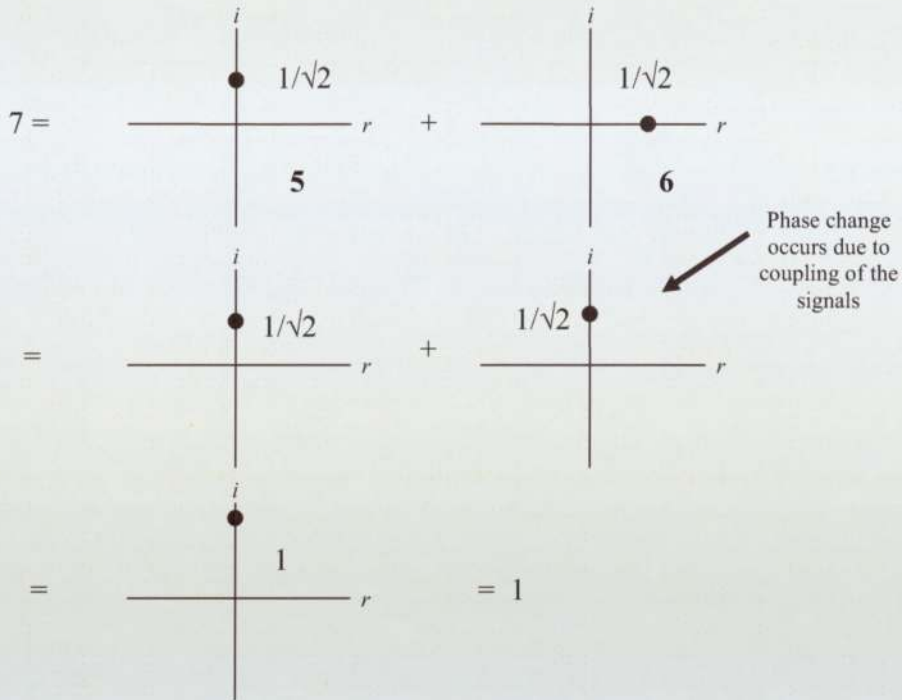
If we have the same constellation diagrams for positions 3 and 4:



There is now a phase change of  $\theta/2$  on one arm and an opposite phase of  $-\theta/2$  on the other introduced by the phase modulators supplying the external voltage, which now gives a constellation diagrams at 5 and 6 of:



To find the output at 7 and 8 it's a case of adding these two diagrams together:



The introduction of these phase changes across the two arms of the modulator has now given an output on the number 7 arm of 1 and on the number 8 arm of 0 with respect to the power levels.

By altering the electric field across these two arms the resulting output of the modulator can be altered to represent different modulation formats.

If we take a look at positions 3 and 4 from figure 1 and take them again as:

$$3 = \frac{1}{\sqrt{2}} e^{i\omega t} \quad 4 = \frac{i}{\sqrt{2}} e^{i\omega t} \quad (2.11)$$

Due to the phase modulators introduction we have ourselves a phase change of  $\theta/2$  on one arm and  $-\theta/2$  on the other which gives us at positions 5 and 6:

$$5 = \frac{1}{\sqrt{2}} e^{i\left(\omega t + \frac{\theta}{2}\right)} \quad 6 = \frac{i}{\sqrt{2}} e^{i\left(\omega t - \frac{\theta}{2}\right)} \quad (2.12)$$

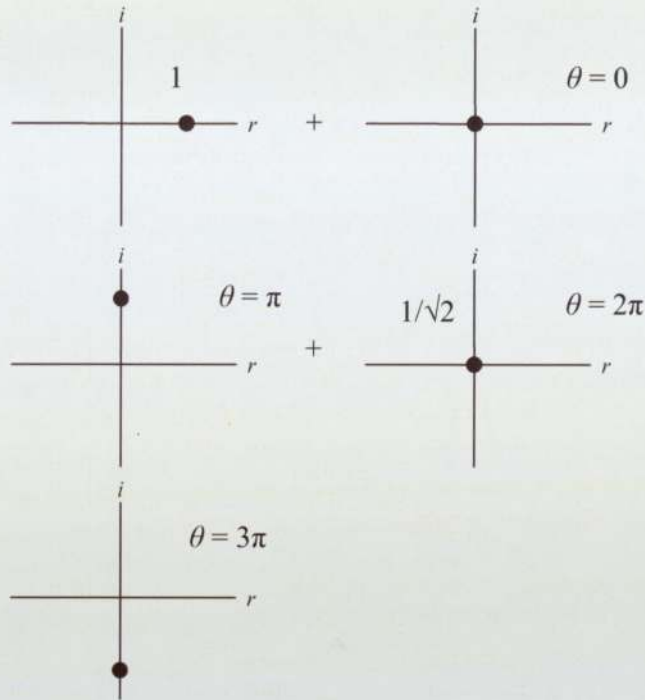
So if will look at the output we get on positions 7 and 8 we have:

$$\begin{aligned} 7 &= \frac{1}{2} e^{i\left(\omega t + \frac{\theta}{2}\right)} - \frac{1}{2} e^{i\left(\omega t - \frac{\theta}{2}\right)} \\ &= \frac{1}{2} \left[ e^{i\left(\omega t + \frac{\theta}{2}\right)} - e^{i\left(\omega t - \frac{\theta}{2}\right)} \right] \end{aligned} \quad (2.13)$$

And using trigonometry formula we produce a signal of:

$$\begin{aligned} &= \frac{1}{2} \cdot 2 \cdot \sin \frac{\theta}{2} e^{i\left(\omega t + \frac{\pi}{2}\right)} \\ &= \sin \frac{\theta}{2} e^{i\left(\omega t + \frac{\pi}{2}\right)} \end{aligned} \quad (2.14)$$

The significance of this equation can be explained by using constellation diagrams and showing the resulting phase changes for  $\theta$  of  $0$ ,  $\pi$ ,  $2\pi$  and  $3\pi$ .



As the phase change occurs across the arm of the modulator the outputted signal alters along the imaginary line of the constellation diagram. This means that the phase of the signal is being altered due to the current applied across the two arms of the modulator which in turn provides the control over what type of modulation format the modulator will output.

For a transmission system the Mach Zender modulator is a device that provides an excellent generation of modulation formats. Optical communication systems are not all created equal and some require different forms of modulation. The Mach Zender modulator, when exposed to different current changes, can generate a modulation format required for the transmission system and if ever the system itself is altered a change in this electrical current can be provide to alter the modulation format. This makes the Mach Zender modulator a stable part of any communication system.

### 2.3 Fibre Design

The communication channel used between optical transmitter and receiver is optical fibre and the type of fibre used on a transmission span is commonly a step-index fibre.

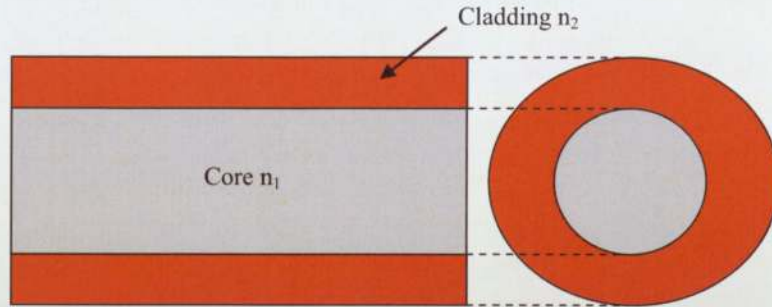


Figure 2.5: Core and cladding of the optical fibre.

The step change in refractive index between the core and the cladding is where this type of fibre gets its name. A silica fibre, it consists of a central core refractive index  $n_1$  surrounded by a cladding of refractive index  $n_2$  [5] as shown in Figure 2.5 And for complete lightwave guidance a reflective angle  $\theta$  has to be greater or equal to the critical angle  $\theta_c$ , given by:

$$\sin \theta_c = \frac{n_2}{n_1} \quad (2.15)$$

Also the fractional index change  $\Delta$  is also important:

$$\Delta = \frac{n_1 - n_2}{n_1} \quad (2.16)$$

This index change is always positive as for the critical angle to exist  $n_1$  must be larger than that of  $n_2$ .  $\Delta$  should also be as large as possible so that the maximum amount of light is coupled into the fibre.

Also on most transmission fibre the number of electromagnetic modes transmitted down the fibre waveguide is one. This single mode fibre has the advantage over multi-mode

fibres, as the broadening of the pulses for each mode due to different transit times which produces inter-modal dispersion and a degradation to the transmitted signal. For single mode fibres to be produced the core of the fibre is reduced to less than 10 $\mu\text{m}$ , where in multi-mode fibre it is approximately 50 $\mu\text{m}$ . To know the number of modes a fibre can support the normalised frequency can be calculated, and this is found by:

$$V = \frac{2\pi a}{\lambda} \sqrt{n_1^2 - n_2^2} \quad (2.17)$$

Where  $V$  is the normalised frequency,  $a$  the fibre core radius and  $\lambda$  the free space wavelength, for a step-index fibre,  $V < 2.405$  for a single mode. [6]

### 2.3.1 Fibre Losses

There are many reasons why the transmitted signal through optical fibre may experience attenuation to its transmission power. Many of these losses can be avoided if good transmission management is adhered to, but there are losses that also occur, that transmission management and system setup has to compensate for.

One of the main forms of loss in fibre is *Absorption*. Most of the modern day fibres are very pure but *intrinsic absorption* can still occur at higher wavelengths. Due to electronic and molecular transitions and vibrations due to chemical bonds absorption of this kind happen in the ultraviolet region and between the 7-12  $\mu\text{m}$  in the infra red region respectively. [5]

Also the presence of impurities in the fibre results to *extrinsic absorption*. The main source for this type of absorption in fibres is the presence of water vapour. A vibration of the OH ion occurs near 2.73 $\mu\text{m}$ . Its harmonic and combination tones with silica produce absorption at the 1.39, 1.24 and 0.95 $\mu\text{m}$  wavelengths. With new kind of fibres known as dry fibre, the OH ion concentration is reduced to such low levels that the absorption at these wavelengths has almost disappeared. [9]

Another form of loss in fibre is *Scattering*. This occurs due to variations in the refractive index throughout the glass in the fibre. As a beam is passed down the optical fibre the energy is scattered due to small variations in the glass. This is known as *Rayleigh Scattering*. [10]

Absorption and Scattering are two forms of losses that can occur during the manufacturing process of the fibre. Losses can also occur when a transmission system is being constructed. One of the main problems from losses in transmission is due to *Bending*. Optical fibres are rarely in spools that are less than 10cm in diameter and this is because the sensitivity of the transmitted signal can be affected by a bend in the fibre especially at longer wavelengths. This is important to note as most transmission monitoring is done at long wavelengths. It has been noted that a single-mode fibre bent into a single 32nm loop, up to additional 0.5dB attenuation can occur. But a fibre with the same core diameter looped a 100 times at 50nm diameter will produce no more than 0.1dB attenuation. [7]

As well as the physical losses mentioned above there is also the degradation of the signal as it propagates along the fibre. As optical signals travel through long fibres a significant time offset proportional to the distance develops between different wavelengths, causing the optical pulses to widen and cross over. This effect is known as dispersion.

## 2.4 Dispersion

The width of a pulse propagating in an optical fibre increases with the distance of propagation. The pulse of light consists of photons and the velocity of propagation of each photon is not the same and this produces dispersion. Dispersion,  $D$  can be defined as:

$$D = \frac{d\tau}{d\lambda} \quad (2.18)$$

Where  $\lambda$  is the wavelength and  $\tau$  is the variation of propagation time. The different propagation of velocities of light through any device is known as chromatic dispersion.

Chromatic dispersion appears for two reasons. The first being material dispersion which occurs due to the fact that the refractive index of the silica, the material used to make the fibre, is frequency dependent and this is the principle component of chromatic dispersion given by:

$$D_m = \frac{\lambda}{c} \left| \frac{d^2 n_1}{d\lambda^2} \right| \quad (2.19)$$

Where  $c$  is the speed of light and  $n_1$  the core refractive index. The other reason is waveguide dispersion. This effect occurs from a change in wavelength and where the energy of the mode propagates, in the core or the cladding and is given by:

$$D_w = - \left[ \frac{n_1 - n_2}{\lambda c} \right] \frac{V d^2 (Vb)}{dV^2} \quad (2.20)$$

Where  $n_2$  the refractive index of the cladding,  $V$  the normalised frequency for the fibre and  $b$  the normalised propagation. The total dispersion is a combination of these two dispersive effects. At wavelengths that are longer than the Zero Material Dispersion (ZMD) point for most fibres material and wavelength dispersion have opposite components and can therefore cancel each other out. So by altering the fibre core diameter and refractive index difference between the core and cladding of the fibre, it is possible to shift the zero of the chromatic dispersion to the low loss regions of the 1300-1500nm wavelengths. This has been done and it has resulted in single mode fibre (SMF) having a ZDW at 1310nm.

Most transmission systems use SMF and the typical chromatic dispersion is approximately 17ps/nm/km. The amount of chromatic dispersion depends on the operationally wavelength of the system, the slope of the curve and the wavelength that the fibre has zero dispersion. Using the formula:

$$D = \frac{S}{4} \left( \lambda - \frac{\lambda^4}{\lambda_0^3} \right) \quad (2.21)$$

Where  $S$  is the slope of the dispersion curve, which we will give as  $0.09\text{ps/nm}^2/\text{km}$ , the zero dispersion  $\lambda_0$  at  $1310\text{nm}$  and the operation wavelength  $\lambda$   $1550\text{nm}$ , we have a resulting dispersion;  $D$  of  $17.08\text{ps/nm/km}$ . [7] This resulting number 17 is typical of most SMF fibres.

To cancel out the dispersion that occurs with SMF, dispersion compensating fibre (DCF) have been designed that adds negative dispersion. The combination of SMF and DCF is aimed at producing zero dispersion at different wavelengths this and other methods are discussed in chapter 4.

## 2.5 Bit Error Rate and Q

Performance measurements of transmission system are usually presented as Q or BER (Bit Error Rate). [The BER defines its ability to identify incorrect bits by the receiver decision circuit.] If we have a BER of  $2 \times 10^{-6}$ , this corresponds to an average of 2 errors for every one million bits. A commonly used level for receivers is to be below a BER of  $1 \times 10^{-9}$ . The receiver sensitivity is then defined as the minimum average received power by the receiver to operate at a BER of  $1 \times 10^{-9}$ . [4] Q, which is usually defined in dB, is a statistical measurement of an optical performance of a digital channel, with the modulation format and the signal-to-noise ratio being a couple of parameters that can affect the level of Q that a system will have. From point to point (start to finish) on a communication system Q is used to measure the total performance of the transmission system were BER is general used at the receiver.

## 2.6 Optical Receiver

The optical receiver performs the opposite application to that of the transmitter, as it converts the optical signal back into an electrical form and recovers the data transmitted. One

of the main controlling effects of a receiver is the receiver sensitivity, with the main governing factor being the Bit-Error Rate (BER), which defines its ability to identify incorrect bits by the receiver decision circuit. With the introduction and improvement of forward error correction (FEC) techniques which is a method of correcting received bits that are known to be at error, BER of a level of  $1 \times 10^{-3}$  can be achieved.

One of the main factors in a communication system that can control the level of the BER is the amount of noise that has corrupted the transmitted signal. The transmitted signal is subjected to different conditions during its transmission. If the signal is being transmitted over a distance where amplification of the signal is required, the transmission will be subject to a condition known as noise which is generated by the device that provides the amplification.

This optical signal to noise ratio (OSNR) is defined as the power ratio between the signal and the noise as:

$$OSNR = \frac{P_{Signal}}{P_{Noise}} \quad (2.22)$$

The noise and the signal have to be measured at the same point in the transmission system as well as at the same bandwidth, and this measurement is often one done at the receiver.

## 2.7 Optical Amplifiers

In an optical communication system the transmitted signal become attenuated by the optical fibre as it propagates along. There is also extra loss that accumulates from the different components, such as couplers and multiplexers that reduce the strength of the signal so much that detection of the signal becomes impossible. A method to combat this signal degradation was the introduction of regenerators. These devices work by taking the transmitted signal at set wavelengths along the span and convert them from optical to electrical signal and then tidy the signal before retransmit it.

The problem with regenerators is that they are specific to transmission bit rates and modulation formats. The introduction of optical amplifiers has provided a more flexible method for the regeneration of a transmitted signal. Optical amplifiers are insensitive to a

change in bit rates and signal formats, and they can also amplify several transmission channels. The negative side for amplifiers is that they introduce extra noise to the transmission system. When several amplifiers are passed through, the accumulated noise can introduce a significant amount of errors to the transmitted signal.

### 2.7.1 Stimulated Emission

For amplifiers the key physical phenomenon for the signal amplification is *stimulated emission*. If a laser-active atom or ion is in an excited state it may after some time spontaneously decay into a lower energy level, releasing energy in the form of a photon emitted in a random spatial direction. This process is called spontaneous emission. However, it is also possible that the photon emission is stimulated by incoming photons, if these have a suitable photon energy (or optical frequency); this is called *stimulated emission*. In that case, a photon is emitted into the mode of the incoming photon. In effect, the power of the incoming radiation is amplified.

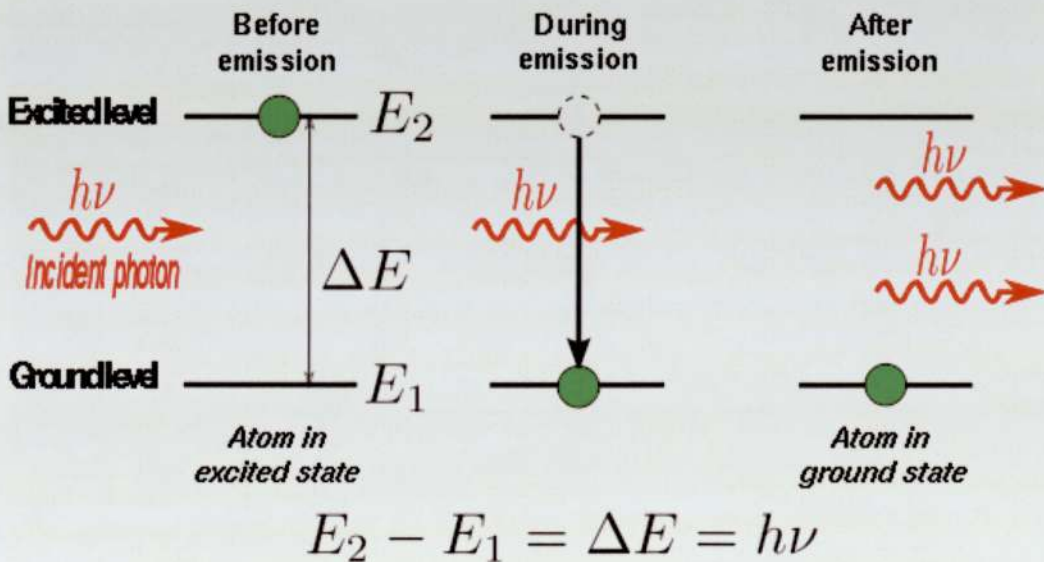


Figure 2.6: Fundamental three processes occurring between two energy state of an atom. [13]

Figure 2.6 shows how the three processes of stimulated emission occurs where  $\nu$  is the frequency and  $h$  is Planks constant. One of the amplifiers in communication systems to use this stimulated emission process is the Erbium-Doped Fibre Amplifier. An amplifier that uses a slightly different method to provide amplification to a signal is a Raman Amplifier.

### 2.7.2 Erbium-Doped Fibre Amplifiers

An Erbium-Doped Fibre Amplifier (EDFA) contains of a length of silica fibre whose core is doped with ionized atoms  $\text{Er}^{3+}$  from the earth element erbium. A signal pump laser at a wavelength of usually 980nm or 1480nm is coupled into the fibre and there is usually an isolator to prevent any unwanted reflections entering the EDFA, as shown in Figure 2.7. Most EDFA's use 980nm pump lasers as these laser are commerically available and can provide more than 100 mW of pump power. [4]

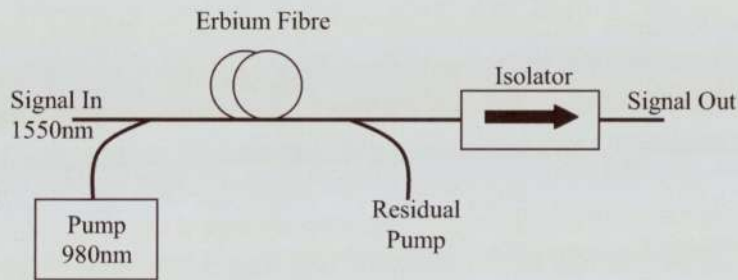


Figure 2.7: An EDFA

With the advantages of using compact and reliable pump lasers, the fact that its an all fibre device and that it introduces no crosstalk when amplifying show the EDFA to be a valuable component for communication systems and it is one of the most commonly used devices for amplification.

### 2.7.3 Amplifier Noise

The ultimate limiting factor for most communication systems is the amplifier noise. [13] For a lumped EDFA the impact of the amplified spontaneous emission (ASE) is quantified through the noise figure  $F_n$  is given by  $F_n = 2n_{sp}$ . The spontaneous emission factor  $n_{sp}$  depends on the relative populations of  $E_1$  and  $E_2$  of the ground and excited states (shown in Figure 2.6) as  $n_{sp} = E_1 / (E_1 - E_2)$ . EDFAs operate on the three level pumping scheme so  $E_1 \neq 0$  and  $n_{sp} > 1$ . So this means the noise figure for EDFAs is expected to be no larger than the ideal level of 3dB. [A more typical noise figure for amplifiers is 6-8 dB.] [4]

The ground and excited levels of  $E_1$  and  $E_2$  vary along the length of the fibre due to their dependence on the pump and signal powers. As a result of this the noise figure becomes dependent on the amplifier fibre length and the pump power just as the amplifier gain does. This leads to it being difficult to achieve high gain, low noise and high pump efficiency. The main limitation is imposed by the ASE travelling backward towards the pump which results in the pump power being depleting. [4]

The relative low noise levels of EDFAs makes them ideal choice for wave-division-multiplexed systems. However in long haul transmission systems the employment of multiple EDFAs required to amplify the signal due to the distance travelled, reduce the performance of the system due to the accumulative noise build up from each amplifier.

### 2.7.4 Raman Amplifiers

Raman amplifiers use stimulated Raman scattering which is explained later in section 5.2. With stimulated emission where the incident photon stimulates an emission of another identical photon without losing energy but with stimulated Raman scattering the incident photon gives up its energy to create another photon at a lower energy and lower frequency (inelastic scattering); the remaining energy is absorbed by the medium in the form of

molecular vibrations (optical photons). [4] What this means is the Raman amplifier has to be pumped optically.

The Raman gain spectrum is fairly broad and has a peak gain at about 13THz below the frequency of the pump signal used. In the near-infrared region of interest for communications, this peak gain corresponds to a wavelength separation of 100nm. So if a fibre is pumped by a high power laser gain can be provided to other signals with a peak gain 13THz below the pump frequency. Which means if we pump at 1460-1480nm this will provide Raman gain in the 1550-1600nm communication window. [11]

The advantage of Raman amplification over EDFA's is that due to the Raman effect amplification can be provided to any wavelength, where the EDFA's are restricted to providing gain in the L and C-bands (1528-1605nm) of the communications window.

Raman amplification relies on simply pumping the same silica fibre that is used for the transmission of the communication signal so it can be used as a lumped or discrete amplifier as well as a distributed amplifier. For the case of the lumped amplifier the Raman amplifier consists of a long fibre reel with the correctly selected pump lasers. For the case of distributed Raman amplifier the fibre can simply be the fibre span that is being used as the transport medium for the communication system with the pump attached to one end of the span. [11] The main purpose at present for Raman amplifiers is to provide additional gain in a distributed manner to EDFAs in ultra long haul systems.

The gain that can be achieved by the distributed Raman amplifier method can be used to provide an Ultra-long Raman Fibre Laser (URFL) which is a new form of amplification scheme which provides an equal gain to all wavelengths in a transmission fibre and this scheme will be looked at and explained in depth in chapter 5.

## **2.8 Multiplexing**

In multiple channel systems there is the need for wavelength selection technologies. In optical systems this wavelength selection is performed by filters. The optical filter

performs simple tasks such as selecting one wavelength and rejecting others and there are optical filters which perform tasks to multiplex and de-multiplex wavelengths in wavelength division multiplexed (WDM) system.

A multiplexer is the combination of several signals at different wavelengths on individual input ports and outputs them on one single common port, where the de-multiplexer performs the opposite function. The method and these devices are used in WDM systems as well as in larger wavelength cross connectors and wavelength add/drop multiplexers. [11]

There are different forms off add/drop multiplexers, many however need to alter the transmitted optical to electrical signal then back to an optical signal. Due to the high speeds of communication transmissions now needed, this transformation between these two mediums slows the communication network down. This has led to the introduction of Reconfigurable Optical Add/Drop Multiplexers (ROADM).

The ROADM is a multiplexer that has the ability to switch communication channels at the wavelength layer. These types of multiplexers appeared originally on long-haul dense wave division multiplexing (DWDM) communication networks, but they started to appear on optical metro systems to cope with the high speed demands and traffic volume. A ROADM also equalises all signal power across all wavelengths, which reduces the need for costly signal amplifying equipment such as optical amplifiers. [12] Due to its channel switching the length of fibre that a transmitted signal is travelling along may vary. As mentioned in section 2.3 this may have altering effects to the level of dispersion upon the transmitted signal so extra dispersion management maybe required.

## **2.9 Conclusions**

There are many important components that make a transmission communication system function and each component of the system has to be measured and setup to perform at their optimum.

For the transmitter, having the correct generated light source is not enough for the modern day communication systems. A method of modulation to help generate the correct communication format is also required. The Mach Zehnder modulator is a device that is very valuable to a transmission system as it can be used to produce different forms of modulated signal with the simple alteration of different phase levels by the change of small current amounts.

When a signal has been transmitted it must have a bit-error-rate at a limit that the receiver can fully recover the signal correctly. This has to be maintained for the complete transmitted system length. Due to the fact that the signals will degrade along the optical fibre, and if the transmission length is too great for the signal to be received correctly then a form of amplification of the signal is required. The choice of amplification however has to be considered carefully, as amplification schemes bring their own problems such as extra noise to the system which in turn can degrade the transmitted signal.

The combination of transmitter, modulation format, amplification scheme, fibre interactions and receiver are all important for all transmission systems. With the modulation format, fibre interactions (dispersion principally) and the amplification scheme all being looked at in the following chapters of this thesis.

## Chapter 3

### Narrowband Optical Filter Demodulation

#### 3.1 Introduction

When designing an optical communication system one of the first considerations to be taken is what type of modulation format will be used for the transmitted data. The output of an optical source is usually modulated by applying an electrical signal, either to the optical source or to a separate external modulator. With the increase in demand for greater speeds and more data transmission around communication networks there is becoming a need for the use of more efficient forms of modulation formats. The research into modulation formats has now having a large amount of time devoted to it.

The introduction of different modulation formats being used to transmit information on, it has also driven the requirements of demodulation. There has been a push over recent years for the use of phase modulated transmission but most optical receivers require the information to be in the amplitude domain. There are devices such as delay line interferometers that can perform the transfer of phase information to amplitude information but they all have their limits, so the search for more efficient methods of demodulation have been researched.

#### 3.2 Modulation Formats

There are two main choices of pulse duty cycle regimes, the Return-to-Zero (RZ) and Non-return-to-Zero formats a diagram of which can be seen in Figure 3.1. For the RZ format each pulse representing 1 bit is shorter than the bit slot and the amplitude returns to zero before the bit period is over and with the NRZ format the optical pulse remains on throughout the whole bit slot and does not drop to zero between two or more successive 1 bits, meaning that the pulse width varies due to the pulse pattern, but for RZ it does not. [4] Each method has its own advantages. The NRZ format has a smaller bandwidth because the on-off

interaction occurs less, but the tolerances for pulse spreading are tighter compared to the RZ format.

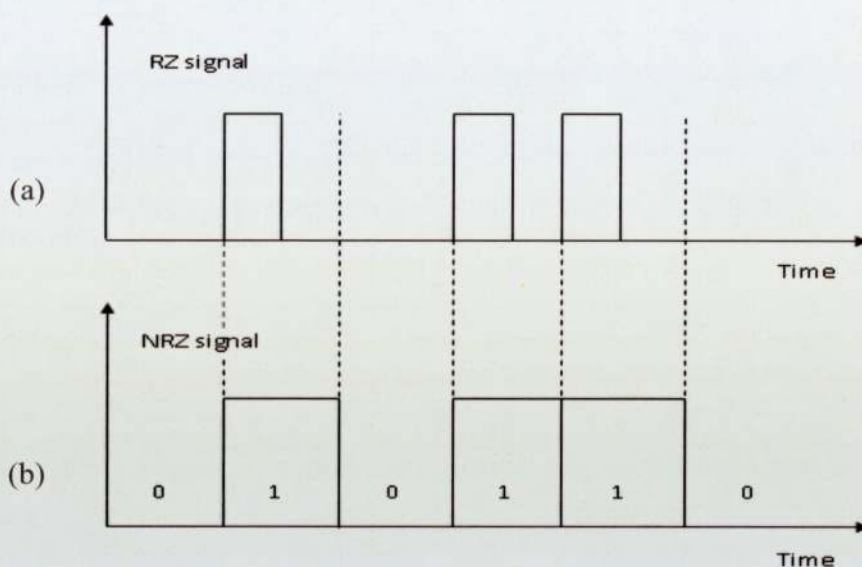


Figure 3.1: Modulated signals (a) return-to-zero and (b) non-return-to-zero.

The choice of which physical variable that is required to be modulated to encode the data on the optical carrier has to be taken. The optical carrier before modulation is in the form:

$$\mathbf{E}(t) = \hat{\mathbf{e}}A \cos (\omega_0 t + \Phi) \quad (3.1)$$

Where  $\mathbf{E}$  is the electric field vector,  $\hat{\mathbf{e}}$  is the polarization vector,  $A$  is the amplitude,  $\omega_0$  is the carrier frequency and  $\Phi$  is the phase [14]. From this the amplitude, frequency or phase can be chosen to be modulated. Depending on how the carrier is shifted between the two levels of a binary digital signal these modulation technique can also be applied to the digital case and these techniques are called Amplitude-shift Keying, Frequency-shift Keying and Phase-shift Keying.

### 3.2.1 Amplitude-shift Keying

Amplitude Shift Keyed (ASK) is one form of modulation that is a variation in the amplitude of a carrier wave. The change in what the modulated signal, as in Figure 3.2(a), varies the amplitude of the carrier signal in Figure 3.22(b). The frequency and the phase of the carrier signal are not altered and remain at a constant. The amplitude level of the carrier signal is commonly viewed as binary logic, with high amplitude as a 1 and low amplitude as a 0. The carrier signal in the modulation format of ASK is often known as ON/OFF keying due to the fact that a binary logic of 0 represents the absence of any carrier signal.[15]

The modulation format of ASK has been in use on transmission systems for some time but due to the increase of transmission speed a lot of work has been now done on Phase Shift Keyed (PSK) modulation formats. PSK has the advantage over ASK due to its ability to help the receiver maintain its synchronisation.

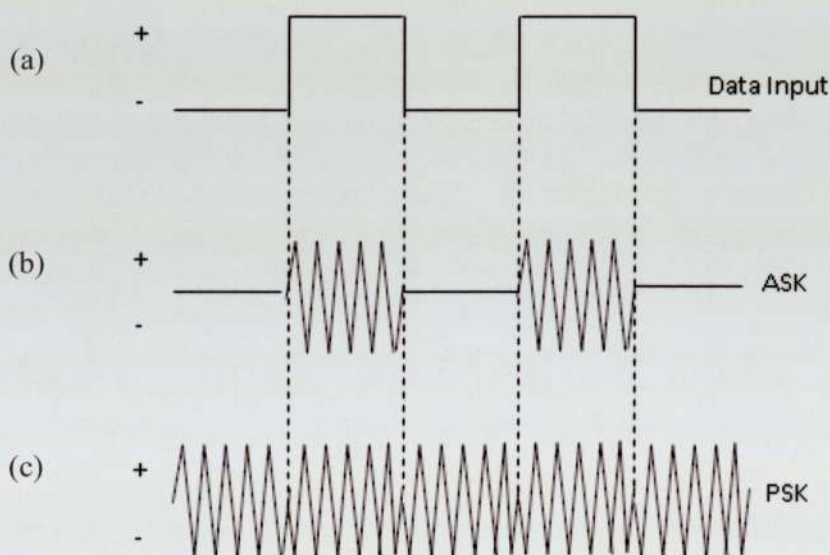


Figure 3.2: The (a) data input and the corresponding modulating formats of (b) amplitude shift keyed and (c) phase shift keyed.

### 3.2.2 Phase-shift Keying

PSK works by modulating the phase of the carrier signal. In PSK a phase is chosen to represent a 0 and another is used to represent 1. When there is a change in the modulated signal as in Figure 3.2(a), this then leads to the shifting of the phase by  $180^\circ$  from its current position to represent a 1 as shown in Figure 3.2(c) and the phase is not changed to represent a 0. To perform this phase shift differential coding is used and this form of modulation transmission is known as Differential Phase Shift Keyed (DPSK) modulation. [15]

### 3.3 Differential Encoding

The signal format of a transmission system may be required, due to transmission constraints or speed of transmission, to be altered from ASK to PSK modulation formats and this can be done and explained by differential encoding. A method for shifting the phase of the modulated transmitted signal is that of differential encoding. As shown in section 2.2.1 a Mach Zender modulator can be used to generate a phase modulated signal and this method can be used in differential encoding.

Transmission Data <sub>+</sub>		1	0	1	1	0	1	0	0	0	1
Encoded Data	1	0	0	1	0	0	1	1	1	1	0
Phase of Data	180	0	0	180	0	0	180	180	180	180	0
Decoded Phase		+	-	+	+	-	+	-	-	-	+
Decoded Data		1	0	1	1	0	1	0	0	0	1

Table 3.1: Encoding and decoding using differential encoding.

The method works by first taking a reference bit of either a zero or a one, (for the example shown in Table 3.1 the reference bit used is a one). This first reference binary bit becomes the first bit of encoded data sequence. Then this first bit of the data encoded sequence is added to the first bit of the transmitted sequence the result of which forms the second bit of the encoded sequence. If the two added bits, the encode and transmitted are the same (both one or both zero) the resulting encoded bit becomes a zero, but if there is a difference between the two bits the encoded bit becomes a one. The second bit of the encoded sequence is then added to the second bit of the transmission data to produce the third bit of the encoded sequence and so on. Table 1 explains how the encoding of the transmitted data works.

The phase of the now encoded data now needs to be decoded. The method used is one similar to that of a Delay Line Interferometer which will be discussed later in the chapter. The encoded data is decoded by taking the phase of the data bit and comparing this with the phase of the data bit that follows. The difference in phase between these two bits is compared, and if there is a change in phase the decoded bit is seen as high (positive) or if there is no change in the phase the decoded bit is seen as low (negative). Once again Table 3.1 show's how this decoding method would work. Differential Encoding can be used as method of demodulation of a DPSK signal.

### **3.3.1 Demodulation**

The transmission of PSK modulation formats means, as stated, that the DPSK format requires demodulation at the receiver. The detection of PSK data can be and is still done by the use of conventional square law detectors, which means the phase information is needed to be demodulated into the amplitude domain.

This demodulation can be achieved by using methods such as coherent detection [16] and bit delay interferometer [17]. These two methods, however, add complexity at the receiver. So the method of using narrowband filtering has been proposed [18] as an alternate

method of demodulation and has in the past been demonstrated at 10 Gb/s for single ended [19] and balanced detection [20]. Also with the correct filtering properties it has been shown a system performance improvement is achievable [21].

### 3.4 Delay Line Interferometer

As stated The Delay Line Interferometer (DLI) is a device commonly used for the demodulation of PSK into the amplitude domain and uses a similar method to that of the differential encoding.

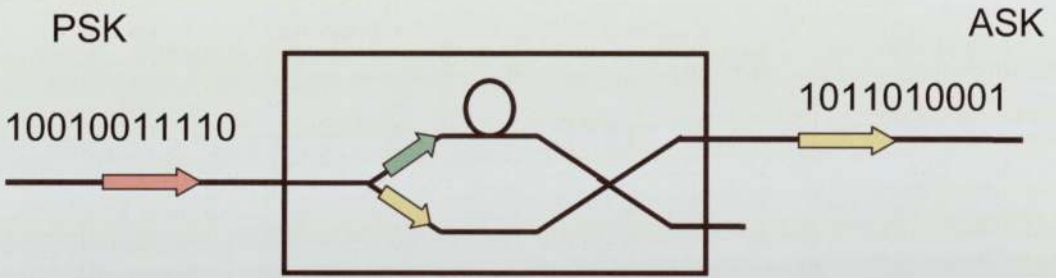


**Figure 3.3: The Delay Line Interferometer with a modulated PSK signal input. One arm introducing a one bit period delay and the combination of the phase difference producing a ASK signal.**

Figure 3.3 shows how a DLI works. An input of the transmitted PSK signal is coupled into the DLI. This signal is then split 50/50 within the DLI and each arm has a copy of the transmitted PSK signal. One of the arms in the DLI subjects the transmitted data to a delay of one bit period. These two signals are then combined together, and there is an interaction between the two different phases of the transmitted signals.

<b>PSK Input</b>	$\pi$	0 + ↓	0 + ↓	$\pi$	0	0	$\pi$	$\pi$	$\pi$	$\pi$	0	
<b>PSK Delay by 1 bit</b>		$\pi$ ↓	0 ↓	0	$\pi$	0	0	$\pi$	$\pi$	$\pi$	$\pi$	0
<b>ASK</b>		$\pi$	0	$\pi$	$\pi$	0	$\pi$	0	0	0	$\pi$	

Table 3.2: The phase combination of the two PSK transmitted data patterns where one pattern is delayed by one bit and the resulting ASK bit pattern generated.

Table 3.2 explains this phase interaction, and as can be seen it is similar to that of the differential encoding, where the combination of the two adjacent phases generate a bit sequence which give either a high or low bit output depending on the phase interaction of the two bits.

Due to the way the phase combination of the PSK data and the PSK data that is delayed by one bit period, the DLI produces two outputs. The one output being the constructive ASK signal and the other being the destructive ASK signal, with the constructive and destructive signals being opposite to each other. In Figure 3.4 the two ASK outputs due to the PSK input can be seen.

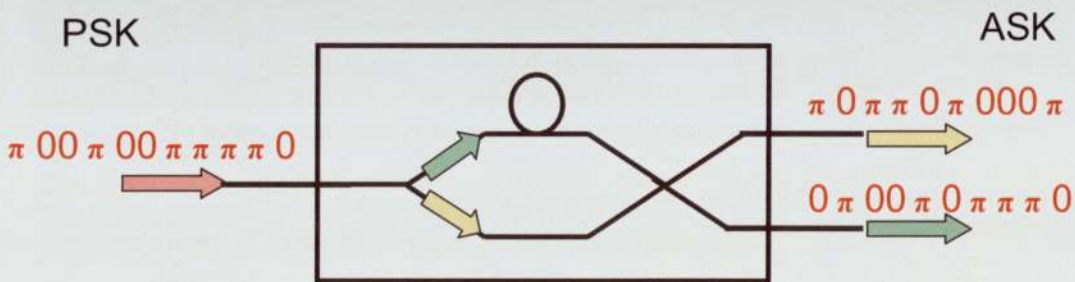
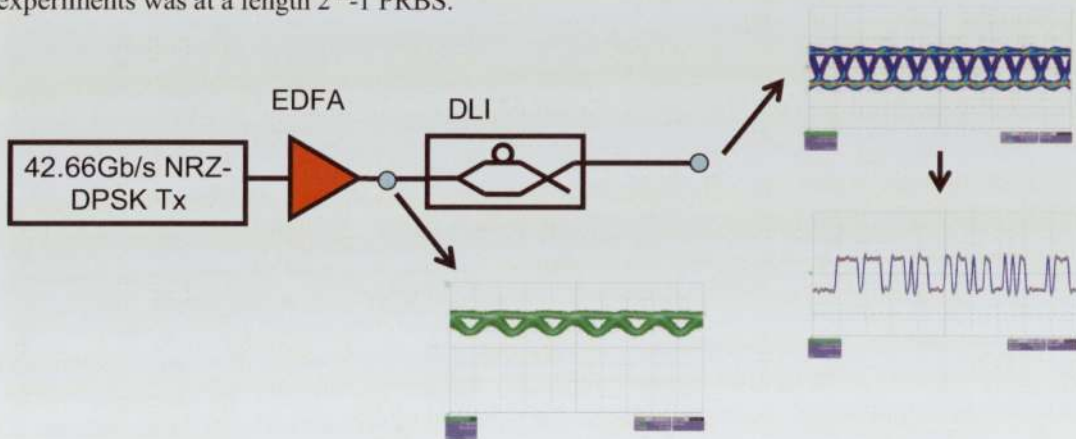


Figure 3.4: The Delay Line Interferometer with a modulated PSK signal input, and the constructive and destructive ASK outputs.

These two outputs of constructive and destructive signals can be combined to improve the received signal. The balanced input of these two signals can improve the receiver sensitivity of the received signal, which improves the total system performance.

### 3.4.1 Delay Line Interferometer experimental results

An experiment was setup to measure the output of a DLI from a resulting NRZ-DPSK transmitted signal input the results taken were then used to provide a measurement baseline for further demodulation experiments. To perform the measurement an external cavity laser was tuned to a wavelength of 1554.62nm and was modulated with the use of a Lithium Niobate Mach-Zehner modulator to produce NRZ-DPSK data. The modulator was biased at the null and was driven with a 2 x Vpi data pattern at 42.66 Gb/s. The data pattern used for this experiment was a pseudo random bit sequence (PRBS) which would mean that there would be no need for any extra additional data pre-coding., and the word length for the experiments was at a length  $2^{31}-1$  PRBS.



**Figure 3.5: DLI with a NRZ-DPSK 42.6 Gb/s data input with eye shown. Output on one arm of the DLI showing the eye and data output.**

The transmitted signal was subjected to a pre-amplification from an Erbium Doped Fibre Amplifier (EDFA) and then connected into the DLI. The signal out of the DLI was then detected by a photo-receiver and the information received was viewed on an oscilloscope. In Figure 3.5 the eye of the DPSK signal that was transmitted was first viewed on the

oscilloscope to give a visual confirmation of the NRZ-DPSK transmission. The diagram also shows the signal that was received after the DLI. From the eye diagrams it can be seen that the information received is that of a ASK signal. The diagram also shows the received data pattern. The data pattern measurement was taken at a pattern length of  $2^7-1$  PRBS this was to allow bit synchronous triggering of the OSA which aided the visual analysis of the transmission.

As previously mentioned the DLI provides constructive and destructive outputs. The results of this were also taken and the data outputs can be seen in Figure 3.6. The outputs for each arm show the constructive and destructive data patterns and they can be seen to be opposite to each other. From either of these outputs the ASK information can be observed.

Knowing how the received signal after a DLI should appear, it can be possible compare other devices and try and find a different method to produce similar results.

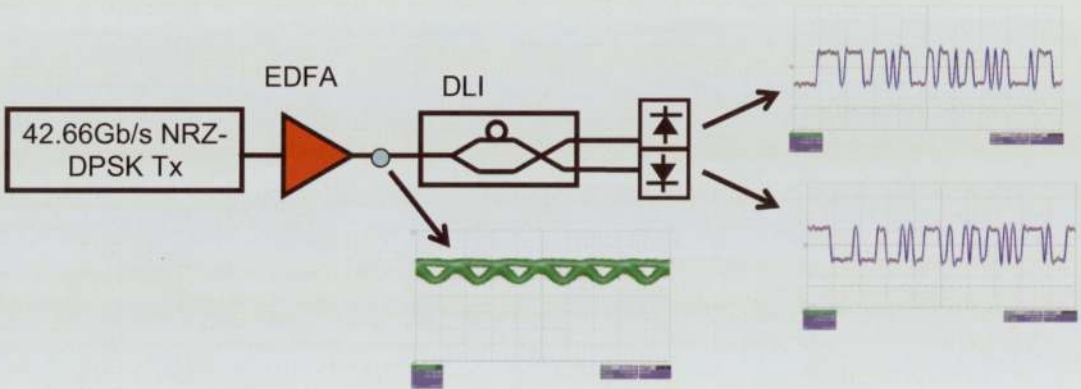


Figure 3.6: The output on both arms of the DLI showing the constructive and destructive data outputs.

### 3.5 DPSK Filter measurements

As stated the use of a filter to demodulate a DPSK signal to ASK can be possible. Previously taken measurements have been done at data rates of 10 Gb/s. The baseline measurements for the DLI were taken at 42.6 Gb/s and so the filter measurements that were taken were taken at this same data rate.

A narrowband filter with a Gaussian profile, which has a bandwidth set at 0.25nm, was used and the transmission setup for the experiment was the same as that for the DLI as

shown in Figure 3.7. A transmission wavelength of 1554.62nm was used and the filter was set to this carrier wavelength.



Figure 3.7: Filter experiment setup.

The data pattern of the receive signal was observed on the OSA. Figure 3.8 (b) shows that when filtering the transmitted signal at the carrier wavelength the data pattern output viewed can be seen to replicate that of the constructive received signal of the DLI.

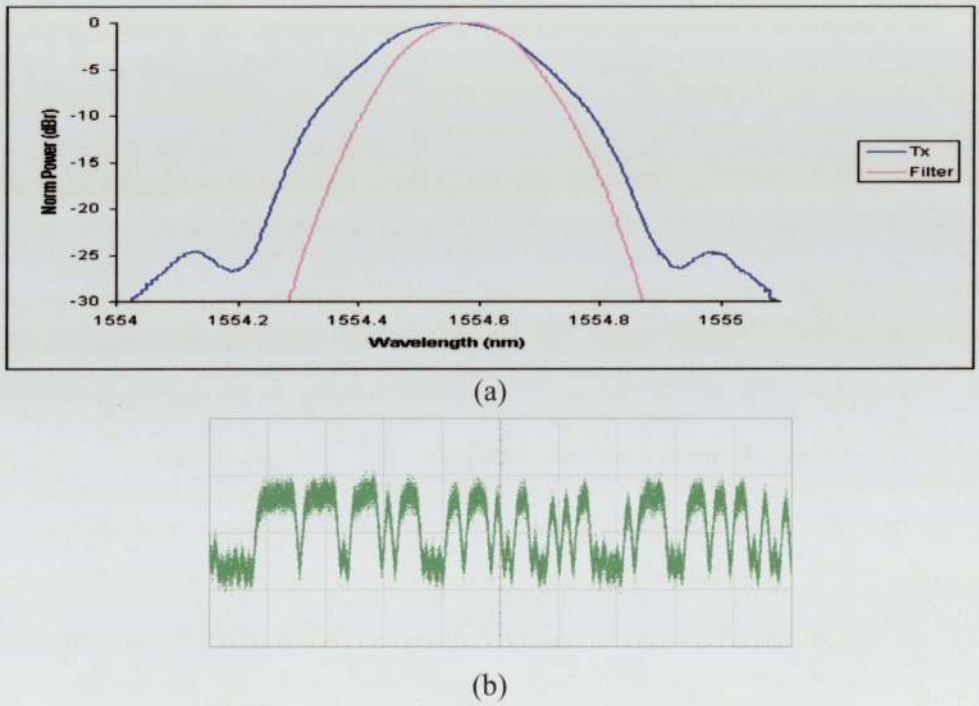
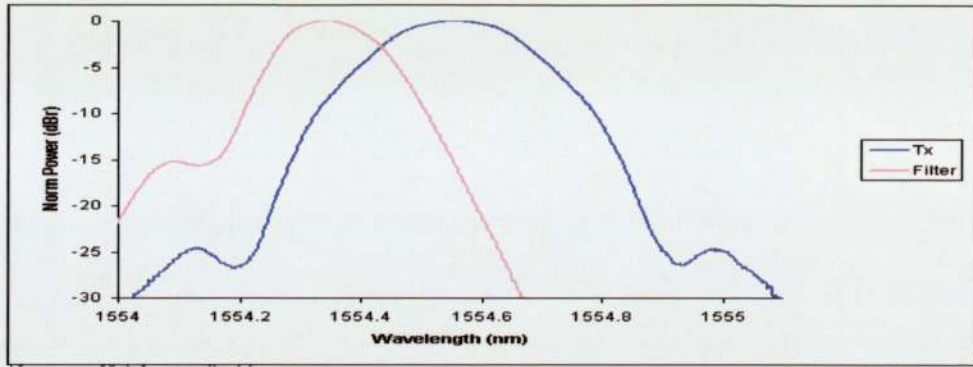
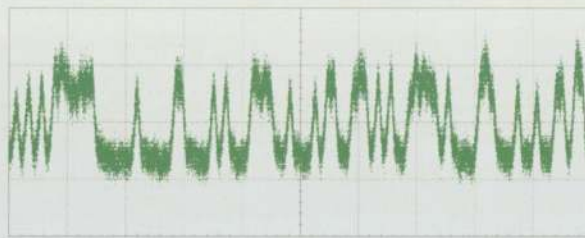


Fig 3.8: The spectrum of the (a) carrier wavelength and filter, with (b) data pattern after the filter.

To measure the effect of the wavelength dependence of the narrowband filter, its wavelength was altered relative to that of carrier wavelength with the resulting data patterns observed. As shown in Figure 3.9 (b) it was possible to obtain a data pattern that was comparable to that of the destructive output of the DLI with a different wavelength.



(a)



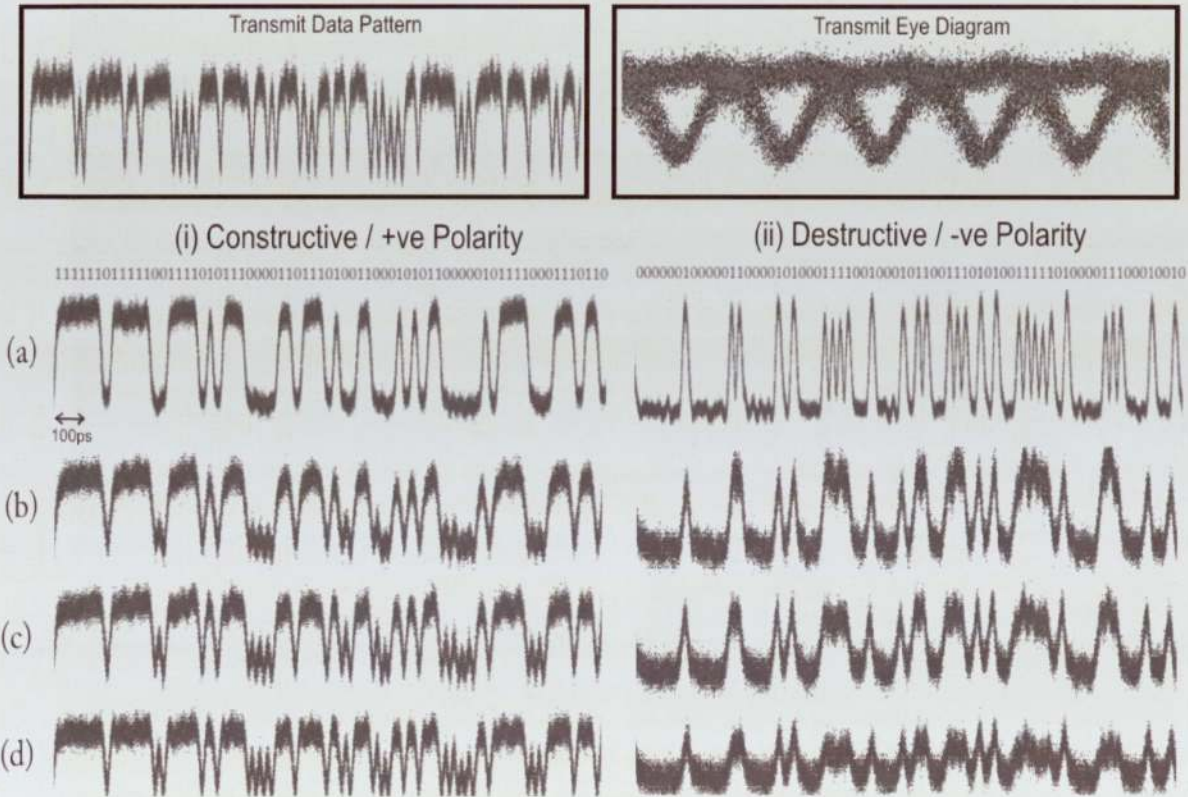
(b)

Fig 3.9: The spectrum of the (a) carrier wavelength and filter, with (b) data pattern after the filter.

Having the filter set at the lower or higher sideband of the carrier wavelength, was when the data pattern appeared to be similar to that of the destructive DLI output. Both sidebands for the transmission produced the same data pattern response. The results show that it is possible with the use of a narrowband filter to perform demodulation for DPSK transmitted data. To demodulate positive polarity data, which is equivalent to the constructive port of the DLI, the filter is aligned with the carrier frequency of the signal, which selects the constant phase part of the signal. When the filter is offset relative to the carrier frequency to the sideband which carries the phase transition information is selected whilst the constant phase carrier is rejected, which in-turn gives the negative polarity data, the equivalent to the destructive port of the DLI. A comparison of the DLI and the bandwidth filter can be seen in Figures 10 (a) and (b).

### 3.6 Delay line Interferometer and Filter Demodulation

The filter bandwidth used for the previous experiments was 0.25nm (31 GHz). An experiment with different bandwidths was performed and the measurements taken. The bandwidth of the filters was increased from 0.25nm to 0.45nm (56 GHz). As can be seen in Figure 3.10, the wider the filter bandwidth the poorer the demodulation performance. The narrowest filter available for the measurements was the 0.25nm bandwidth filter and the results do show that even this filter may have had too large a bandwidth. On the zero rail of the demodulated 0.25nm bandwidth filter received data pattern, the residual intensity transitions can still be seen. These are the artefacts of the phase transitions of the transmitted signal that have not been filtered away fully. These artefacts however are reduced considerably when compared to that of the wider bandwidth filters.



**Figure 3.10:** (a) DLI (i) Constructive port, (ii) Destructive port, (b) 0.25nm filter, (c) 0.35nm filter, (d) 0.45nm filter. For filters column (i) shows filter & carrier frequency aligned, column (ii) show filter offset 42.7GHz from carrier frequency. For reference the binary bit sequences are also shown.

From the resulting data pattern measurements shown in Figure 3.10, it is clear that a DPSK modulated transmitted signal can be demodulated by a narrowband filter to produce similar results to that of a DLI. The filter bandwidth does appear to have an important role to play but the resulting ASK data can be seen to be demodulated correctly.

### 3.7 Filter Receiver Penalty measurements

With a  $2^{31}-1$  PRBS word length, receiver sensitivity measurements were taken to measure the performance of the different bandwidth filters along with the baseline measurements for the DLI. The measurements for the DLI were all done as single ended detection. The experimental results were taken with the use of error analyser to measure the Bit Error Ratio (BER) and a variable optical attenuator (VOA), which was used to alter the power received as shown in the experimental setup in Figure 3.11.

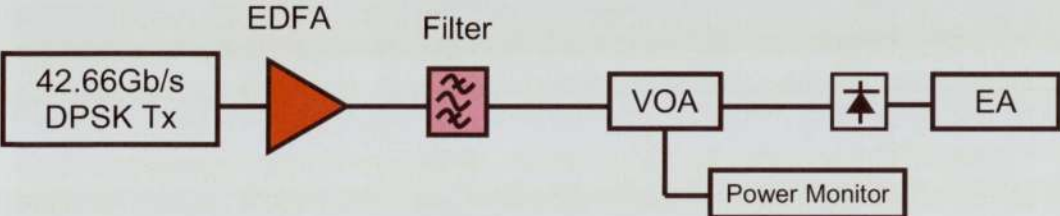
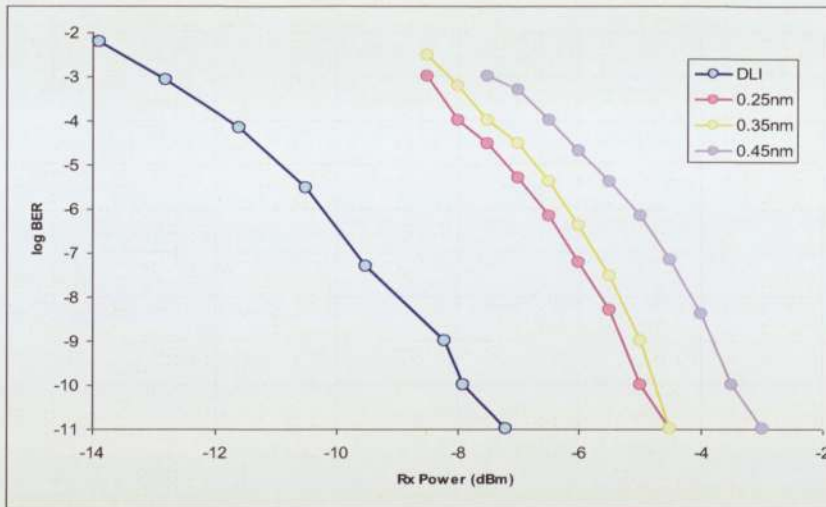


Fig 3.11: The output on both arms of the DLI showing the constructive and destructive data outputs.

By altering the received power the BER was taken and the results are shown in Figure 3.12. The results taken confirm the performance improvement of a narrow filter bandwidth, the narrower the bandwidth the better the performance of the filter. When comparing the filter performance to the DLI however, there is a performance penalty to incur. The best performing filter, the 0.25nm filter, does however have a performance penalty of 2 dB to that of the DLI.



**Figure 3.12: Receiver Sensitivity Measurements.**

This performance penalty could possibly be improved by the introduction of an optimal filter for demodulation. A decreased filter bandwidth is one possible method to improve the performance, but however this decreasing of the filter bandwidth may not improve the penalty performance by a great deal. The results show that reducing the filter bandwidth of 0.1nm, from 0.35nm to 0.25nm only gave a penalty improvement of 0.1 dB. The results shown in figure 12 are taken for perfect wavelength alignment. The interferometer nature of DLI's, mean that any small drift in the free spectral range of the device or any wavelength drift of the source laser could produce a dramatic impact on the device performance.

### 3.7.1 Filter Detuning Measurements

Using the same experiment setup as used for the performance penalty measurements, the transmission wavelength of signal was altered and the power penalty for a BER of  $1 \times 10^{-9}$  was taken for the DLI and each filter. The results taken were plotted and are shown in Figure 3.13.

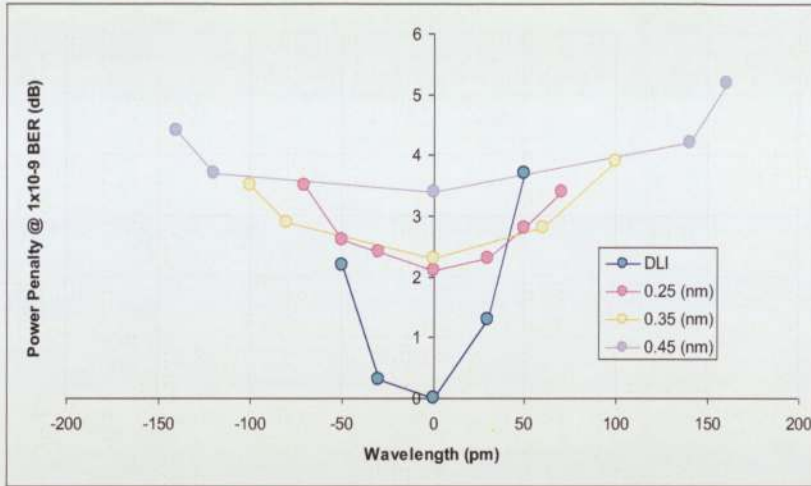


Figure 3.13: Detuning Penalty.

From the results it can be seen that from the shape of the curves is that the tolerance of the narrowband filters is significantly higher than that of the DLI. A steep curve for the DLI results in the device receiving a penalty of 2 dB at +/- 50pm wavelength detuning. The DLI curve cross the filter curves at approximately +/-50pm and it is from this point that that filters outperform the DLI. The curves for the filter results provide a flatter response and the results show that wider the bandwidth the greater the tolerance. It can also be seen that the filter at 0.35nm can provide a broader tolerance curve with a small degradation of 0.1dB compared to that of the 0.25nm filter. It should be noted that these values of wavelength drift are higher than that of a typical wavelength division multiplexer.

### 3.8 Conclusion

From the results it has been shown that narrowband optical filtering can be used for the demodulation of 42.66 Gb/s phase shift keyed data and can perform as well as a Delay Line Interferometer. The DLI does provide a better performance penalty measurement compared to the filters but the filter technique does outperform the DLI when transmission system is subjected to a wavelength drift of +/- 50pm.

When transmitting a 42.66 Gb/s NRZ-DPSK, the best performance filter demodulation was that of the 0.25nm filter bandwidth. As already stated this filter bandwidth

could be further reduced to improve the penalty performance, but from the results taken the penalty performance may not receive any significance improvement.

Increasing the bandwidth of the filter from 0.25nm up to 0.35nm can give a significant improvement to the tolerance of wavelength drift with very little penalty.

The filter bandwidths used in these experiments, as well as the Gaussian passband shapes used for the 42.6 Gb/s demodulation are similar to those that installed in 10 Gb/s wavelength de-multiplexers. This means that this technique of demodulation can be used on transmission system already in use. The method of DPSK demodulation by filter can remove the need for the DLI, which is a device that is wavelength sensitive and any drift that occurs may reduce the demodulation performance.

## Chapter 4

# Optical Tuneable Dispersion Compensator

### 4.1 Introduction

The distance a signal can be transmitted through optical fibre is controlled by the amount of loss that the signal has during transmission and the effect chromatic dispersion has upon that signal. When loss over a distance is needed to be compensated in a transmission system, as stated in section 2.7 optical amplifiers can be use to boost the transmitted signal. For systems that are running at 2.5 Gb/s, this is where loss is the limitation that dominates. Chromatic dispersion becomes the major limitation at greater data rates. [22]

### 4.2 Chromatic Dispersion and Group Delay

Chromatic dispersion is the variation in the velocity of light according to wavelength, and due to this variation, the pulses of a modulated light source are caused to broaden when travelling through a fibre, which then increases the bit error rate. As mentioned in section 2.4, when looking at chromatic dispersion the main concept to consider is that of optical phase. Optical phase gives a mathematical relationship between group delay and chromatic dispersion. Group delay is defined as the first derivative of optical phase and chromatic dispersion the second derivative of optical phase with respect to optical frequency [23]. These quantities are represented as:

$$\text{Group Delay} = \frac{\delta\Phi}{\delta\omega}$$

$$\text{Chromatic Dispersion} = \frac{\delta^2\Phi}{\delta\omega^2}$$

$\Phi$  = Phase

$\omega$  = Wavelength

These two phenomena occur because all optical signals have a finite spectral width, and different spectral components will propagate at different speeds along the length of the fibre. One cause of this velocity difference is that the index refraction of the fibre core is

different for different wavelengths. This is called material dispersion and is the main cause of chromatic dispersion.

#### 4.2.1 Dispersion techniques

With more work being done at greater transmission rates solutions to manage the dispersion prior to regeneration of the transmitted signal are now in demand. The method that has been used to compensate for chromatic dispersion has been historically the use of Dispersion Compensating Fibre (DCF), where DCF is a fibre that has been specifically designed to disperse the propagating light in the opposite direction to that of the dispersive effect within the transmission fibre. This means the broadening effects that have occurred during the transmission are re-shaped and the transmission can be recovered.

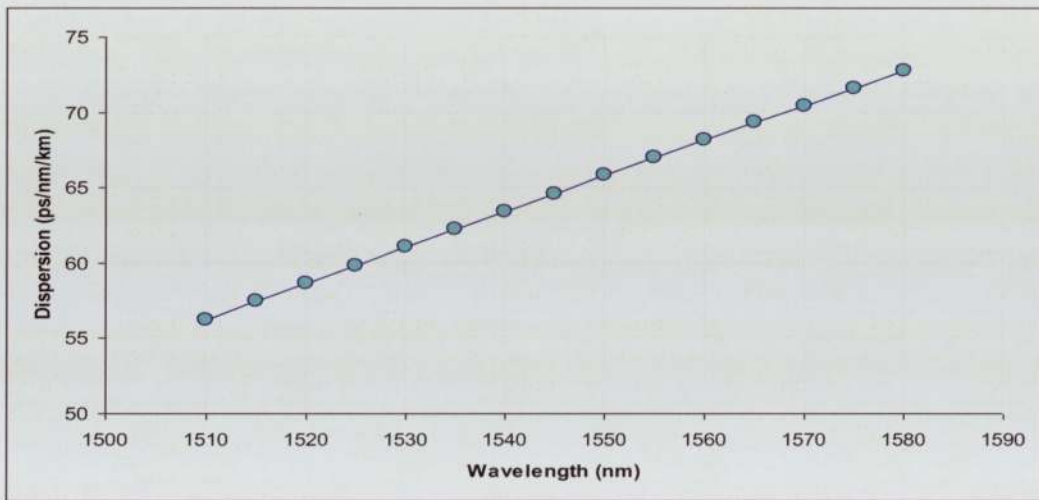


Figure 4.1: Dispersion in SMF.

If we look at a trace of the dispersion slope of 80km of single mode fibre (SMF), with the transmission across the c-band, as shown in Figure 4.1 it can be seen the dispersion increases in a linear fashion as there is an increases in wavelength. This means that the DCF is required to be designed and be able to compensate for this chromatic dispersion and will need to have an opposite dispersion slope.

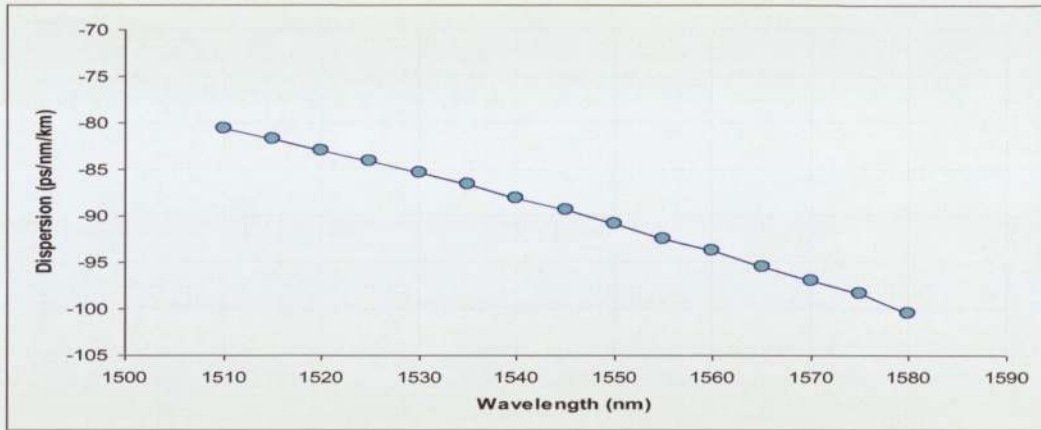


Figure 4.2: Dispersion in DCF.

Looking at the trace in Figure 4.2 which shows the dispersion slope for DCF designed to compensate for 80km of SMF, it can be seen that the slope is indeed opposite to that of the SMF.

In transmission spans these two forms of fibre are coupled together and a dispersion map is generated and as shown in Figure 4.3, the amount of dispersion at any given transmission wavelength can be found. The ideal solution from the combination of the SMF and DCF would be the removal all of the dispersion effects upon the transmitted signal at the required wavelength.

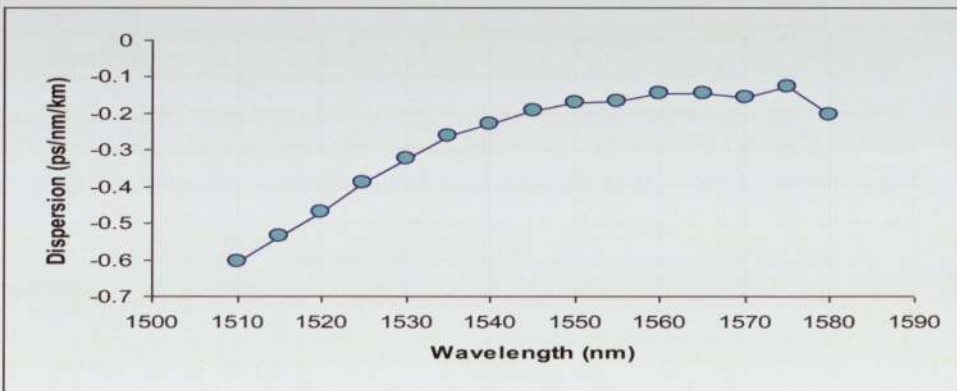


Figure 4.3: Combination of SMF and DCF.

From Figure 4.3 it can be seen that there is a limit for the DCF due to the slope matching between the two types of fibre. The DCF's ability to compensate for different

channels at different wavelengths is poor. The channels at either end of the band have larger levels of residual dispersion meaning that extra pre or post dispersion compensation will be required. This however is an impractical solution due to the amount of reels of fibre that would be required at each node for each channel at custom made lengths, which is an economically poor solution.

The solution for the problem has been the introduction of Tuneable Dispersion Compensators (TDCs). TDCs are becoming more and more inevitable as the data rates increase on fibre-optic transmission systems.

### **4.3 Tuneable Dispersion Compensators**

TDCs are now become important components of long haul transmission setups. They are beginning to be used in the transmission span as well as being used in tandem with the DCF to compensate for residual dispersion that occurs after the DCF, which in a sense is giving the dispersion compensation of the DCF a tweak. There are now also tighter tolerance levels of dispersion for networks running at 40 Gb/s and above.

TDCs also give the advantage of the dynamic way of how they function. The dispersion that the TDC can compensate and therefore control can be altered to suit any change that may occur to the transmitted signal. Even if this change be due to a change in the distance that the signal is transmitted over due to reroute or any external effects such as temperature or bending.

There have been several different solutions introduced as TDCs these include chirped fibre Bragg gratings [24] which can be tuned by either strain or temperature. Also there are virtually image phased arrays [25] and multi cavity etalons [26]. The chirped fibre Bragg grating has the advantage of having low loss and is fully compatible with optical connectors but the main advantage would be for a device that reduces the group delay ripple and supply multi-channel compensation. These advantages are available with the use of thin film Gires-Tournois etalons (GTE) [27] but they suffer from high insertion loss. It was reported in [28] about the fabrication and the demonstration of two in-fibre distributed Gires-Tournois etalons

(DGTEs) used for dispersion compensation. This device was then increased to a three DGTE structure [29] and the results published.

Using, this three DGTE TDC, further investigations were carried out to find further improvements for the device.

#### **4.3.1 Three Distributed Gires-Tournois Etalon TDC**

The configuration of the three Distributed Gires-Tournois Etalons (DGTEs) can be seen in Figure 4.4. The DGTEs were written using a frequency doubled argon ion laser (244nm) together with a chirped phase mask. Each DGTE was formed with two overlapping chirped fibre Bragg gratings of the same chirp rate but of different strength as explained in [28]. The dispersion of the TDC is determined by the shape of the combined group delay (GD) and different dispersion settings. This is achieved by properly arranging the relative wavelength positions of the group delay peaks of the three DGTEs. [29] The alteration of these three wave peaks is performed by altering the temperature across the DGTEs and this control of temperature is performed by altering current settings of thermoelectric coolers (TECs), which are connected to the DGTEs. The three DGTEs all have a group delay response at the same oscillation period but they all have different amplitudes, due to the different reflectivities of the three gratings. It's the combination of these three different group delay responses that determine the level of dispersion compensation gained. So, ultimately it's this alteration to the TECs, that in-turn alters the level of dispersion compensation produced by the device.

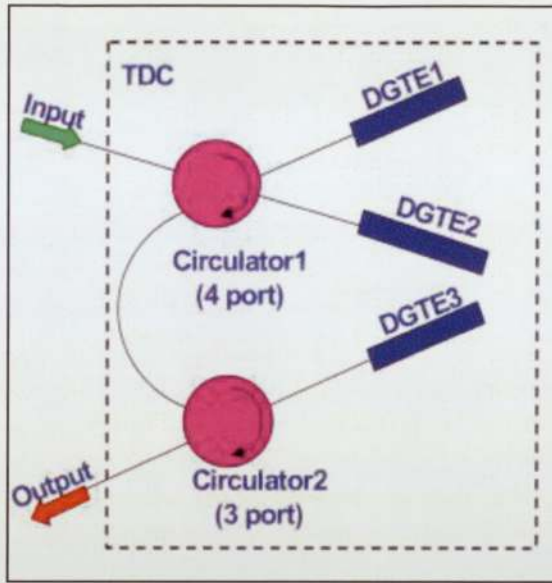


Figure 4.4: The configuration of the TDC based upon three DGTEs. [28]

#### 4.4 TDC experimental Setup.

Previous results showed that the three DGTE could perform over a dispersion tuning range of  $\pm 500$ ps/nm over a usable bandwidth of 20 GHz [29]. It was decided that further experimentation was to be performed on the device to see if the capabilities of the device could be improved.

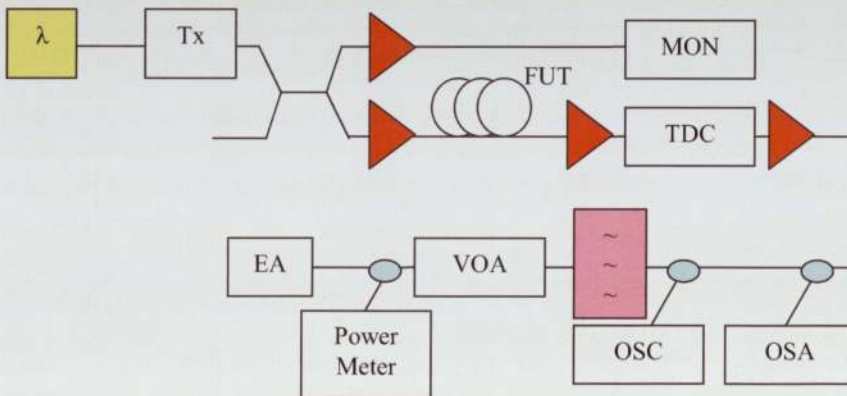


Figure 4.5: The configuration for the experimental results.

From the experimental setup in Figure 4.5 it can be seen that a light source at a wavelength from the ITU grid, in this case 1554.54nm, was modulated with a word length of  $2^{31}-1$  by a

transmitter (Tx) and connected to a 3dB coupler. From one arm of the coupler the transmitted eye of the signal was monitored (MON) to ensure that the transmission remained stable. From the other arm of the coupler the signal was amplified onto the fibre under test (FUT). Amplifiers were introduced into the experimental setup to compensate for losses that may occur due to the length of fibres used. In this setup a pre-amp and booster were introduced which is also typical of a transmission system.

Different lengths of fibre which have different levels of dispersion were placed as the FUT and it was after the FUT that the TDC was placed to compensate for these different levels of dispersion. The output signal from the TDC was then monitored on an optical spectrum analyzer (OSA), an oscilloscope (OSC) and there was also an error-analyzer (EA) to ensure that the signal was that of an error free one.

The measure of the positive and negative dispersion abilities of the TDC for the FUT in the experiment was performed with different lengths of fibre for both SMF and DCF.

**4.4.1 Transmission Measurements**

The length of the fibre was altered until the fibre length reached was considered the optimum for an error-free signal. This was decided by the state of the received eye at the OSC compared to the transmitted eye at the MON; this was also backed up by the bit error measurement at the EA. The resulting TEC settings were then noted, and then the individual TECs were altered and any performance improvements recorded.

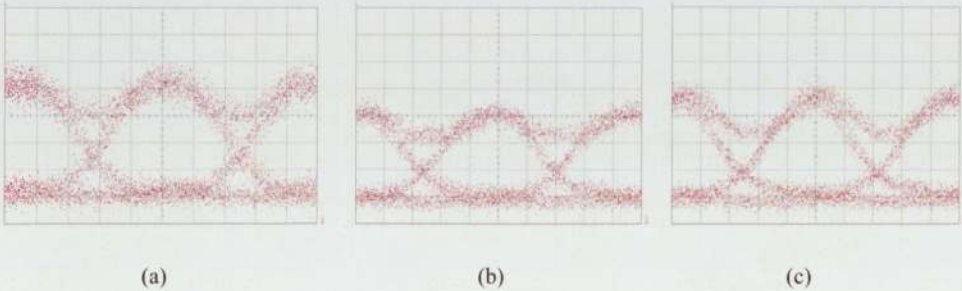


Figure 4. 6: Transmitted eye (a) and the received eyes for 80km SMF (b) and 60km DCF (c).

From the eye diagrams in figure 4.6 it can be seen that the TDC could compensate SMF and DCF fibre for, was 80km and 60km respectively. The dispersion for each fibre is approximately 17.5 ps/nm/km, which means that the TDC compensated for 1400ps/nm, which was the dispersion generated by the SMF and -1050ps/nm the dispersion generated by the DCF.

[These results gained showed that the TDC can compensate for dispersion levels of +1400ps/nm and -1050ps/nm, which is a greater level of dispersion compensation than of the previous thought level of +/-500ps/nm.]

The previous TEC settings were:

For the +500ps/nm: -	Tec1 42.7°C	and -500ps/nm: -	Tec1 23.4°C
	Tec2 36.4°C		Tec2 10.0°C
	Tec3 40.8°C		Tec3 44.3°C

Table 4.1: Previous TEC settings.

Taking a look at the TEC settings for the dispersion levels now, with have:

For +1440ps/nm: -	Tec1 14.0°C	and -1050ps/nm: -	Tec1 18.0°C
	Tec2 14.0°C		Tec2 48.7°C
	Tec3 42.3°C		Tec3 45.9°C

Table 4.2: New TEC settings.

From the TEC settings shown above there is no obvious coloration between the change in temperature for each DGTE and the performance of the TDC. It does show that a manipulation of the temperature across the DGTEs can in-turn alter the combination of all three group delays in such a way that the higher levels of dispersion compensation is achievable.

The TDC showed that it can compensate for dispersion for a wavelength that is on the ITU grid. The performance of the TDC off the ITU grid was also measured to observe any possible effects due to an alteration in wavelengths.

#### 4.4.2 Change in Transmission Wavelengths

Performing the same experiment as previous and having 60km DCF placed as the FUT the wavelength of the transmitted signal was altered to a position that was in-between two ITU grid channels at 1554.74nm.

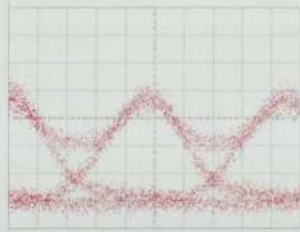


Figure 4.7: Received eye after 60km DCF at 1554.74nm

The resulting measurements from the transmitted experiment show that it was still possible for the TDC to completely compensate for the dispersion generated through the 60km of DCF fibre even at a different wavelength. The eye from the experiment is shown in Figure 4.7. It has to be noted that the TEC settings were altered slightly to gain an error-free received signal.

A second measurement at a wavelength of 1554.22nm, which is just offset from an ITU channel by 0.2nm was also performed and again from this resulting eye capture shown in Figure 4.8 it can be seen that the TDC can compensate for the dispersion at this given wavelength.

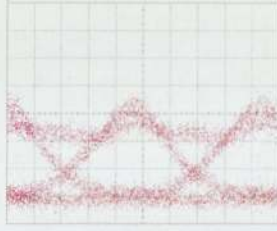


Figure 4.8: Received eye after 60km DCF at 1554.22nm

From the dispersion compensation achieved by the TDC at these three different wavelengths it has shown that the TDC can compensate for any given wavelength by altering the temperature across the DGTEs by the TECs.

#### 4.4.3 TDC Wavelength Sweep Measurements

From the previous experiments it was found that an alteration of transmission wavelength would mean that for the TDC to compensate, the temperature levels across the DGTEs also needed to be altered. Knowing that the TDC could compensate dispersion at one wavelength for certain TEC settings, a sweep of different wavelengths could be performed to see if it was possible for the TDC to compensate for dispersion at different wavelengths but with fixed TEC settings.

Using the same experimental setup as previous, and setting the TECs to compensate for 60km DCF at a wavelength of 1554.54nm, the transmission wavelength was swept from 1554.14nm to 1556.94nm a total bandwidth of 350GHz.

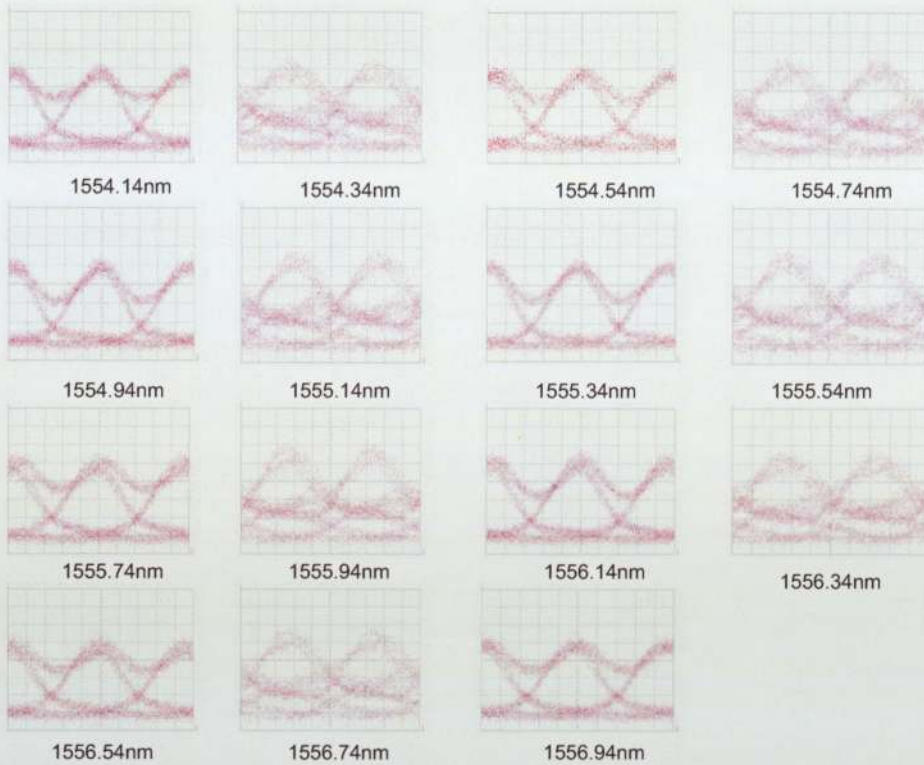


Figure 4.9: Received eyes after 60km DCF

As can be seen from the results in Figure 4.9 the TDC compensates for different wavelengths while the TEC levels are fixed. The results shown are at 25GHz steps and from the gained eye patterns it can be noted that a pattern is clear to see. A good eye can be clearly seen at every 0.4nm or 50GHz step. This shows that the TDC has a periodic response. The wavelengths that the TDC has compensated are all on the ITU grid.

A larger range of measurements were then performed to ensure that this effect is noticeable at a greater range of wavelengths. So with the TDC again compensating for 60km DCF and the TEC settings fixed, the wavelength sweep was increased to a bandwidth of 2200GHz at 1534.94nm to 1556.14nm.

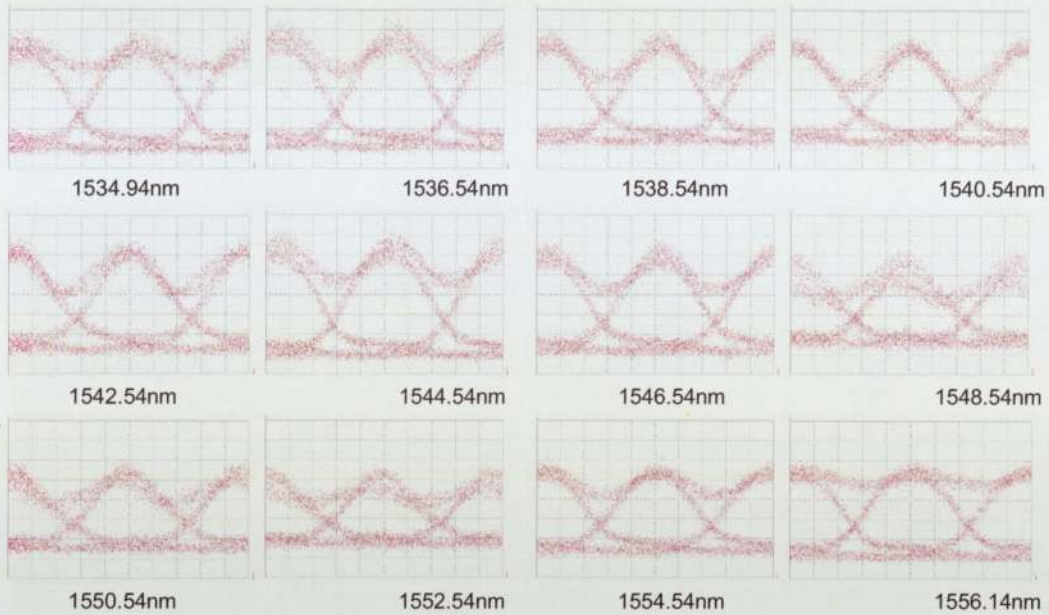


Figure 4.10: Received eyes after 60km DCF

The eye diagrams in Figure 4.10 show the wave sweep measurements across the wider bandwidth with the each eye captured at 2nm (250GHz) steps. The results show that the periodic response still occurs across a wider bandwidth.

The TDC does show that it has the ability to compensate for the dispersion generated by the fibre over a wide range of wavelengths. The next step was to measure the bandwidth tolerance of the TDC. This measurement can be done, by once again sweeping the transmission wavelength but this time by altering the wavelength by smaller steps and once again looking at the eye diagrams produced. Using the 60km DCF as the FUT and altering the wavelength of the transmission wavelength by 0.01nm around a central wavelength of 1554.74nm, the received eyes for each wavelength was monitored and as shown in figure 4.11 the following results captured.

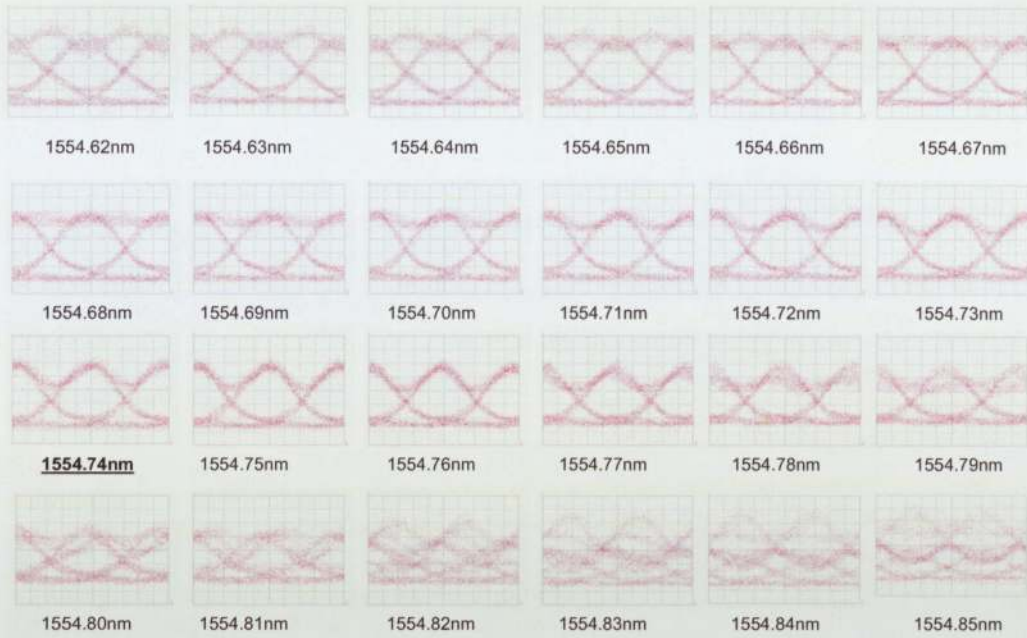


Figure 4.11: Received eyes after 60km DCF

From measurements the bandwidth of the TDC can be easily made out. From the central wavelength of 1554.74nm there is a good eye response from wavelengths 1554.701nm to 1554.78nm, which gives the TDC a total bandwidth of 0.08nm / 10GHz.

#### 4.4.4 TDC Signal Sensitivity

The tolerance of the device to any wavelength drift is important. The previous set of results provided us with a known bandwidth for the device and it's the BER within this bandwidth that was measured. The BER of a transmitted signal is an important baseline measurement of any transmission system. It is possible with forward error correction (FEC) coding to recover a signal that has a BER better than  $1 \times 10^{-3}$ , so each transmission system is designed to have a BER equal to or better than this level.

Another important consideration of a transmission system is the optical signal to noise level (OSNR). The size of an OSNR can determine the performance of all transmission systems with the component with the lowest tolerance to OSNR being the controlling factor.

Using the same system setup used for the previous measurements a controlled noise floor was injected into the system after the TDC as shown in Figure 4.12.

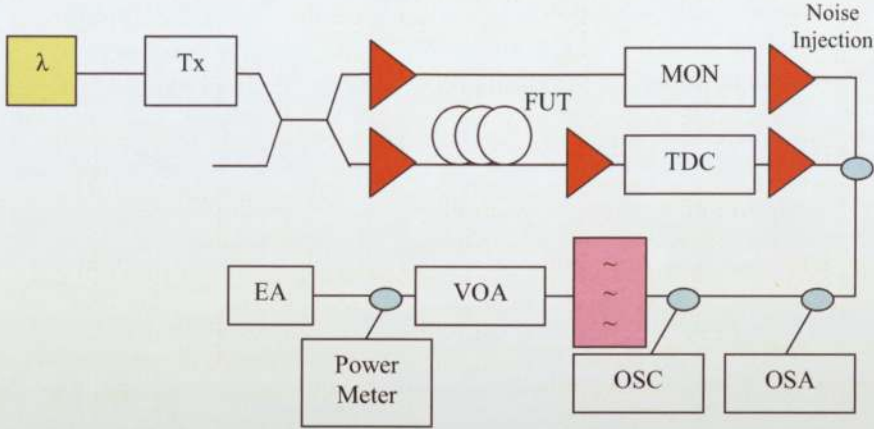


Figure 4.12: Circuit diagram with noise floor injected

Using again the 60km DCF and setting a noise floor to 17.dB sensitivity measurements were taken. The first sensitivity measurements taken were done by fixing the received power, by the use of the VOA to -9dBm. A sweep the different transmitted wavelengths about a central wavelength of 1554.74nm were performed and the BER on the EA recorded.

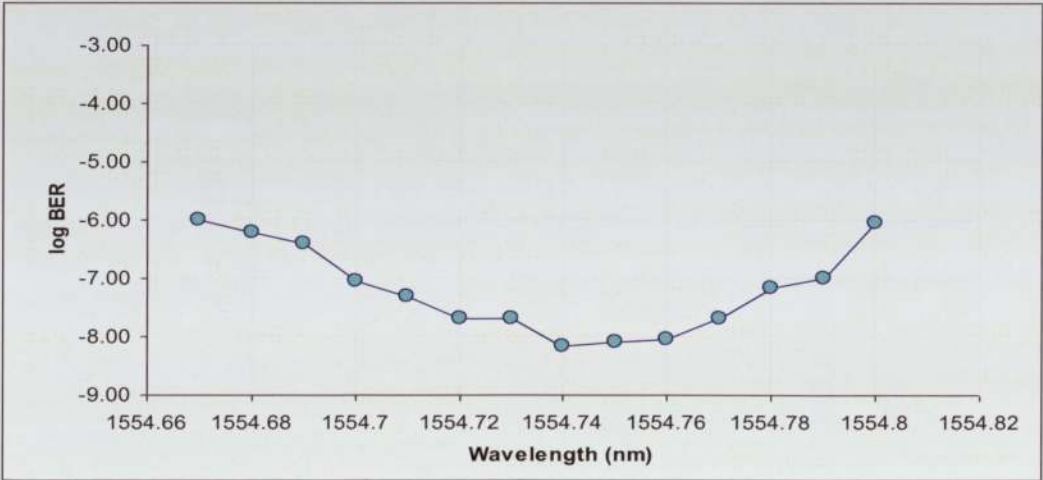


Figure 4.13: Sensitivity measurements

The results in Figure 4.13 show the possible bandwidth of the TDC. It can be seen from the bathtub shape that between the wavelengths of 1554.60nm to 1554.78nm there is a change in the bit rate of 1 and taking this as our bandwidth, we have of 0.08nm / 10GHz about the

central wavelength. When the wave is stepped away from this wavelength errors begin to appear on the received signal.

This next procedure was to measure the sensitivity due to the change in received power. This was by performed altering the received power with the use of the VOA in the system and measuring the BER from the received signal on the EA. The measurement was at first taken at a central wavelength of 1554.74nm this wavelength was then again altered to wavelengths above and below this to measure any positive or negative differences that may occur due to an alternate wavelength.

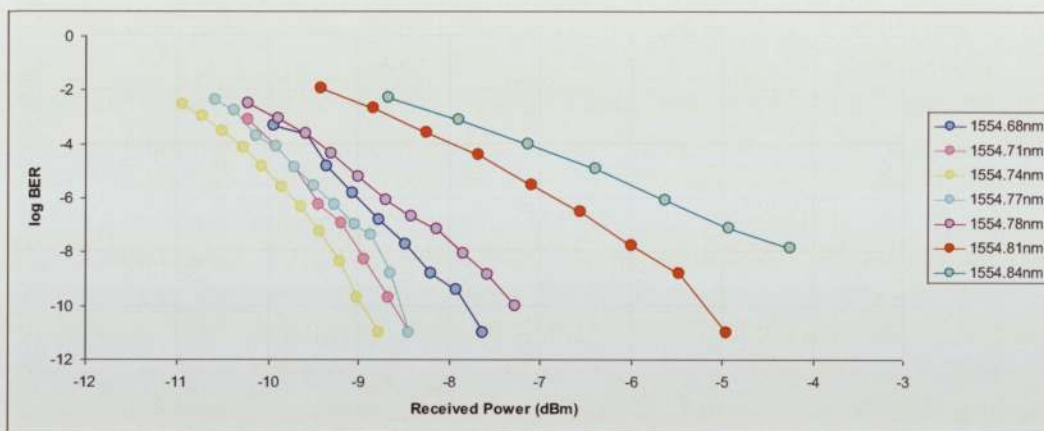


Figure 4.14: Sensitivity measurements

As can be seen in Figure 4.14 the results show that at the optimum wavelength provides the best sensitivity as expected. However wavelengths still within the bandwidth of the device still provide a reasonable response. As the wavelengths are altered and moved further away from the central wavelength the sensitivity of the system becomes worst.

#### 4.4.5 TDC Profile

From the measured and recorded eye diagrams taken in section 3.3.2, it can clearly be seen that the TDC has a periodic response. To confirm this, the profile of the TDC was measured. This was done by measuring the resulting group delay from the device compensating for 60km DCF on dispersion measuring equipment.

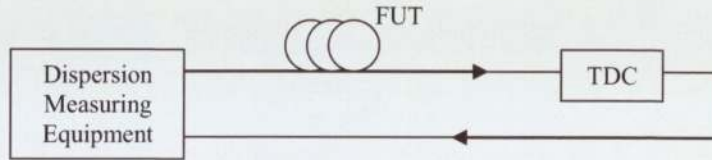


Figure 4.15: Group delay TDC measurement setup.

The measurement is taken by a light source from the dispersion measurement equipment that sweeps through different wavelengths. These wavelengths are then transmitted through the FUT and then into the TDC, which is setup to compensate for the FUT at different wavelengths of 1554.22nm, 1554.54nm and 1554.74nm. The signal from the TDC is then coupled back into the dispersion measurement equipment which then calculates the group delay.

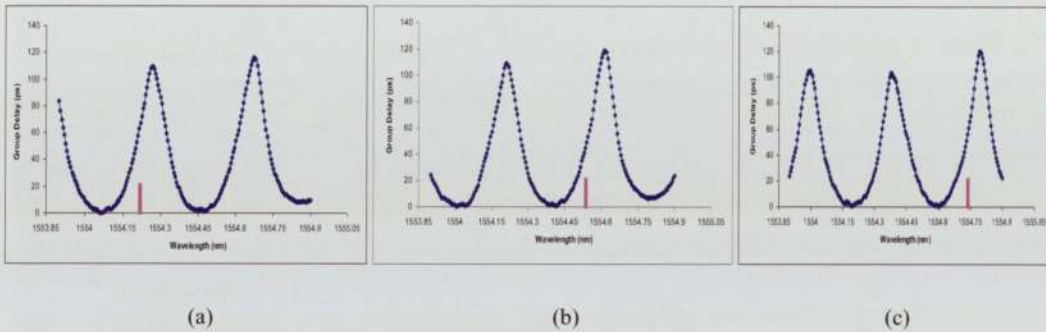


Figure 4.16: TDC Group Delay profile of device compensating for 60km DCF @ 1554.22nm (a), 1554.54nm (b) and 1554.74nm.

From the profiles in Figure 4.16 the group delay measurements for the TDC the periodic nature of the results can be seen. The pink marker represents the transmitted wavelength the TDC is compensating for. What can also be seen from figure 16 (a) to (c) is the shift of the group delay due to the change in TEC settings, this is the collective response of the three DGTEs when the temperature across them is altered. From the group delay measurements it is possible to produce the dispersion profile of the TDC. As can be seen in Figure 4.17 the dispersion maps produced show the periodic nature of the TDC again. The yellow line on the graphs represents the amount of dispersion that the TDC is compensating for, with again the

pink markers being the wavelength that the TDC is compensating for. As shown the peak of the dispersion compensation is at the wavelength that the device is set to compensate for.

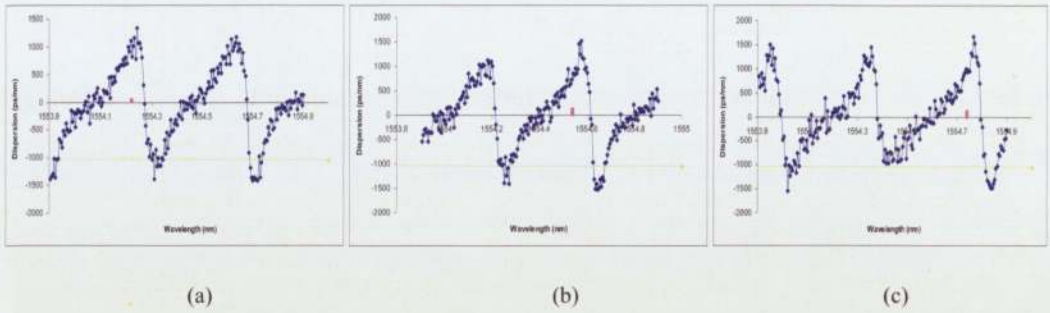


Figure 4.17: TDC dispersion profile of device compensating for 60km DCF @ 1554.22nm (a), 1554.54nm (b) and 1554.74nm.

### 4.5 DPSK compensation

As mentioned in chapter 3, with data rates increasing there is becoming a switch towards different types of data format transmission with DPSK being the most popular. The transmission results with the TDC have so far been done at the modulated format of ASK, so to ensure that the device has the ability to perform with DPSK modulated data, measurements were done and the eye diagrams of the performance recorded.

Using the same experimental setup used with the ASK modulated format in Figure 5, the DPSK data was transmitted. The transmission was again performed at 10.66 GB/s but with 52km SMF and the TDC compensating at 1554.54nm. As can be seen in Figure 4.18 the eye of the received signal is fully recovered.

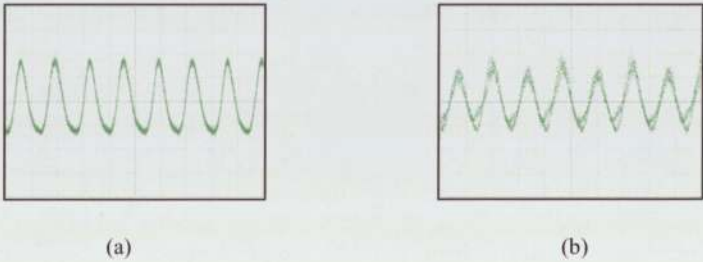


Figure 4.18: DPSK eyes, input (a) and output (b) @ 1554.54nm.

This measurement was performed again at a different wavelength on the ITU grid with the TDC setting fixed and as can be seen with the eye diagrams in Figure 4.19 the signal is again fully recovered and the periodic response can again be seen.

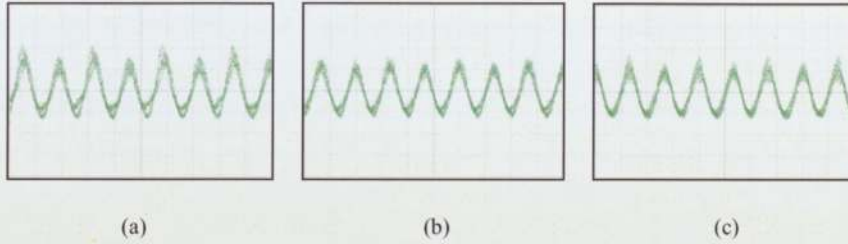


Figure 4.19: DPSK outputs for 1554.13nm (a), 1554.94nm (b) and 1555.34nm.

#### 4.5.1 Multiplexed DPSK

All transmission experiments that have been performed on the TDC have so far been with a single transmitted signal. In a normal transmission system of course, the signals are transmitted on multi-channel systems. For the TDC to become apart of any transmission system it would need to perform with multiple signals being transmitted through it. The device has already shown with its periodic nature that it has the capability to compensate at more than one wavelength at 50GHz spacing. But to ensure that there would be no interference form one channel to another is also a consideration that is required.

To measure this, four channels with 50GHz spacing on the ITU grid were multiplexed together with each wavelength in-turn filtered off and the received eye observed. The transmission setup is shown in Figure 4.20.

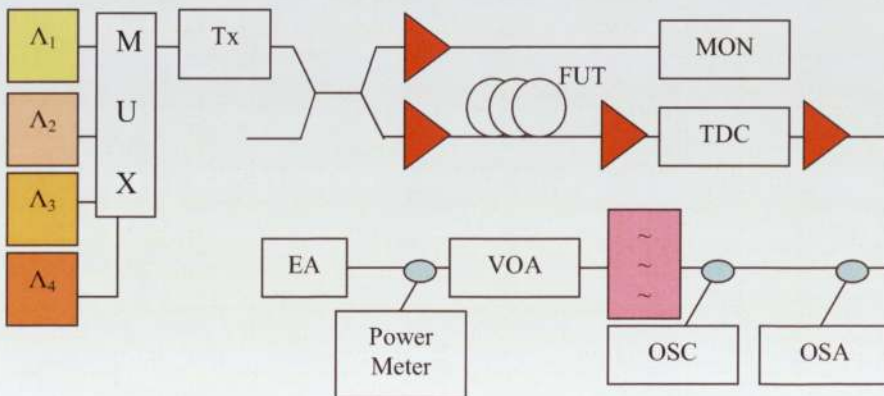


Figure 4.20: Multi-channel transmission setup with DPSK data.

With all channels being transmitted the recovered eyes for each transmission can be seen in Figure 4.21. What can be noted from this is that each eye is fully recovered showing that there is no interference between each channel through the TDC.

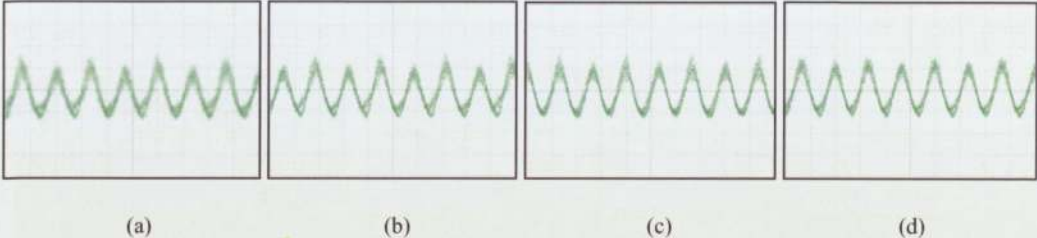


Figure 4.21: The DPSK multiplexed received eyes @ 1554.13nm (a), 1554.54nm (b), 1554.94nm (c) and 1555.34nm.

Further measurements were taken with a DPSK modulated signal with the spacing between the transmitted signals reduced. With the TDC compensating for a transmitted wavelength of 1554.54nm, this was multiplexed together with firstly a wavelength of 1554.22nm which gives 0.3nm / 37.5GHz spacing and then a wavelength of 1554.74nm, a spacing of 0.2nm / 25GHz.

In Figure 4.22 we have the eyes that are been looked at for wavelength 1554.54nm. The resulting eyes in Figure 22 are a combination of the two signals that are spaced by 37.5GHz, where there appears to be no effect to the received signal, but with the combination of the two transmitted signals spaced by 25GHz the recovered signal can be seen to be affected.



Figure 4.22: 1554.54nm output wavelength DPSK eyes for the combination of wavelengths of 1554.54nm and 1554.22nm (a) and 1554.54nm and 1554.74nm (b).

#### **4.6 Adaptive control**

The control of the temperature on the gratings which in turn controls how the TDC compensates for dispersion was all done through a computer program. The information feed back to the computer informed the user of the temperature level of each grating, also on a different point of measurement the information of dispersion level was also read. Taking these two points of information it could be possible to set the TDC up so it could perform its only dispersion recover.

A program was setup to read the dispersion level of the incoming transmitted signal, this information was then relayed back to the TDC. With this information the TDC was programmed to alter the temperature levels on the gratings, while always monitoring the dispersion level at the receiver. By doing this the TDC was able to self compensate for the dispersion. The advantage of this in the real world is that the TDC could be in place at the end of a transmission span and if any drift occurred the TDC could automatically reconfigure the dispersive effects.

#### **4.7 Conclusions**

The ability to compensate for dispersion in a more dynamic way than just the use of dispersion compensating fibre has been shown. The tuneable dispersion compensator has shown that it is a versatile, adaptive and with its all-fibre architecture a device which can prove to be a valuable part of any transmission system.

The device compensated for dispersion levels greater than previously thought, which gives the device greater scope for use. The device also has shown that due to its periodic nature it has the ability to compensate for wavelengths that are equally spaced by multiple of 50GHz. The results taken in these experiments were taken at 50GHz spaced channels which show that the device would fit perfectly with the spacing of the channels on real-world

transmission configurations. This transmission experiments also showed that the transmitted signals do not have to be on an ITU channel. But if the transmission is performed off the ITU grid, all channels will still require 50GHz spacing but it does mean that all wavelengths in the c-band can be compensated for.

Also there is no effect to the TDCs dispersion compensation when switching from ASK to DPSK transmission formats and with more transmission systems using DPSK the devices ability to diversify can only be an advantage.

The levels of compensation from the TDC are not at levels required for long-haul compensation but the device is very suitable for the compensation of signals that are required to be remotely switched on wave division multiplexers. When the signal is switched at the wavelength layer, such as in setups like the ROADM, the slight change in dispersion can be compensated by this TDC.

## Chapter 5

# Ultra-long Raman Laser Transmission

### 5.1 Introduction

It has been shown from previous work that with the use of an advanced second order Raman pumping scheme it is possible to generate quasi-lossless conditions whereby an optical signal can propagate over long distances with very little variation in the optical power level. [5] Taking this knowledge we have explored the possibilities of using optical data that is transmitted through such quasi-lossless fibre spans which may provide a different nonlinear propagation regime to conventionally EDFA and Raman amplified systems.

With this different form of nonlinear propagation regime we aim to show that this alternate form of amplification can perform as well or better than the more traditional methods of amplification. This chapter takes a look at the nonlinear effects in transmission spans and how managing these effects can improve communication systems.

### 5.2 Nonlinear Effects

The response of any dielectric material becomes nonlinear for intense electromagnetic fields including optical fibres. Although silica is intrinsically not a highly nonlinear material the wave geometry that confines light to a small cross section over long fibre lengths makes nonlinear effects important to the design of modern light wave systems.[30]

Nonlinear effects can fall under two categories, the first of these being *stimulated light scattering*, which is the interaction between the light waves and the silica medium. The second set of nonlinear effects is due to the dependence of the refractive index on the intensity of the applied electric field with the most important being *self-phase modulation* and *four-wave mixing*.

### 5.2.1 Stimulated Light Scattering

The effect in the fibre that occurs due to this nonlinear effect is known as *stimulated light scattering* and it's the frequency of the scattered light that is shifted downward during inelastic scattering. The main examples of inelastic scattering are *Raman scattering* and *Brillouin scattering*. [31] Both of these can be understood as the scattering of a photon to a lower level energy photon such that the energy difference appears in the form of a phonon. [4] The difference between the two is that optical phonons participate in Raman scattering and acoustic phonons participate in Brillouin scattering. At low power levels these two forms of stimulated light scattering effects have little effect on the power at the incident frequency, which is where the scattering effect occurs. The problems begin to come into effect at higher power levels.

Once a threshold value is reached for higher powers for both stimulated Brillouin scattering (SBS) and stimulated Raman scattering (SRS) the intensity of scattered light grows exponentially for each. [4]

These two types of scattering SBS and SRS are both similar in their origins but due to different dispersion relations for acoustic and optical phonons it leads to a difference in the effects on the light that each scattering event produces.

These differences are:

- SBS can only occur in the backward direction where SRS can occur in both directions.
- The light that is scattered is shifted in frequency by approximately 10 GHz for SBS but by about 13 THz for SRS. (This shift is called the Stoke shift).
- The spectral gain for Brillouin is very narrow at a bandwidth of less than 100 MHz but for Raman the spectrum size is 20-30 THz. [4]

For the scattering effects the energy is transferred from light wave to another wave at a longer wavelength with the energy absorbed by the phonons. The second wave that is produced is known as the *Stoke* wave. If the first wave is viewed as a ‘pump’ wave that causes amplification to Stoke wave, as the pump propagates in the fibre it loses power and the Stoke wave gains power. [11] For SBS the pump wave is the signal wave and it’s the Stoke wave that is unwanted and for SRS the pump-wave is a high power wave and the Stoke wave generated is the amplified signal wave.

### 5.2.1.1 Stimulated Brillouin Scattering

As mentioned previous, the phonons in SBS are acoustic and the interaction occurs over a very narrow bandwidth. Also the pump and Stoke wave occur in opposite directions, so as long as the wavelength spacing is wide enough SBS should not cause any interaction between the two wavelengths. It’s also important to note that due to the fact the SBS produces gain in the opposite direction to the signal it is important to isolate the transmitter. [11]

The SBS gain coefficient  $g_B$  is approximately  $4 \times 10^{-11}$  m/W, independent of the wavelength. The intensities of the pump wave  $I_p$  and the Stokes wave  $I_s$ , are related by the coupled-wave equation: [11]

$$\frac{dI_s}{dz} = -g_B I_p I_s + \alpha I_s \quad (5.1)$$

And

$$\frac{dI_p}{dz} = -g_B I_p I_s - \alpha I_p \quad (5.2)$$

From these two equations it is possible to estimate the threshold power for SBS. The threshold power  $P_{th} = I_p A_{eff}$ , where  $A_{eff}$  is the effective area of the core:

$$\frac{g_B P_{th} L_{eff}}{A_{eff}} \approx 21 \quad (5.3)$$

Where  $L_{eff}$  is the effective interaction length defined as:

$$L_{eff} = \frac{[1 - \exp(-\alpha L)]}{\alpha} \quad (5.4)$$

And  $\alpha$  is the fibre loss. For optical communication systems  $L_{eff}$  can be approximated by  $1/\alpha$  as  $\alpha L > 1$ . Using  $A_{eff} = \pi\omega^2$  where  $\omega$  is the spot size  $P_{th}$  can be as low as 1mW depending on the values of  $\omega$  and  $\alpha$ . [4] Once this threshold level is exceeded by the launched power the majority of the light is reflected back by the SBS which means the launch power is limited by the SBS threshold.

### 5.2.1.2 Stimulated Raman Scattering

If two or more signals at different wavelengths are injected into a fibre the SRS causes power to be transferred from the lower wavelength channels to the higher wavelength channels as shown in figure 5.1. [11]

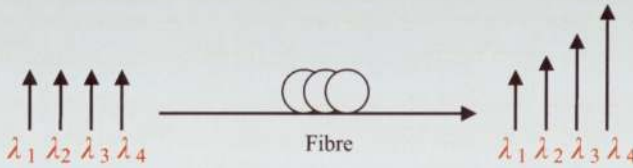


**Figure 5.1: The effect of SRS. Power from the lower wavelengths being transferred to the higher wavelengths.**

The SRS occurs in optical fibre due to the scattering of the pump wave. Looking at the energy-level diagram in Figure 5.2 we can see that some of the pump photons give up their energy to create other photons of reduced energy at a lower frequency, with the remaining energy absorbed by silica molecules which end up in an excited vibration state. The vibration energy levels of silica dictate the value of the Raman shift  $\Omega_R = \omega_p - \omega_s$  and

because an acoustic wave is not involved SRS is an isotropic process and occurs in all directions. [4]

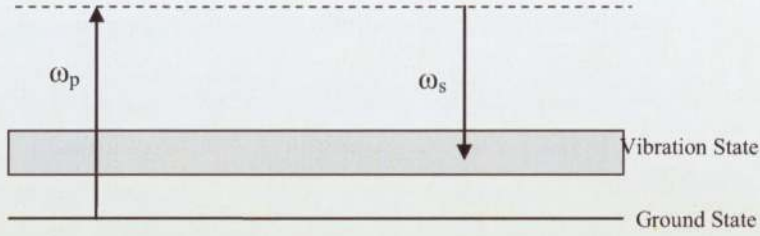


Figure 5.2: Participating energy levels pump frequency  $\omega_p$  and Stoke frequency  $\omega_s$

Like SBS, the SRS process becomes stimulated if the pump power exceeds a threshold limit. As already stated SRS can occur in both the forward and backward direction in optical fibres. The beating of the pump and with the scattered light in these two directions creates a frequency component at the beat frequency  $\omega_p - \omega_s$  which acts as a source that derives molecular oscillations and due to these a positive feedback loop is generated due to amplitude increase of the scattered wave response. [4]

For forward SRS the feedback process is governed by the two coupled equations:

$$\frac{dI_p}{dz} = -g_R I_p I_s + \alpha_p I_p \quad (5.5)$$

And

$$\frac{dI_s}{dz} = -g_R I_p I_s - \alpha_s I_s \quad (5.6)$$

where  $g_R$  is the SRS gain. For backward SRS a minus sign is added to the front of the derivative in equation 5.6. [30]

Raman gain depends on the decay time associated with the excited vibration state. For molecular gas and liquid the decay time is relative long ( $\sim 1\text{ns}$ ) which results in a Raman

gain bandwidth of ~1GHz, for optical fibres this exceeds 10THz. This broadband nature is due to the amorphous nature of the glass as the vibration energy levels of silica molecules merge together to form a band. Due to this merging the Stokes frequency  $\omega_s$  differ from the pump frequency  $\omega_p$  over a large range. The maximum gain occurs when the Raman shift  $\Omega_R \equiv \omega_p - \omega_s$  is about 13THz with another major peak being at 15THz. [4]

The threshold power  $P_{th}$  for Raman scattering, like SBS is defined as the incident power at which half the pump power is transferred to the Stokes field at the output of the fibre of a length L is given as:

$$\frac{g_R P_{th} L_{eff}}{A_{eff}} \approx 16 \quad (5.7)$$

As before  $L_{eff}$  can be approximated by  $1/\alpha$  and if  $A_{eff}$  is replaced by  $\pi\omega^2$  the  $P_{th}$  for SRS is given by: [3]

$$P_{th} \approx \frac{16\alpha(\pi\omega^2)}{g_R} \quad (5.8)$$

The ability to transfer the energy from a pump wavelength to the wavelength of an optical signal by the use of SBS and SRS can be used as an advantage for optical communication system.

### 5.2.2 Self-Phase Modulation

Self-Phase Modulation (SPM) occurs because the refractive index of the fibre has an intensity dependent component. This nonlinear refractive index causes an induced phase shift that is proportional to the intensity of the pulse which means that different parts of the pulse undergo different phase shifts, which leads to the chirp of the pulses. The pulse broadening effects of the chirping enhance the pulse broadening effects of chromatic dispersion. [11] For systems that are operating at and above 10GHz as well as systems that use high transmit powers, SPM has significant ability to increase the broadening affect of the chromatic dispersion as the chirping effect is proportional to the transmitted power.

### 5.2.3 Four Wave Mixing

Four wave mixing (FWM) originates from  $\chi^{(3)}$ . If three optical fields with carrier frequencies  $\omega_1$ ,  $\omega_2$  and  $\omega_3$  co propagate inside a fibre at the same time  $\chi^{(3)}$  generates a fourth field of  $\omega_4$ . This fourth frequency is related to the other three frequencies by  $\omega_4 = \omega_1 \pm \omega_2 \pm \omega_3$ . Several frequencies correspond to different plus and minus combinations most of these however do not build up due to the phase matching requirement. [30]

FWM can be viewed as a scattering process in which two photons of energy  $h\omega_1$  and  $h\omega_2$  are destroyed and their energy reproduced in the form of two new photons of energy  $h\omega_3$  and  $h\omega_4$ . As all four waves propagate in the same direction the phase mismatch can be written as:

$$\Delta = \beta(\omega_3) + \beta(\omega_4) - \beta(\omega_1) - \beta(\omega_2) \quad (5.9)$$

where  $\beta(\omega)$  is the propagation constant for an optical field with frequency  $\omega$ . In the degenerated case,  $\omega_2 = \omega_1$ ,  $\omega_3 = \omega_1 + \Omega$  and  $\omega_4 = \omega_1 - \Omega$  where  $\Omega$  is the channel spacing. Using the monochromatic approximation where  $\beta(\omega)$  expanded in a Taylor series around the carrier frequency up to the third term:

$$\beta(\omega) = \bar{n}(\omega) \frac{\omega}{c} \approx \beta_0 + \beta_1(\Delta\omega) + \frac{\beta_2}{2}(\Delta\omega)^2 + \frac{\beta_3}{6}(\Delta\omega)^3 \quad (5.10)$$

we find that the terms  $\beta_0$  and  $\beta_1$  cancel out and the phase mismatch is  $\Delta = \beta_2 \Omega^2$ . [4] The FWM is completely phase matched when  $\beta_2 = 0$ . Also when the  $\beta_2$  and the channel spacing is too small the FWM process can occur and a transfer of power from each of the channels to its nearest neighbour can happen. This transfer of power can introduce crosstalk which can reduce the system performance.

Most systems avoid FWM by introducing better dispersion management techniques but FWM can be also be used to improve communication systems. FWM can be used to

spectrally invert a signal through optical fibre with a technique that will be looked at in chapter 6 called *optical phase conjugation*, which can be useful for dispersion compensation.

### 5.3 Generating Quasi-lossless conditions

From stimulated Raman scattering (SRS) effects it can be seen if the power threshold produced by a Raman pump is exceeded a Stoke shifted wave occurs and the pump then provides amplification for this stoke shifted wave. SRS produces maximum gain around the standardized band of communications known as the c-band and methods to utilize this method of amplification have been explored. One area that we have been looking at is to take the SRS effect and use this to amplify transmitted signals in c-band region with a technique called *Quasi-lossless* transmission, where the aim is to generate a constant power level throughout a transmission fibre span. This technique takes the Stoke shifted effect and with the use of an *Ultra-long Raman Fibre laser cavity* (URFL) produces nonlinear effects within the cavity which produce the conditions for a second Stoke shift to occur.

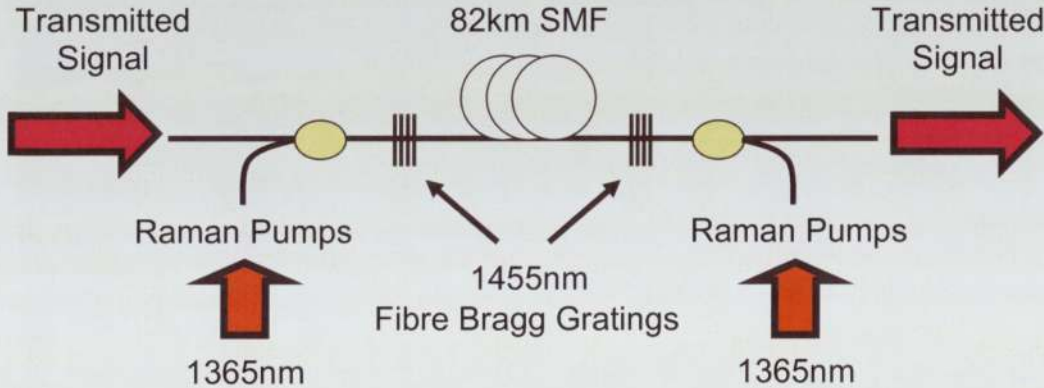


Figure 5.3: Ultra-long Raman Fibre Laser with pumping configuration to produce quasi-lossless conditions

The method to produce Quasi-lossless (QLL) conditions is as explained in [31] but the fundamental configuration is shown in Figure 5.3. The system works by forming a high Q cavity by using a pair of fibre Bragg gratings (FBG) which are placed at both ends of the

transmission span. The FBGs have 99% reflectivity and a spectral width of 1nm at 1455nm. The transmission span is pumped bi-directionally by the Raman pump lasers at 1365nm and this is coupled into the fibre. Through the resulting Raman affect Stoke shifted light is generated in the transmission fibre span and is reflected by the FBGs, which then creates our ultra-long Raman laser cavity. In the URFL nonlinear pump broadening occurs and this combined with the gain generated by the lasing wavelength at 1455nm as well as the primary pump at 1365nm, a second Stoke shift occurs which provides a wide range of amplification over a broad range of wavelengths. The pump and gratings used here are specific to produce gain in telecommunication c-band region but with a different pump and grating setup it would be possible to alter the gain region.

The fibre represented in Figure 5.3 is 82km SMF-28 (single mode fibre) and this will be the fibre used throughout the research into the capabilities of the ultra-long Raman fibre laser. The effects produced by the QLL conditions can be explained by Figure 5.4. The graph shows the results of an (OTDR) trace with regards to the signal power variation due to the distance travelled.

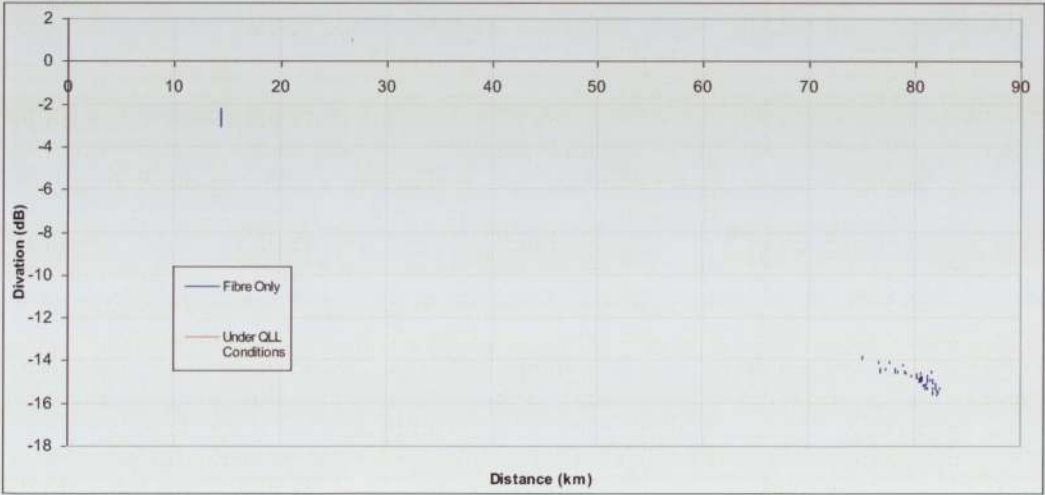
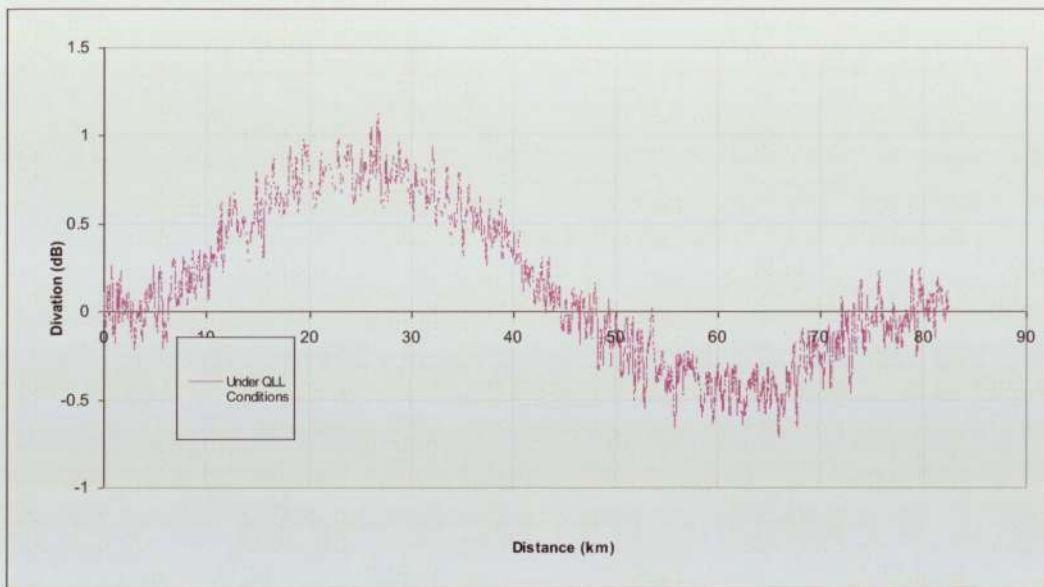


Figure 5.4: OTDR trace of 82km SMF with and without QLL conditions

As can be seen when the fibre is not under the QLL conditions (the blue line) the power variation along the span has a linear decrease. The result shows that a signal transmitted through this fibre span will be subject to the attenuation that is produced. When

the fibre is placed under QLL conditions however (the pink line) and the Raman pump current set accordingly, the power variation along the fibre span is reduced. If we take a closer look at resulting trace for the fibre when under QLL conditions in Figure 5.5 we can see that the output power level is the same as the input power level and that the power varies by less than 1.5dB across the full length of the fibre span. It's this equal power from the input of the fibre to the output that we are aiming for when generating a QLL transmission span.



**Figure 5.5: OTDR trace of 82km SMF with QLL conditions**

The generated QLL conditions give the possibility of a new form of amplification scheme for optical transmission systems. The performance of this new type of amplification scheme has to be measured against a form of amplification scheme that is already being used on communication systems, and the comparisons and differences explored. The commonly used amplification scheme used is that of an erbium doped fibre amplifier (EDFA) scheme. Under the same transmission conditions both schemes the EDFA and the QLL performances will be measured and compared.

## 5.4 Quasi-lossless Single Channel Transmission

For the transmission measurements a single span optical re-circulating loop will be used as shown in Figure 5.6. A single span re-circulating loop was used as it gives control over the distance that a signal is transmitted without having to alter the lengths of fibre that are being placed under test.

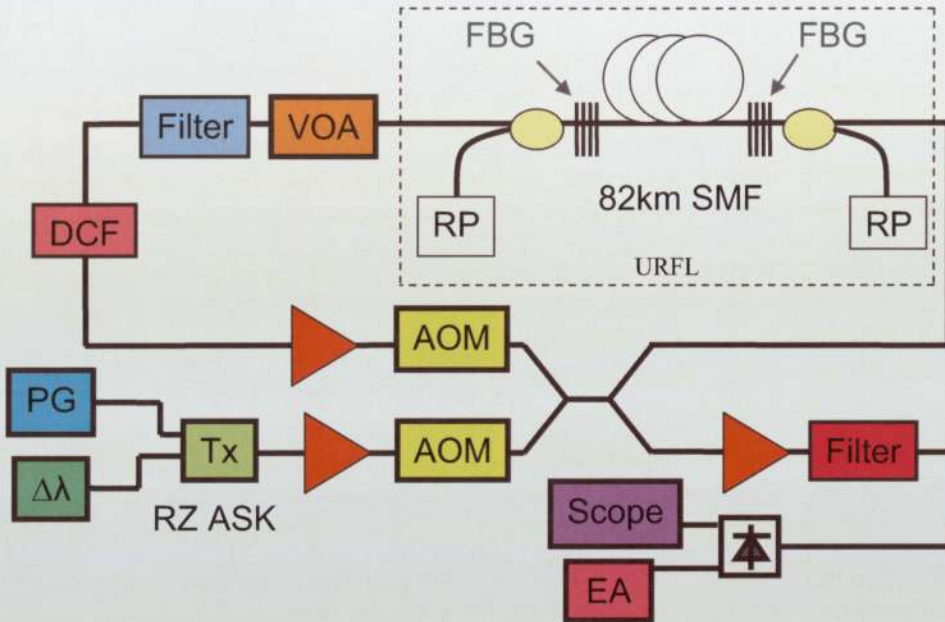


Figure 5.6: Optical transmission loop with URFL

Working through the optical re-circulating loop setup we have a wavelength of 1550nm and a PRBS of  $2^{31}-1$  from a pattern generator (PG) that are modulated to give an RZ-ASK signal that will be transmitted at two different data rates of 10.6 and 42.6 Gb/s. The transmitted signal is then gated onto the optical loop through an acousto-optic modulator (AOM). The signal is then applied through the URFL where it is subjected to the QLL conditions. It is at this point in our loop that the URFL will be replaced by an EDFA, as shown in Figure 5.7 when the comparison of amplification schemes is to be done. The EDFA is required to help compensate for the power loss through the fibre which the URFL is not subject to.

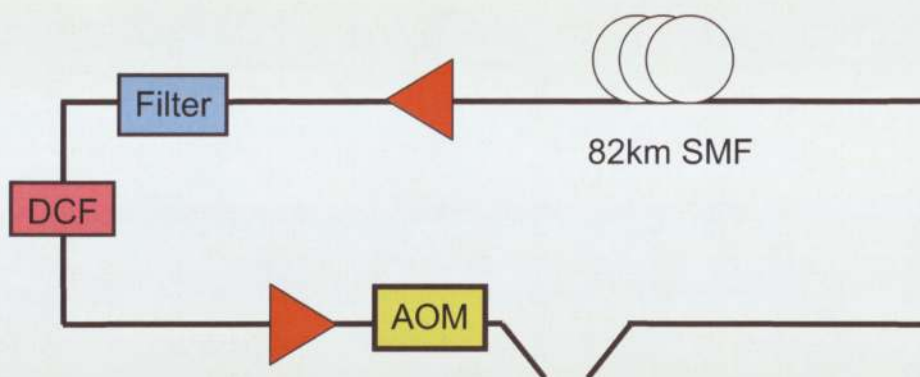
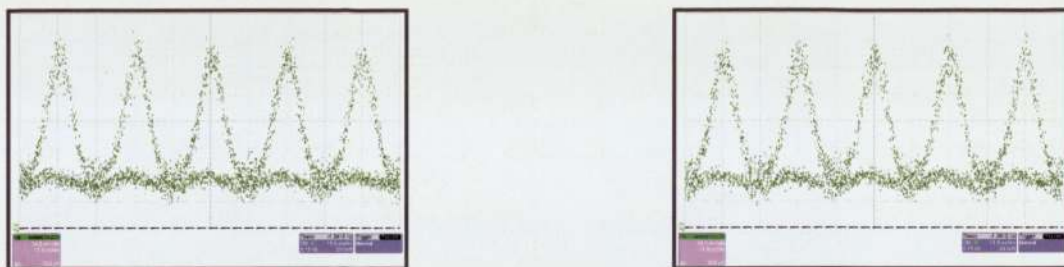


Figure 5.7: Optical transmission loop with EDFA scheme

For the QLL scheme a variable optical attenuator has been placed after the fibre span and this is to control the power levels through the dispersion compensating fibre (DCF) that follows. The power levels for the input and output of the signal through the URFL under QLL conditions are equal but for the EDFA system the power level due to the loss through the fibre is approximately 17dB lower. So this is why the introduction of an EDFA is required to ensure that the power level through the DCF is correct. After the transmission span there is a dynamic gain flattening filter in place, this is to adjust the spectral profile of the two amplification schemes by removing any residual out of band amplification. After the filter we have DCF.

The experiment here has no pre or post dispersion compensation at the loop input or output and all the dispersion compensation for the SMF was provided by the DCF. The eye diagrams in Figure 5.8 show the input and output eyes for once around our transmission loop. The DCF was chosen to provide 100% dispersion compensation at the transmission wavelength for the SMF in our transmission span and this can be seen from the eye diagrams.



**Figure 5.8: Input and output eyes for one loop re-circulation**

After the DCF an EDFA is used to compensate for the losses from the filter, DCF and the insertion losses of the input and output of our re-circulating loop which are generated by the coupler and gating AOM. The signal was then switched out of our loop with another AOM onto the receive path. On this path we have an EDFA which is used to amplify the signal before the receiver. To remove any out of band noise an optical pass-band filter was used before our signal was converted from optical to electrical signal by a photodiode. With the use of an error-analyser (EA) that was synched with the optical data the bit error rate of our transmissions was measured and eye diagrams were monitored on an oscilloscope.

#### **5.4.1 Quasi-lossless Transmission Launch powers**

To ensure that the measurements involving the two types of amplification scheme were comparable the optimum launch power into the transmission fibre for each scheme was found. This measurement was performed by measuring the bit error rate for a fixed received power and altering the SMF launch power. The input power to the DCF was fixed at -4dBm while the SMF launch power was adjusted by the power variation of the EDFA preceding the re-circulating AOM and the launch EDFA at the loop input.

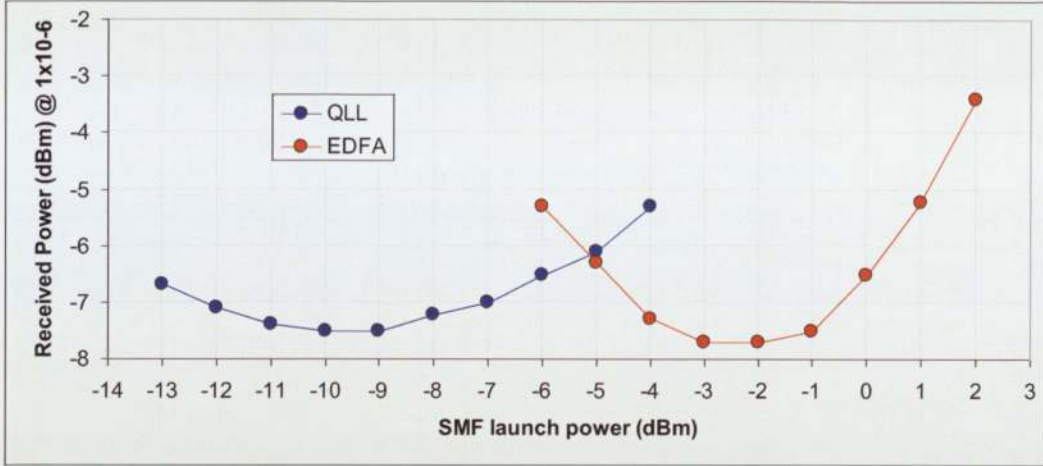


**Figure 5.9: Optimum launch power measurements for QLL and EDFA amplification schemes at a data rate of 10.6Gb/s.**

For the optimum launch power measurements for a data rate of 10.6Gb/s the transmission distance over the SMF used was 3300km and the bit error rate for the received power was  $1 \times 10^{-6}$ . From the results in Figure 5.9 it can be seen that the launch power for the QLL scheme is -10dBm but for the conventional EDFA scheme the launch power required is much higher at -2dBm. This difference in optimum launch powers of 8dBm is indicative of the different power profiles of these two regimes. The system setup for the EDFA has a higher launch power at the start of the transmission fibre which is in a strong nonlinear region but the decay of the signal due to the intrinsic loss along the length of the fibre a reduction in the nonlinear effects occurs. In the QLL scheme the loss across the fibre is less than 1.5dBm meaning that the nonlinear effects that occur along the full length of the fibre span. The more distributed nature of nonlinearities leads to increased degradation of the signal for the QLL system compared to the EDFA scheme if both have the same launch power. This leads to the optimum launch power for the SMF being lower for the QLL than the EDFA system. [33]

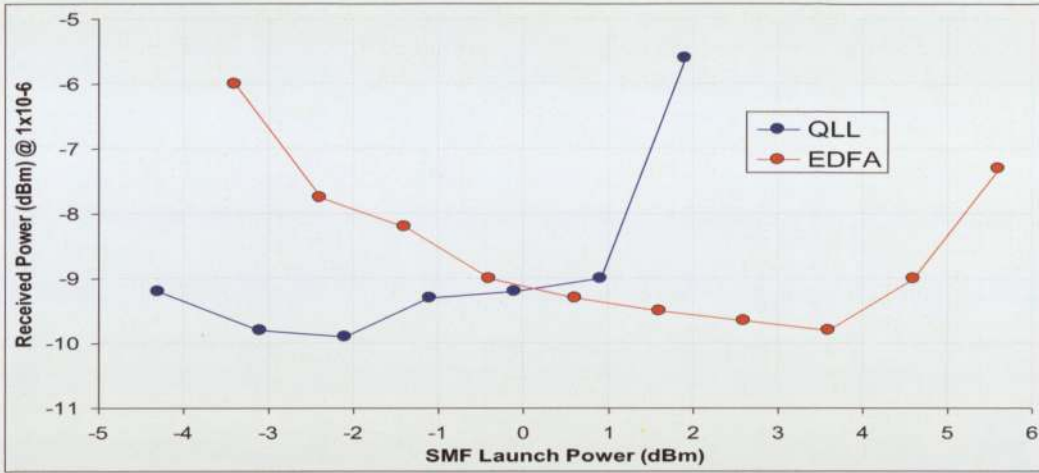


**Figure 5.10: Optimum launch power measurements for QLL and EDFA amplification schemes at a data rate of 42.6Gb/s.**

If we take a look at the optimum launch powers for the transmission fibre at a data rate of 42.6Gb/s in Figure 5.10 we can see that once again the QLL launch power is again lower than the SMF launch power for the EDFA system. The measurements were taken at a distance of 800km with the bit error rate for the received power again taken as  $1 \times 10^{-6}$ .

Now we have an optimum of -2dBm SMF launch power for the QLL system and a launch power of +4dBm for the EDFA system. Once again the reduction in the optimum launch powers for the transmission spans that can be seen is down to the nonlinear effect along the full length of the transmission fibre span.

### 5.4.2 Quasi-lossless Transmission Distances

With the optimum launch powers for each system known, transmission distance measurements can be performed. Using the re-circulating loop configuration in Figure 5.6 the bit error rate for different distances were taken for each amplification scheme at the two different data rates.

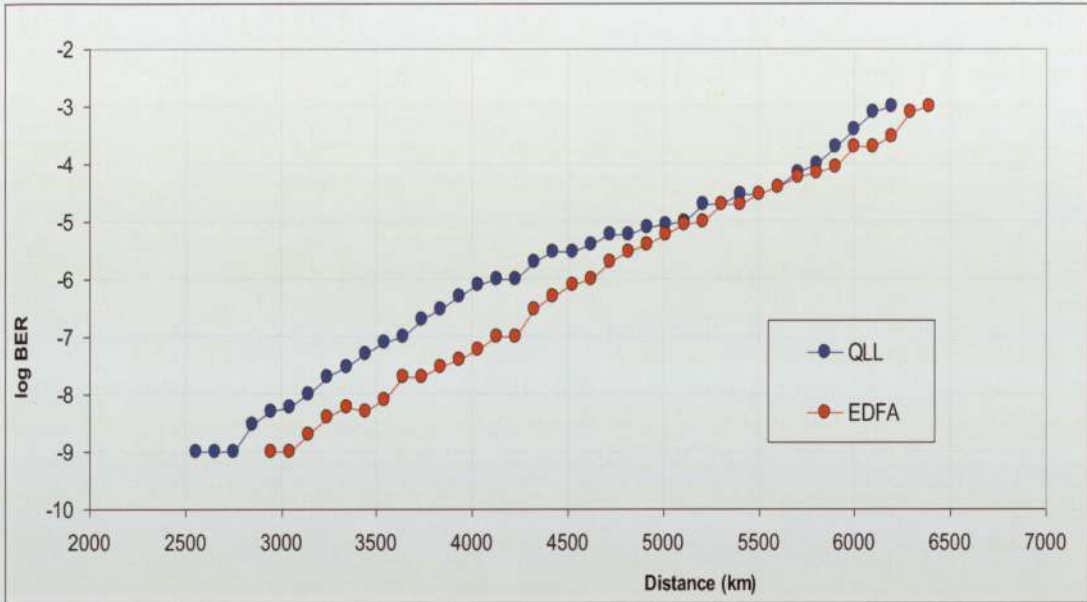


Figure 5.11: Transmission distances for the QLL and EDFA schemes at a data rate of 10.6Gb/s

The results in Figure 5.11 shows the bit error rate versus the transmission distance for the two amplification schemes at a data rate of 10.6Gb/s. From the results it can be seen that the performance of the two schemes is very similar although the launch power for the QLL system is of a lower power. Also the QLL system is subjected to more loss due to the FBGs and coupling in of the Raman pumps which will be looked at in more detail in section 5.4.3. This extra loss however does suggest that the QLL scheme has a better OSNR performance.

The performance measured here was at a data rate, 10.6Gb/s and the transmission distances possible for both schemes where the bit error rate is low enough for forward error correction was that of 6200km. The greater interest however is at the high data rates where transmission systems are now looking to perform due to higher demand of system capacities and faster speeds.

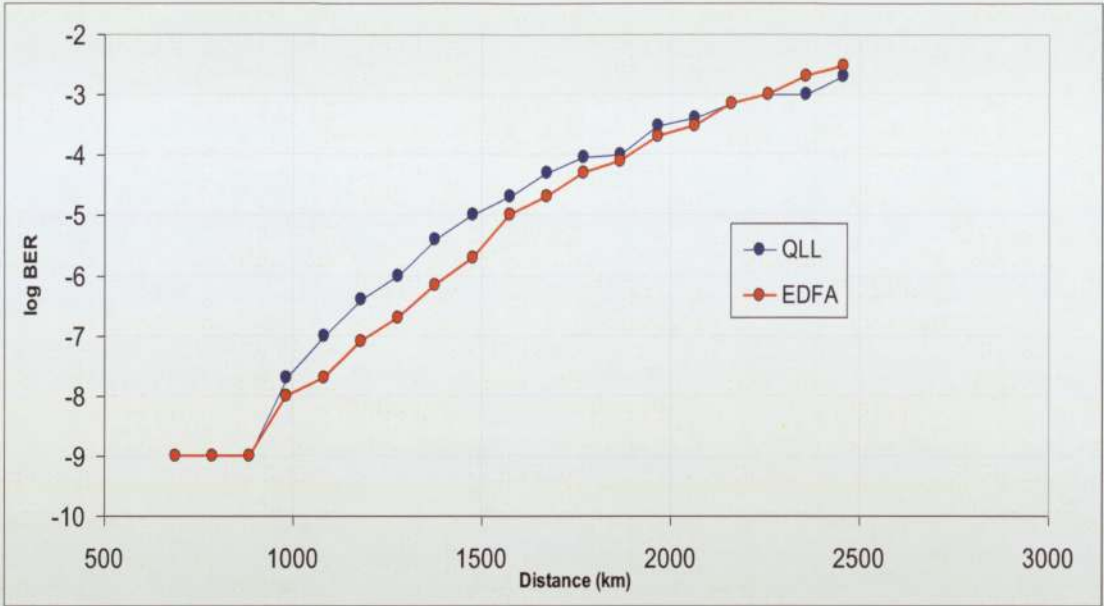


Figure 5.12: Transmission distances for the QLL and EDFA schemes at a data rate of 42.6Gb/s

The transmission results in Figure 5.12 are of the two amplification schemes but this time at the higher data rate of 42.6Gb/s. Once again the performance of the two schemes is similar with both systems reaching a transmission distance of 2200km with the bit error rate lower than the forward error correction limit.

It has to be noted that during these experiments that no RIN degradation was observed. This may be down to the low RIN pumps used with the RIN specification for the pumps being -120dB/Hz and the use of the ultra-long Raman laser cavity.

To ensure that the dispersion levels in the transmitted signals for each system eye diagrams were taken at different distances. Looking at the eye diagrams for the EDFA system in Figure 5.13 and the QLL system in Figure 5.14 it can be seen that throughout the transmission distances achieved there appear to be no dispersive effects on the signal.

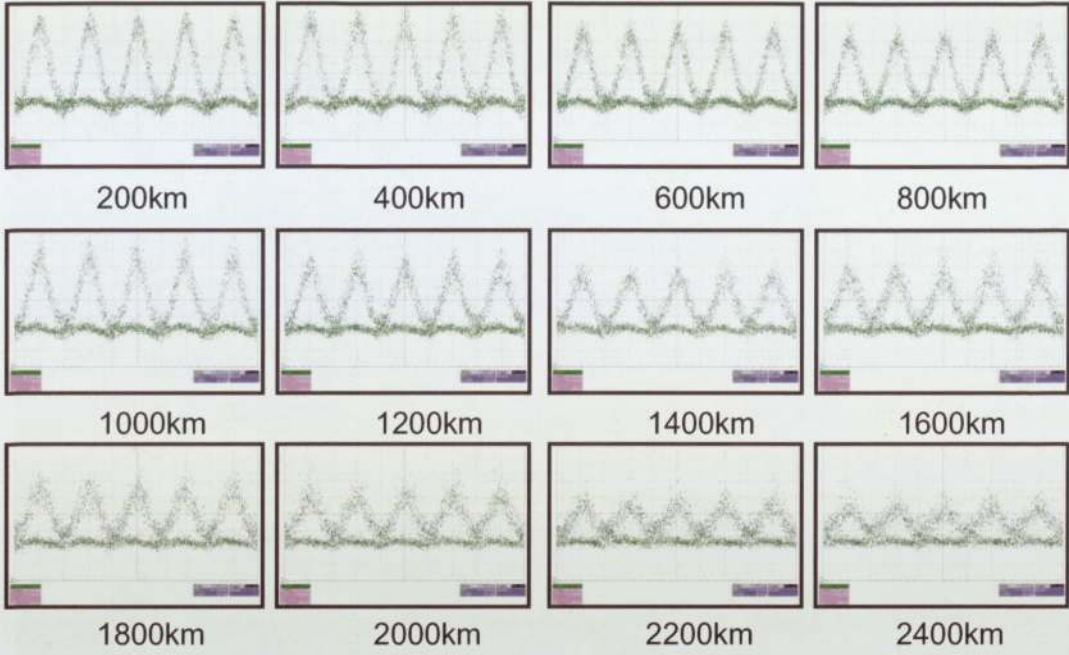


Figure 5.13: Eye diagrams for EDFA transmission system at 42.6Gb/s

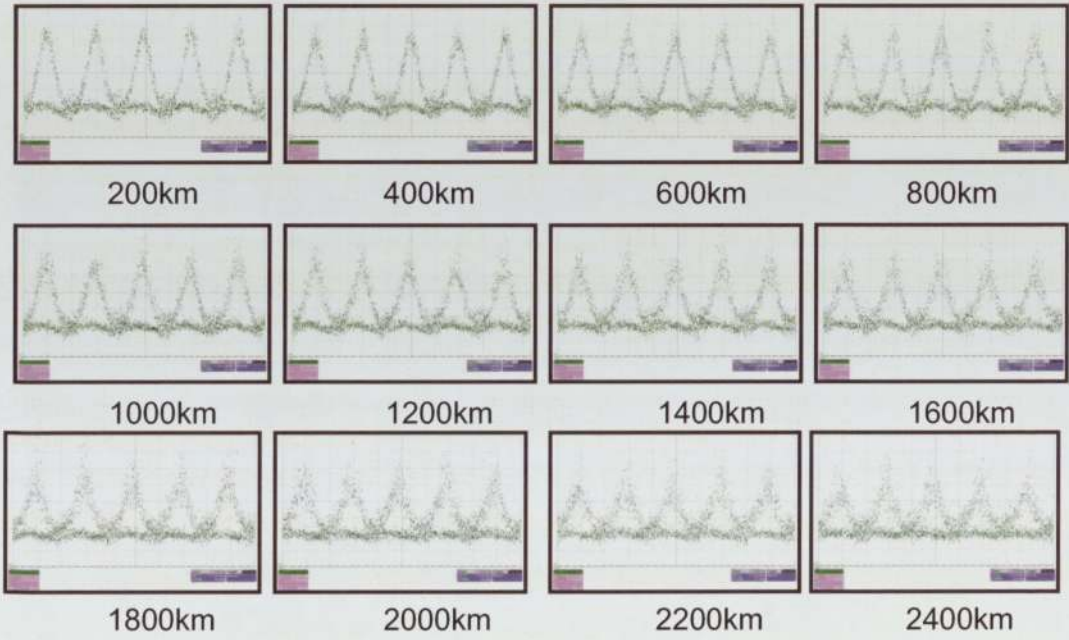


Figure 5.14: Eye diagrams for QLL transmission system at 42.6Gb/s

### 5.4.3 Transmission OSNR

As mentioned previously due to the fact that the two different amplification schemes have the same levels of performance for the transmission of an optical signal and that the QLL system has more loss due to the FBGs and the couple for the Raman pumps, the QLL appears to have a better OSNR performance.

To compare the difference in OSNR between the two schemes firstly the modelled performance of the QLL and EDFA systems was performed. From Figure 5.15 the modelled performance of the EDFA system can be seen.

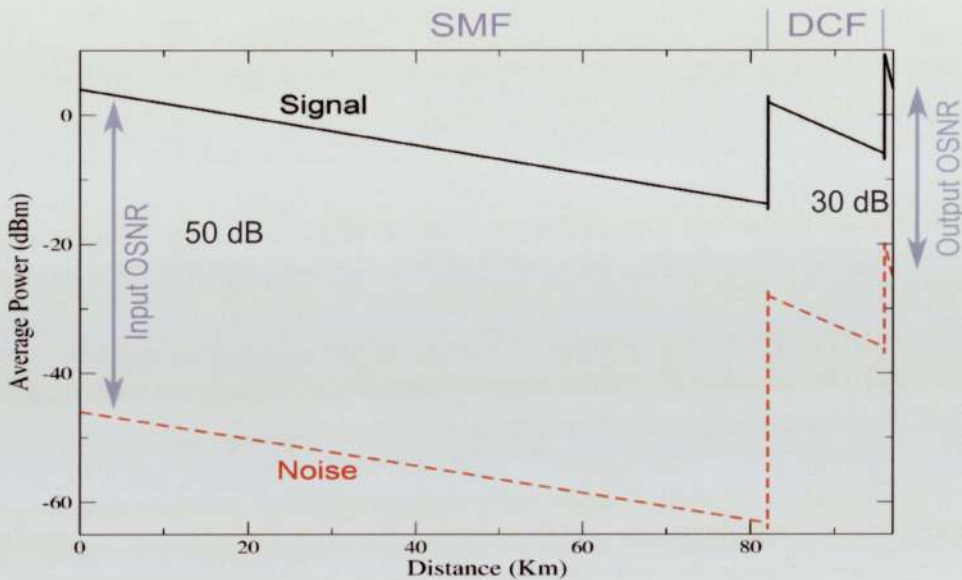


Figure 5.15: Modelled performance of OSNR through the EDFA scheme

With an input OSNR of 50dB the amplified signal and noise both degrade linearly through the transmission SMF fibre span. The signal and noise are both amplified before they are coupled into the DCF with the amplification of the noise being greater than that of the signal. They both again degrade through the DCF in linear fashion before being amplified again. The OSNR that would be now going onto the next transmission fibre span would be of 30dB which gives a total difference of 20dB from the input to the output OSNR.

If we look at the QLL system as shown in Figure 5.16 we can see the results of the modelled performance.

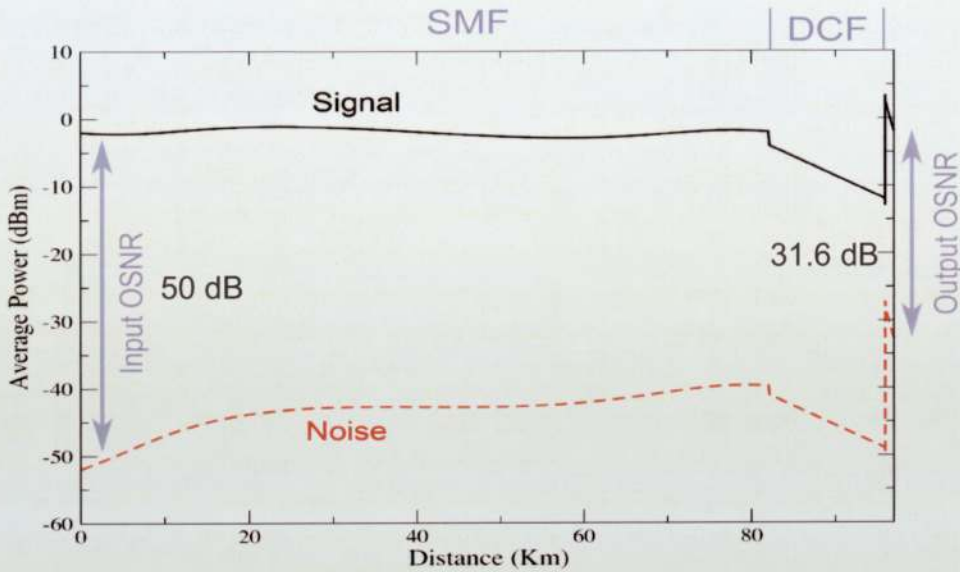
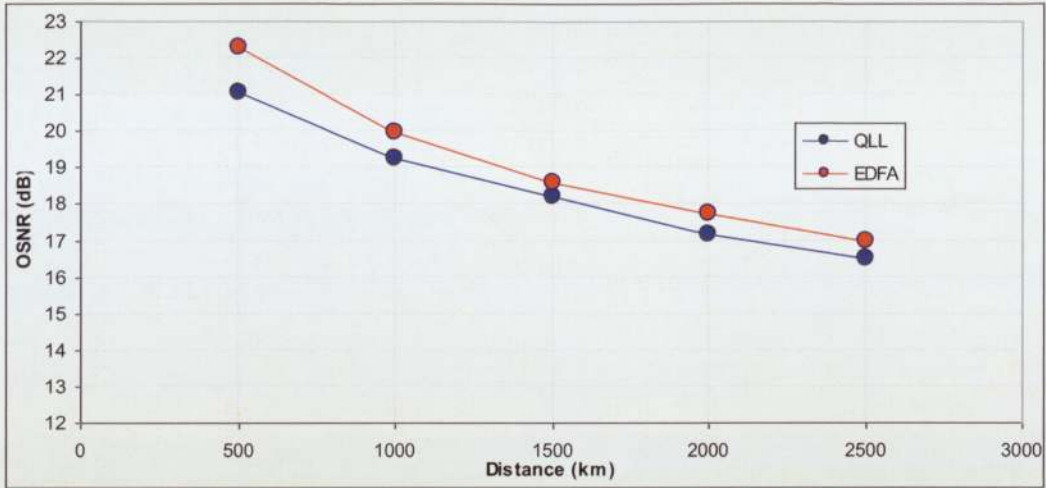


Figure 5.16: Modelled performance of OSNR through the QLL scheme

Again we have an input OSNR of 50dB. As we have almost flat gain across the transmission fibre for the QLL scheme there is little variation off the signal where the noise floor builds up by approximately 10dB across the whole span. The transmission is coupled into DCF where again there is a power degradation and the signal after the DCF is amplified up. From these results it can be seen that the OSNR level is now at 31.6dB which is a difference of 28.4dB from the input to the outputted OSNR. This shows that through the modelled experiment that the QLL scheme does provide an OSNR improvement of 1.6dB.

For the physical measurements the OSNR was measured for different distances for each amplification scheme and the results were plotted against each other as shown in Figure 5.17.



**Figure 5.17: Transmission performance of OSNR through the QLL and EDFA scheme**

From the results above it can be seen that the EDFA scheme appears to perform better than the QLL scheme. These results differ to that of the modelled results. The explanation of this can be easily explained with the use of Figures 5.18 and 5.19.

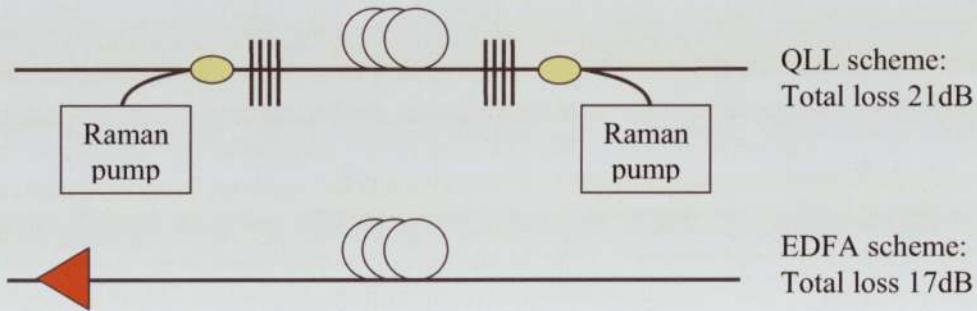


**Figure 5.18: Losses through the QLL and EDFA scheme**

The total losses for each amplification scheme vary due to the different configurations. The QLL scheme is subject to extra loss from the couplers for the Raman pumps and the fibre Bragg gratings as shown in Figure 5.18 which is a total of an extra loss of 4dBm. A method to compare the performance of the two amplification schemes with the same loss is to keep the couplers and the gratings from the QLL system in the transmission system setup for the EDFA measurements as shown in Figure 5.19.

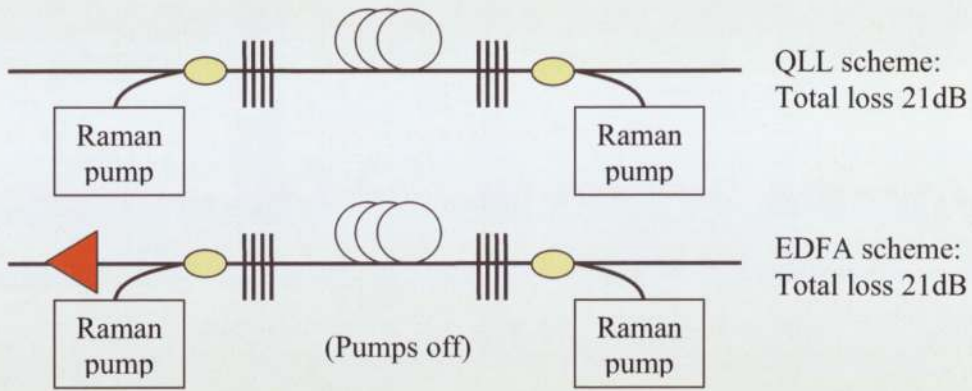


Figure 5.19: Equal losses through the QLL and EDFA scheme

With both schemes now under the same loss conditions the QLL scheme has a better OSNR than that of the EDFA as shown in Figure 5.20.

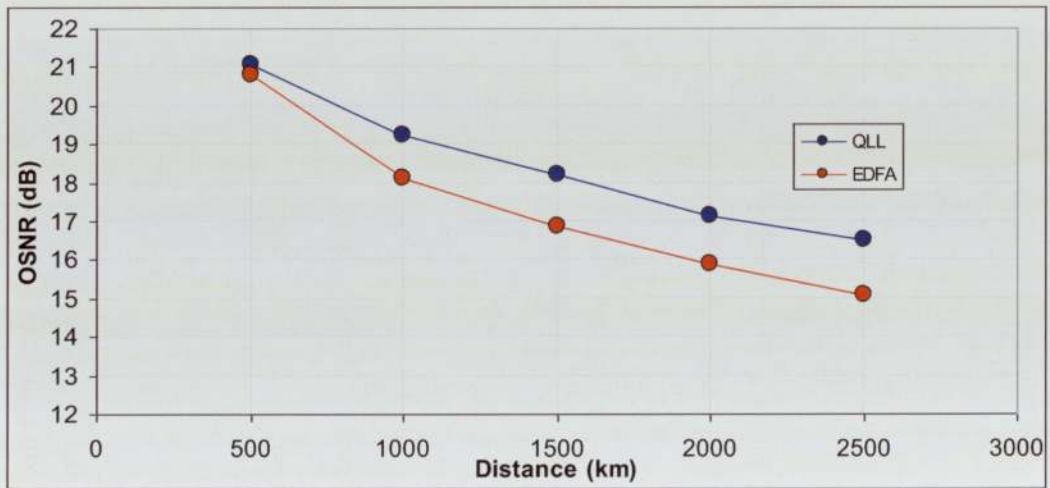


Figure 5.20: Transmission performance of OSNR through the QLL and EDFA scheme with equal losses

The results show that the OSNR performance of the QLL scheme is approximately 1.5dB better than that of the EDFA scheme. The OSNR measurement different between the two schemes is important as the OSNR is a major factor when producing an optical transmission system and here the QLL scheme does perform better than that of the EDFA scheme.

## 5.5 Quasi-lossless Multi-Channel Transmission

All the previous experiments were done with the use of single channel transmission and it has been shown that with the use of an ultra-long Raman fibre laser that quasi-lossless conditions can be produced and transmission at a data rate of 42.6 Gb/s is possible. [7]

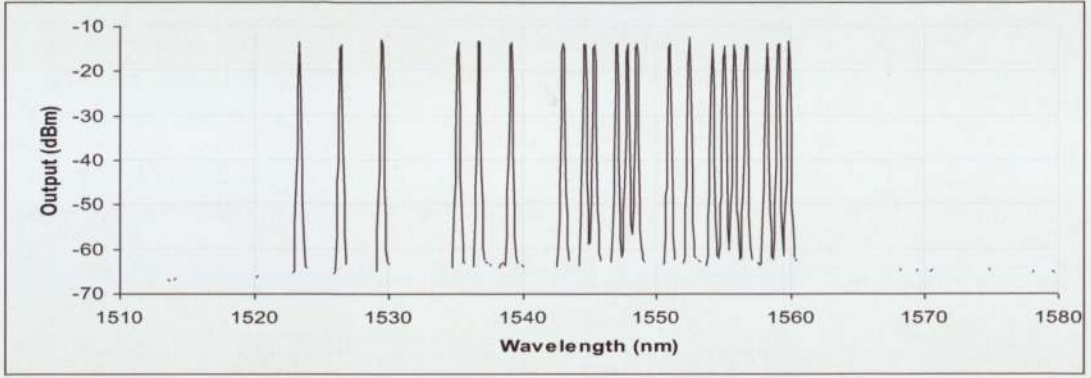
To prove that the ultra-long Raman fibre laser can be applied to more real world situation the performance of the amplification process was applied to a DWDM application. Once again the broadband gain effect was compared to that of the more conventional EDFA system.

Using the same experimental setup as in Figure 5.6, twenty one channels at a data rate of 42.6Gb/s were multiplexed together. The same URFL and EDFA systems that were used to perform the single channel measurements were used here.

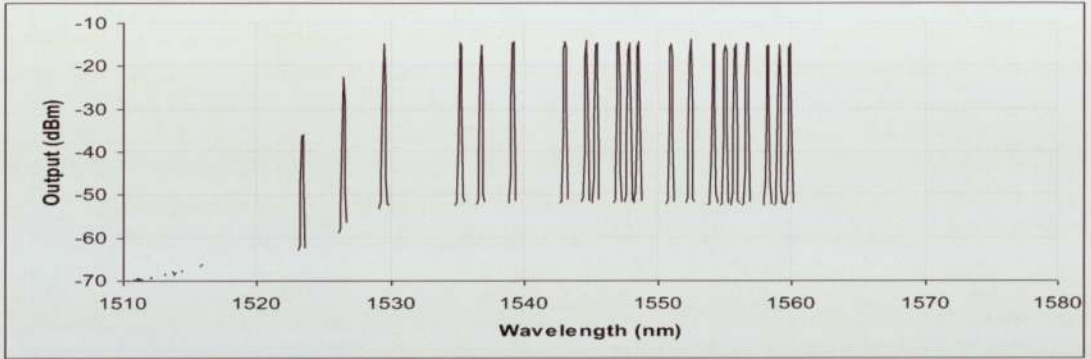
### 5.5.1 Bandwidth

For our experiment the maximum available channels we had was twenty one and the channels were spread across the telecommunications c-band. Eighteen of the channels used were fixed while three of the channels were used to alternate between higher and lower wavelengths. Some of the channels were tightly spaced (100GHz) spacing to replicate true telecommunication systems to see if any interference from channel to channel occurs while being amplified under quasi-lossless conditions. The reason for the three floating channels was to measure the bandwidth capabilities of each amplifier scheme.

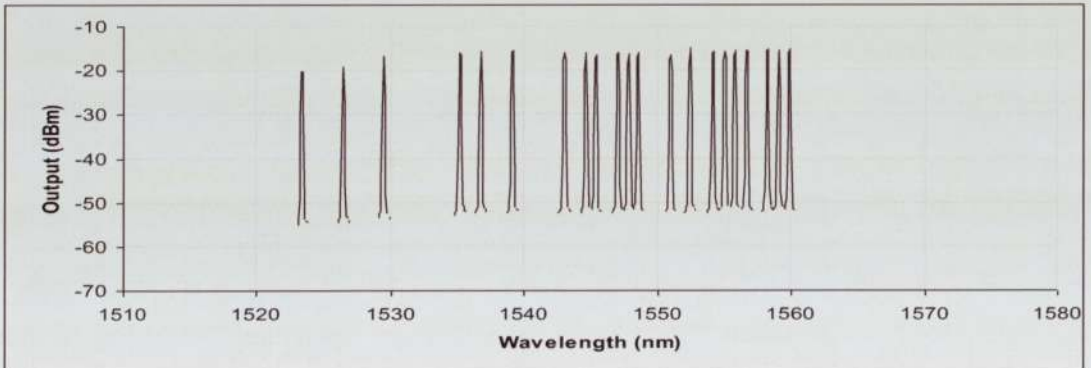
For each amplifier scheme the input and output powers were set to the optimum values used for transmission so that the spectral representation is of those of an actual system configuration. The URFL input power was 4dBm and the EDFA input power -6dBm and the output power for both amplification schemes was at 4dBm. (It has to be noted that no pre-emphasis for the input channels was used and that the EDFA spectrum was set to be flat across the c-band).



(a)



(b)

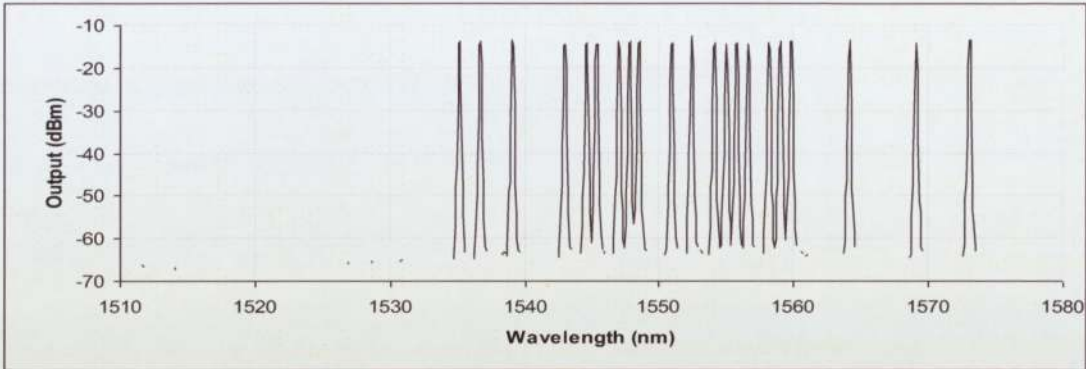


(c)

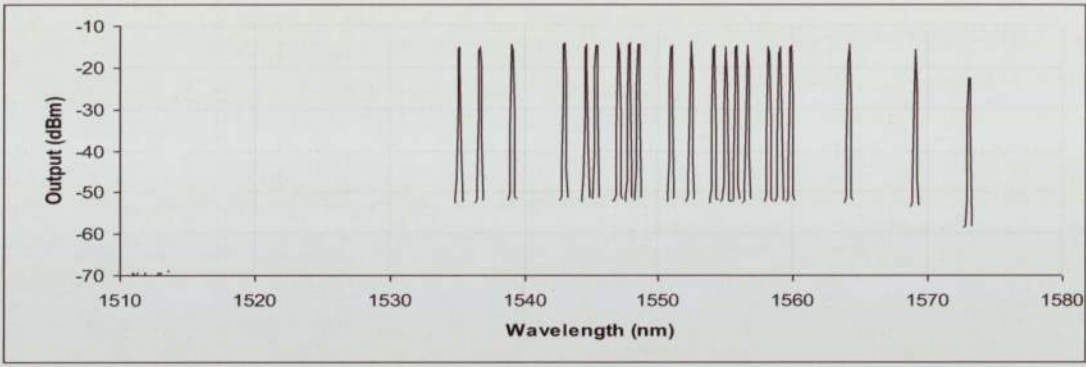
**Figure 5.21: Lower wavelengths spectrum of 21 channel input (a) and EDFA amplification (b) URFL (c) amplification schemes outputs**

From the results in Figure 5.21 it can be seen that for a give input (a) that the URFL (c) provides a broader gain bandwidth than that of the EDFA (b) scheme. The characteristic of the EDFA system is to have a sharp decrease around the 1530nm region but for the URFL this decline is one of a gradual one. If a measurement at a 3dB gain reduction point is

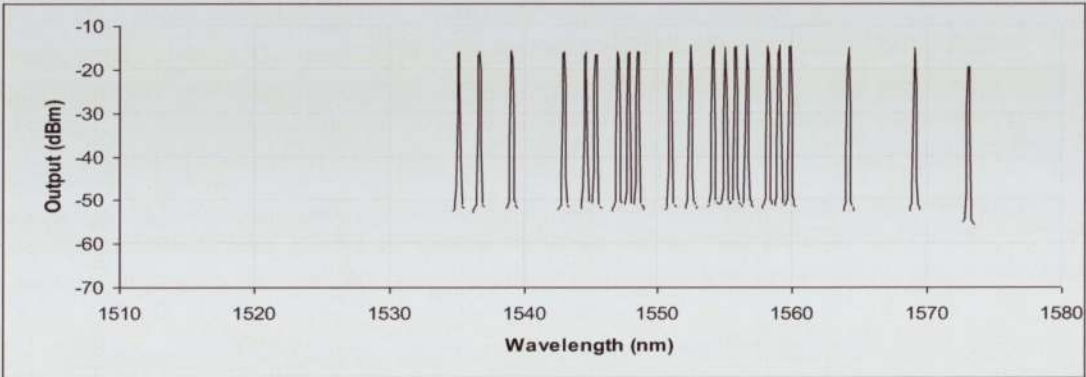
compared for the two amplifiers for the EDFA this would correspond to a wavelength of 1528nm and for the URFL this would be 1523nm which gives a difference of 5nm (625GHz).



(a)



(b)



(c)

**Figure 5.22: Higher wavelengths spectrum of 21 channel input (a) and EDFA amplification (b) URFL (c) amplification schemes outputs**

From the spectrums in Figure 5.22 it can be seen that there is also an increase in bandwidth for the URFL scheme at the higher wavelengths compared to the EDFA scheme. The extra bandwidth coverage may not be as large as at the lower wavelengths with the 3dB gain

reduction at 1573nm for the URFL condition and 1571nm for the EDFA condition, a difference of 2nm (250Ghz).

At the 3dB gain reduction point the overall bandwidth for the QLL scheme is 50nm where the EDFA scheme is 43nm in total bandwidth. What this tells us is that the URFL has a greater useable gain flatness region that can extend beyond the c-band compared to that of the gain flatness of an EDFA based system.

**5.5.2 Transmission**

Twenty CW c-band lasers were coupled together using an array waveguide multiplexer (MUX) then modulated with a 42.6Gb/s  $2^{31}-1$  PRBS RZ\_ASK test pattern at the transmitter (Tx) and then transmitted on the re-circulating loop configuration in Figure 5.6.

The results gained are similar to the single channel transmission results as they show that the two types of amplification schemes have similar outcomes. Both of the systems were reduced down to error rates of  $2 \times 10^{-3}$  (the forward error correction limit) at a distance of 1071km.

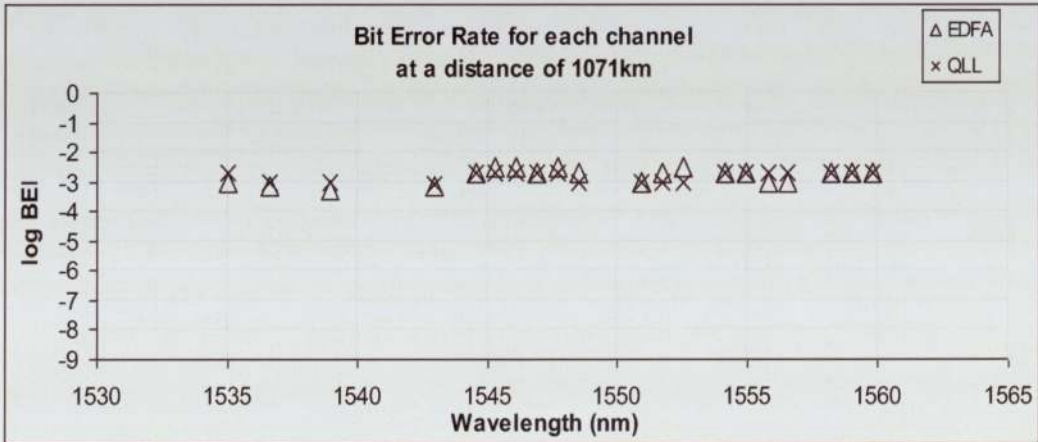


Figure 5.23: Transmission results for EDFA and URFL WDM schemes

It has to be noted here that the purpose of this experiment was not to determine absolute transmission limits but to compare the two types of amplification schemes under the same conditions. With re-circulating loop configurations there are high round trip losses that

can be experienced but both of the transmission schemes here are subjected to these same losses.

The use of wavelengths for this experiment was restricted by the bandwidth of the EDFA used. The full gain bandwidth capabilities of the URFL shown in the previous section could not be tested as this was outside the EDFA gain bandwidth also the additional re-circulating loop losses restricted the measurements.

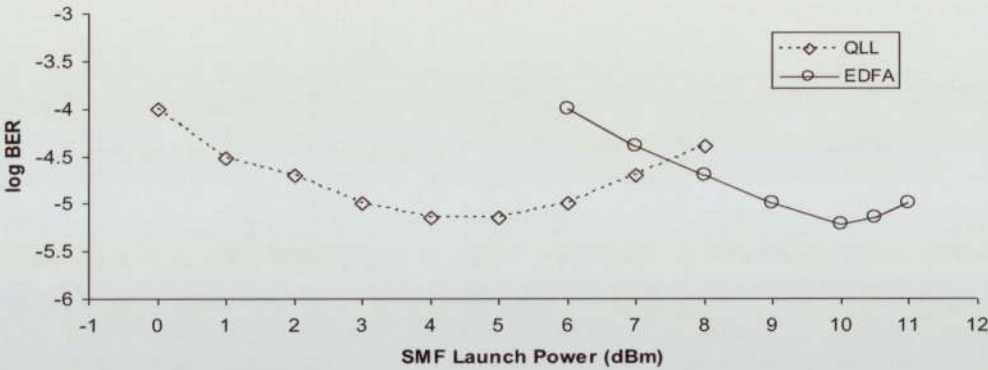


Figure 5.24: Launch powers for EDFA and URFL WDM schemes

Once again with respect to the launch powers the URFL provides a lower required launch power for the SMF compared to EDFA scheme. With launch power for the URFL being around 4dBm and 10dBm for the EDFA system and this 6dBm lower required power is down to the near constant power level provide by the quasi-lossless transmission conditions. So once again we can provide a significant reduction to nonlinear impairments without incurring a noise penalty with the URFL compare to the EDFA system.

### 5.6 Conclusion

With nonlinear effects on transmission systems there can be a negative effect to the communications setup. With the need for greater capacity and higher data rates the effects of

the nonlinear interactions begin to play a greater role. From the work shown in this chapter it is possible to use these effects to improve your transmission system.

With the single channel experiments we showed for the first time the ability to transmit data using quasi-lossless conditions. [33] The transmission system performance was similar to that of the conventional EDFA transmission systems in use today. The quasi-lossless scheme however was subject to more loss than that of the EDFA scheme and the removal of this loss could improve the capabilities of the quasi-lossless scheme. One of these improvements that were found from the experimental results would be to the OSNR for the system, which is one of the most important system considerations for optical communications.

Also the optimum launch power for the quasi-lossless scheme was lower than that of the EDFA which would, through this lower power provide a transmission system with a greater nonlinear tolerance.

When performing the multi-channel experiments the same conclusion as the single channel experiments could be drawn. Again the transmission performance of the quasi-lossless system was similar to that of the EDFA system even though again it was subject to extra losses of the fibre Bragg gratings and couplers. The launch powers were again different with the power for the quasi-lossless system being lower than that for the EDFA. The interesting thing to come from the multi-channel transmission results was the difference in gain bandwidth for each scheme.

The gain bandwidth for the ultra-long Raman fibre laser was wider than that EDFA scheme and it was also flatter. The gain bandwidth region cover the complete c-band region, as did the EDFA but the ultra-long Raman fibre laser could also give amplification to regions beyond this where the EDFA can not. The extra 7nm (875GHz) can give coverage to an extra 8 channels on a 100GHz spaced transmission system or 16 channels on a 50GHz system.

This extended c-band coverage with lower required launch powers that provide no degradation in the transmission abilities compared to that of the EDFA scheme show the ultra-long Raman fibre laser technique as an effective amplification technique.

# Chapter 6

## Optical Phase Conjugation

When transmitting a signal over great distances and attempting to reduce or remove the effects that occur during transmission forms of management along the transmission line are put in place to correct the problems at a given distance along these transmission lines. Another way of solving this problem would to reverse the altering effects at the half way point of the transmission. A method of doing this is called Optical Phase Conjugation (OPC).

This process involves the use of nonlinear optical effects to precisely reverse the propagation direction of each plane wave in an arbitrary beam of light, thereby causing the return beam to exactly retrace the path of the incident beam. The process is also known as wave-front reversal or time-reversal reflection. [35]

OPC as a process is by which a light beam interacting in a nonlinear material is reflected in such a manner as to retrace its optical path.

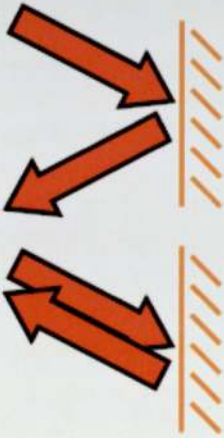


Figure 6.1: The reflective effect of (a) a Conventional mirror and a (b) phase conjugated mirror.

Figure 1 shows how such an interaction can occur. The image-transformation properties of this reflection are radically different from those of a conventional mirror. The incoming rays and those reflected by a conventional mirror are related by reversal of the component of the wave vector which is normal to the mirror surface. Thus a light beam can be arbitrarily redirected by adjusting the orientation of a conventional mirror. In contrast, a phase-conjugate reflector inverts the vector quantity so that, regardless of the orientation of the device, the reflected conjugate light beam exactly retraces the path of the incident beam.

## **6.1 Introduction**

In high bit rate communication links, optical nonlinearity along the link and their interplay with the chromatic dispersion is one of the main sources of signal distortion. In order to reduce the impact of nonlinearity on the optical transmitted signal in the fibre the introduction of a method called Optical Phase Conjugation (OPC). The introduction of an OPC device in the centre of a transmission link, as suggested by mid-span spectral-inversion (MSSI) technique. [36] The technique is extremely promising as in principle it allows compensating for both dispersive and nonlinear effects.

The only problem with MSSI is that it can not be introduced to an optical transmission system that is already installed, due to the fact that its effectiveness is strongly affected by the power asymmetries and fluctuations along the transmission link, the OPC can only be used in specific configurations that satisfy mid-nonlinearity temporal inversion (MNTI) requirements. [37]

Another possibility for the use of OPC is to combine it with QLL transmission system. As shown in chapter 5 the power variation in such transmission spans is minimal which closely approximate the ideal lossless configuration required for MSSI implementation.

## **6.2 The OPC device**

The OPC device that will be used in this experimentation is a device based on the cascading technique into a high efficient 67nm long waveguide realized by reverse-proton-

exchange on a periodically-poled lithium-niobate (PPLN) substrate. In order to achieve the polarization independence of the apparatus a polarization-diversity scheme, which was reported in [38] was used.

### 6.3 OPC in a lossless transmission span.

The traditional method of compensating dispersion in a transmission system is the use of dispersion compensating fibre, so the OPC technique was measured compared to this method. Using the lossless method used in the previous chapter the effectiveness of an OPC system in a lossless transmission span the OPC device was placed into the transmission loop and the DCF removed, as shown in Figure 2.

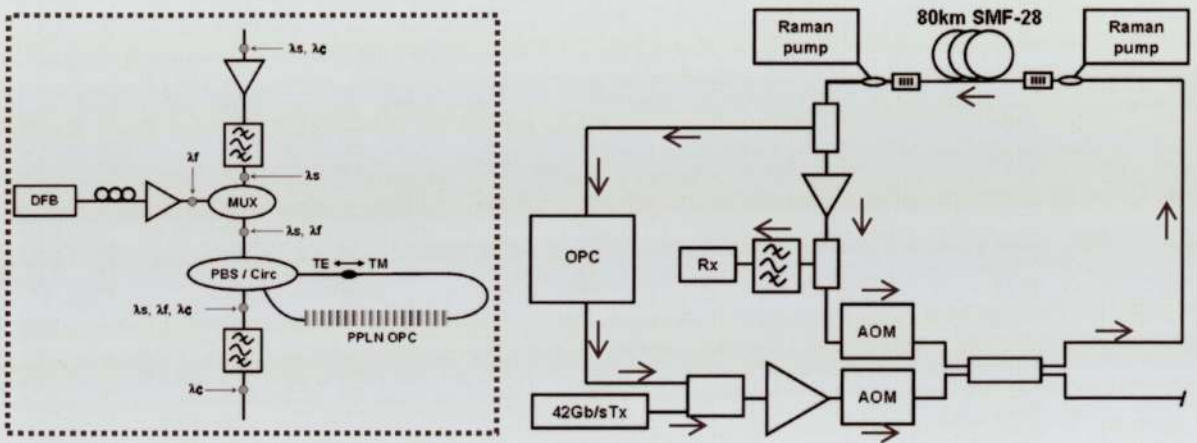


Figure 6.2. Recirculating loop configuration and OPC set-up

#### 6.3.1 Comparison of Optimum Launch powers.

For the performance of the OPC technique and the technique with the DCF the launch power tolerance for each setup were measured and compared. This was done by measuring the Q-factor penalty (best BER performance) compared to the optical power launched into the two different propagating spans. Making this measurement allows us to see the possible effects of the non-ideal power settings upon the two different transmission systems.

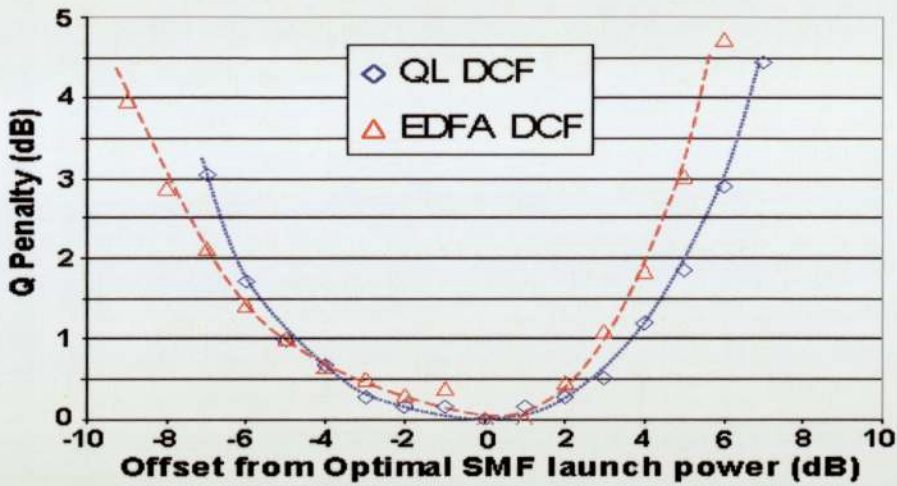


Figure 6.3. Q-penalty as a function of optical launch power, comparing the difference between an EDFA and QL link. Dispersion compensation obtained with DCF.

If look at Figure 3 we can see that when using the DCF in the transmission span with the QLL and the EDFA system configurations there is no significant improvement for the system tolerance due to the alteration to the amplification scheme. The reason that this occurs is that the nonlinearity can be compensated independently of the structure of the amplification scheme. But if we look at the results in Figure 6.4 when the OPC scheme is introduced to replace the DCF we can see significant differences.

When the OPC scheme is used with the lumped amplification there is no nonlinear compensation due to the MSSSI implementation. Figure 4 shows that the combination of OPC and EDFA give and power tolerance of approximately 7 dB at a penalty level of 1 dB. If we however look at the results of the QLL and OPC scheme combination we can see that the power tolerance is improved to 12 dB at a penalty level of 1 dB. This is due to the OPC allowing for compensation to the slight nonlinear distortions that affect the pulse propagation.

Another point that has to be noted when taking these measurements was the difference in launch powers required for each transmission system. For the OPC and QLL scheme the optimum transmission power was at -5dBm, where for the combination of OPC and EDFA this was at a higher power level of 2dBm.

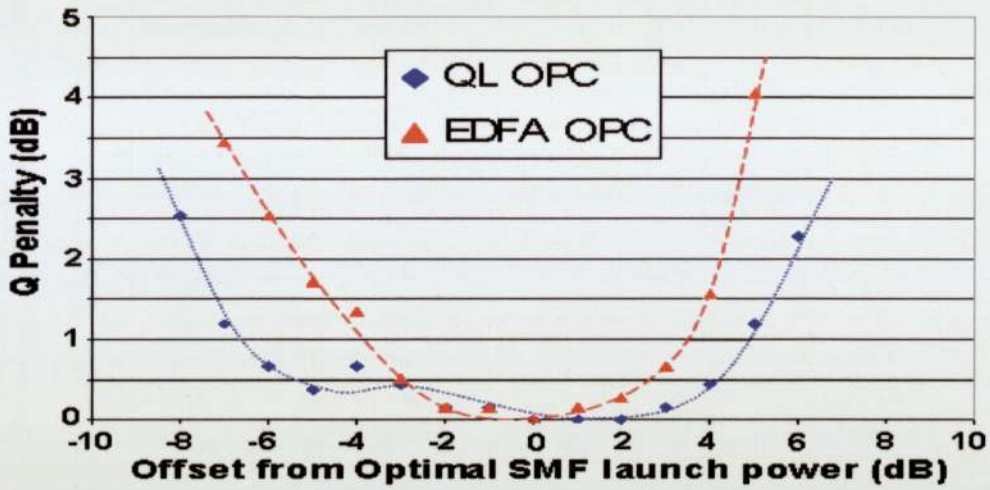


Figure 6.4. A comparison between EDFA and QL link with dispersion compensation is obtained by OPC.

When we compare the results for the QLL transmission scheme for both OPC and with the use of DCF, (as shown in Figure 6.5) we can that the combination of QLL and OPC do provide a greater power tolerance than that of the QLL scheme with the DCF.

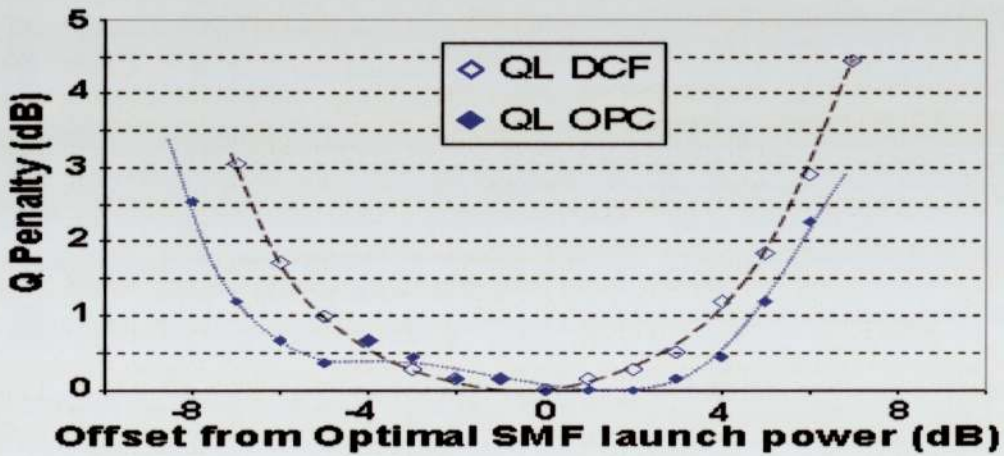


Figure 6.5: Comparison of launch power tolerance between QL link using DCF and OPC using DCF.

### 6.3.2 Transmission Distances.

To compare the transmission capabilities of the combination of the QLL and OPC schemes with the QLL and DCF combinations, the two configurations were placed into transmission loops and the received BER were measured at different distances and the two compared.

The results in Figure 6 show the results of these two transmission experiments. As can be seen for the short distances the performance of QLL-DCF combination is better than the QLL-OPC, this can be but down to the optimization of the OPC scheme. During the experiments there appeared to be some minor problem with the high power amplifiers used in the setup. The amplifiers seem to produce ASE noise level that generated the problem, the scheme however is being optimised to solve this problem and so therefore an improvement in performance at short distances is expected.

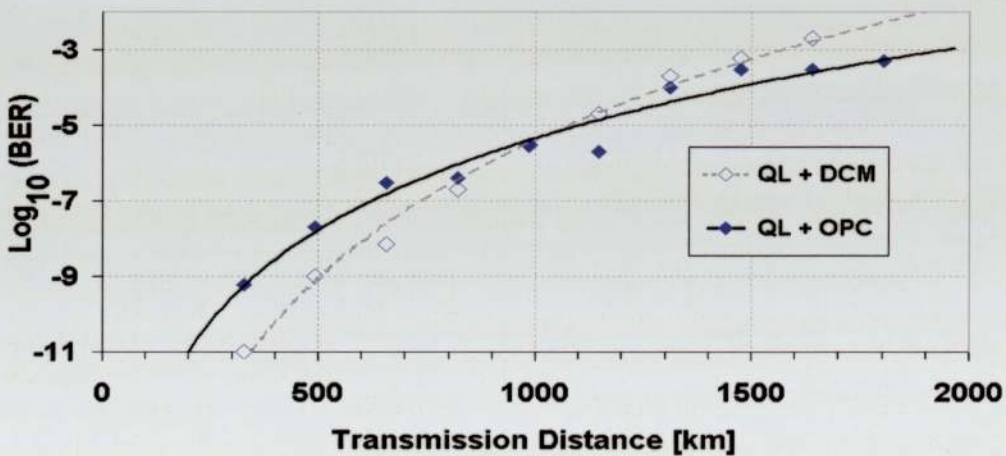


Figure 6.6: BER curve as a function of the system length comparing the QL with DCF and QL with OPC system configurations.

As for the longer transmission distances it can be seen that the QLL-OPC system provides better BER results than that of the QLL-DCF system. This is down to the amount of nonlinearity produced on the fibre. For the QLL-DCF system, even if the nonlinear effects are small they are can still accumulate while propagating during transmission. On the QLL-OPC

system however any nonlinear distortion that occurs should be completely removed. Another reason for the improved transmission at the greater distances for the QLL-OPC scheme compared to the QLL-DCF scheme is due to accumulative ASE noise. The QLL-OPC scheme introduces an OSNR reduction just on the whole transmission distance, the QLL-DCF scheme however introduces an OSNR reduction every span due to the amplification required to compensate for the signal attenuation produced by the DCF. This accumulative noise adds up and has a major effect on the overall performance of the transmission distance.

## 6.4 Conclusions.

From the results shown here it can be seen that some advantage can be gained by the use of the OPC system configuration. The introduction of OPC in a QL system is the most interesting and important part of the research done. As the introduction of OPC would remove the need for DCF spools and therefore the related amplifiers, which introduce extra noise to the system.

The problem with the OPC system is that it is required to part of the transmission scheme in situation and can not be added to existing transmission systems. So if this method of transmission was preferred it will mean that whole transmission systems would require replacing which would become a great expense. However as transmission systems age and communication speeds increase communication systems will require replacing and this is when the introduction of OPC-QL transmission schemes can be introduced.

## Chapter 7

### Conclusion

Life at the start of the twenty first century for the majority of people involves the use of some form of communication system. Be it in the form of business or for leisure purposes the transmission systems that are used are required to carry vast amounts of information and at extremely quick speeds as well as performing at very high efficient levels. The aim of the majority optical research is to find solutions that can help fulfil these demands. One of the major effects that occur in a transmission system is that of dispersion. The work shown here in this thesis has been all performed to determine what possible directions can be taken through the use of new and unique transmission systems to solve the problem of dispersion in transmission systems.

The first two chapters of the thesis are an introduction to fibre optic communications systems and is a look at the background of the subject. In chapter 3 there is a look at how the use of different modulation formats used to carry the transmitted signal can be used to aid the ability of the communication system. The research highlighted that the introduction of a narrow band filter at the receiver can be used to help recover and demodulate a transmitted signal. The results presented show that it would be possible with the use of a filter and at a high data rate of 40 GHz, it is possible to recover a differential phase shifted keyed (DPSK) signal. The filter used is one that is similar to wave division multiplexers (WDMs) that are already in use in transmission systems, meaning that this technique can be easily introduced to modern day transmission systems.

Chapter 4 looked at a common problem for all optical communication transmission systems, dispersion. A transmitted signal is subjected to dispersive effects when travelling down an optic fibre and these effects can cause information to become lost. The most common method which has been in practice for sometime in optical transmission systems is the use of dispersion compensated fibre which is placed in a system and is matched to give the opposite dispersive effects of the transmission optical fibre. This method is a static form

of compensation. Due to the increase in the demands on transmission systems extra transmission routes are introduced and this is where a static form of dispersion lets the system down as the DCF provides a fixed level of compensation, this where the research work in chapter 4 can offer a solution.

The introduction of a tunable dispersion device has been shown in this thesis to provide a suitable method of dispersion compensation in a transmission system. The device can be used at the receiver end of a transmitted system to provide the similar dispersive effects of dispersion compensation fibre (DCF). The advantage of a tunable device is that it can be used as a stand alone device to provide dispersion compensation or in conjunction with dispersion compensation fibre. When being used with DCF the tunable device can be an aid to fine tune the received signal.

An interesting point that was found during the investigation of the DCF device was the periodic performance of the device. The importance of the wavelength has a great effect on how much compensation is available from DCF, it is wavelength dependent. The periodic function in with the tunable device has been shown to prove similar results at different wavelengths, and the research shows that this device can be used in a multi-channel transmission scheme.

The Quasi-lossless method explored in chapter 5 is a new novel method for optical communication transmission. Using the ultra-long Raman laser in the transmission span gives an amplification scheme, which is not only comparable to a conventional EDFA amplification scheme but can also provide some improvements.

The experimental worked showed that it was possible with both single and multi channel transmission to provide across a fibre span of a dispersion level of almost zero. The work on the single channel experiments showed for the first time how a scheme like this would perform and gave an insight in to what possible improvements to a transmission system could be provided. The scheme not only provided a dispersion level of almost zero across the whole transmission span but introduced a lower optimum launch power which would itself help reduce the interactions from non-linear effects.

The results from the multi-channel experiments also provided encouraging results. The scheme again out performed the more tradition EDFA method of amplification. The amplification levels at all the different channels in the c-band all produced a near zero dispersion level but the QLL scheme provided something a little extra than the EDFA scheme. The QLL showed it could provide an equal level of amplification over a wider range of the c-band compared to that of the EDFA scheme.

The ability to provide an equal level of amplification at a wider range across the band and also produce a dispersion level of almost zero, has given evidence that the QLL scheme is a scheme that can be considered ahead that of the EDFA scheme when transmission systems are being considered.

The advantages of QLL scheme found in chapter 5 were then used to provide interesting experimental work with the OPC method shown in chapter 6. Due to the fact that the OPC method requires minimal variation in power across the transmission span the results in chapter 5 showed that the QLL scheme could provide this.

From the results it was shown that the combination of the QLL and OPC provide a higher launch power tolerance compared to a combination of EDFA and OPC. This in turn should produce a better performing transmission with a lower chance of noise and non-linear effects due to reduced need for extra amplifiers in the transmission span.

With the social media and video streaming constantly growing at a rapid rate, researcher into how to improve network systems on how to expand and improve speed without reducing quality is always being strived for. The work in this thesis has been motivated by this requirement and the results achieved have been another step forward in optical communications.

## **Publications**

- [1] “42.6Gb/s RZ-ASK transmission over 2500km using quasi-lossless transmission spans”, L. Barker, A. E. El-Taher, M. Alcon-Camas, J-D Ania-Castanon and P. Harper, CLEO EU CII.2 MON, (Munich) 2009.
- [2] “Optical Phase Conjugation for Dispersion and Nonlinearity Compensation in a 1600km, 42 Gb/s Quasi-Lossless System”, P. Minzioni, P. Harper, V. Pusino, L. Barker, Ca. Langrock, M. M. Fejer, J-D Ania-Castanon, I. Cristiani, V. Degiorgio, Advances in Optical Sciences: OSA Optics & Photonics Congress NThA5, Hawaii, 2009.
- [3] “Optical Communications Applications of Ultra-long Raman Fiber Lasers”, P. Harper, L. Barker, A. E. El-Taher, M. Alcon-Camas, J-D Ania-Castañón, S. K. Turitsyn, I. Bennion, Invited paper International Conference on Optical Communications and Networking, Beijing, China, 2009. ICOCN (Beijing) 2009.
- [4] “Extended bandwidth for long haul DWDM transmission using ultra-long Raman fiber lasers” L. Barker, A.E. El-Taher, M. Alcon-Camas, J.D. Ania-Castanon , P. Harper ECOC PP3 Torino (2010).

## **Bibliography**

- [1] [www.it.kth.se/docs/early\\_net](http://www.it.kth.se/docs/early_net).
- [2] D.Koeing, 'Telegraphs and Telegrams in Revolutionary France', *Scientific Monthly*, 431 (1944).
- [3] Fibre-optic comms systems 3<sup>rd</sup> edition, agrawal.
- [4] G.P. Agrawal, *Fibre-Optic Communication Systems*, Third Edition, John Wiley & Sons, New York, 2002.
- [5] Joseph c. palais, fibre optic communications 4<sup>th</sup> ed, 1998
- [6] E.E.Basch, *Optical-Fiber Transmission*, 1986
- [7] John Lester Miller, *Optical communications Rules of Thumb*, 2003
- [8] M.J.N. Sibley, "Optical Communications", 2<sup>nd</sup> edition
- [9] G.A. Thomas, B.L. Shraiman, P.F.Glodis, and M.J.Stephan, *Nature* 404, 626 (2000)
- [10] M.Born and E.Wolf, *Principles of Optics*, 7<sup>th</sup> ed, 1999
- [11] Rajiv Ramaswami and Kumar N. Sivarajan, *Optical Networks*, 2002
- [12] [www.infocellar.com/networks/networks/new-tech/ROADM/ROADM.htm](http://www.infocellar.com/networks/networks/new-tech/ROADM/ROADM.htm)
- [13] k.kikuchi, *electronic letters*, 26, 1851 (1990).
- [14] J.Gower, *Optical Communication Systems, Second Edition*, Prentice Hall, Europe, 1993.
- [15] Turboblogsite.com
- [16] D-S Ly-Gagnon, K.Katoh, and K.Kikuchi, "Unrepeated optical transmission of 20 Gbit/s quadrature phase-shift keying signals over 210 km using homodyne phase-diversity receiver and digital signal processing", *Electronic Letters*, Vol 41, No.4, pp.206-207.
- [17] A.H. Gnauck, S.Chandrasekhar, J.Leuthold, and L.Stulz, "Demonstration of 42.7-Gb/s DPSK receiver with 45 photons/bit sensitivity", *Photonics Technology Letters*, Vol 15, No 1, pp. 99-101.

- [18] D. Penninckx, H.Bissessur, P.Brindel, E.Gohin, and F.Bakhti, "Optical differential phase shift keying (DPSK) direct detection considered as a duo binary signal", *ECOC*, 2001, WeP40, pp. 456–457.
- [19] D.Gatti, G.Galzerano, P.Laporta, S.Longhi, D.Janner, A Gugliera, and M.Belmonte, "Demonstration of differential phase-shift keying demodulation at 10 Gbit/s optimal fiber Bragg grating filters", *Optics Letters*, Vol 31, No 13, pp.1512-1514.
- [20] L.Christen, Y.K.Lize, S.Nuccio, J-Y.Yang, P.Saghari, A.E.Willner, and L.Paraschis, "Fiber Bragg Grating Balanced DPSK Demodulation", *Lasers and Electro-Optics Society*, pp 563-564, 2006
- [21] C.Malouin, J.Bennike and T.J.Schmidt, "Differential Phase-Shift Keying Receiver Design Applied to strong Optical Filtering", *Journal of Lightwave Technology*, Vol. 25, No 11, November 2007.
- [22] G.P.Agrawal, *Fibre Optic Communication Systems* (Wiley and Sons, NY, 1997), Chap 9.
- [23] LUNA TECHNOLOGIES, optical component DNA.
- [24] B.J. Eggleton, A. Ahuja, P.S. Westbrook, J.A. Rogers, P. Kuo, T.N. Nielsen, B. Mikkelsen, *J. Lightwave Technology*, 18 (2000) 1418.
- [25] G.H. Lee, S. Xiao and A.M. Weiner, 'Programmable, polarization-independent, and DWDM-capable chromatic dispersion compensator using a virtually-imaged phase-array spatial light modulator', *Optical Fiber Communications Conference*, (OFC 2006), Anaheim, USA, 2006 (OThE5).
- [26] L.M. Ludardi, 'Tunable dispersion compensation at 40 Gb/s using a multicavity etalon all-pass filter with NRZ, RZ and CS-RZ modulation', *IEEE J. Lightwave, Tech*, 2002,20 (12) pp 2136-2144.
- [27] D.J. Moss, S. McLaughlin, G. Randell, M. Lamont, M.Ardekani, P. Colbourne, *OFC 2002 Paper TuT2*.

- [28] Xuewen Shu, Kate Sugden, Philip Rhead, John Mitchell, Ian Felmeri, Glynn Lloyd, Kevin Byron, Zhijian Huang, Igor Khrushchev and Ian Bennion, *Tunable Dispersion Compensator Based on Distributed Gires-Tournois Etalons*, *Photon. Technol. Lett.* **15**, NO.8, August 2003
- [29] Xuewen Shu, Karen Chisholm, John Mitchell, Ian Felmeri, Phil Rhead, Andrew Gillooly, Kate Sugden and Ian Bennion, *Tunable Dispersion Compensator Based On Three Distributed Gires-Tournois Etalons*, *Opt. Comms.* **251** 59-63 (2005)
- [30] G.P.Agrawal, *Nonlinear Fiber Optics* 3<sup>rd</sup> Edition, 2001
- [31] R.W.Boyd, *Nonlinear optics*, 1992
- [32] Ania-Castañón, Juan D.; Karalekas, V; Harper, Paul and Turitsyn, Sergei K. (2008). Simultaneous spatial and spectral transparency in ultralong fiber lasers. *Physical Review Letters*, 101 (12), p. 123903.
- [33] Harper, Paul; Barker, L.; El-Taher, Atalla; Alcon-Camas, M.; Ania-Castañón, Juan D.; Turitsyn, Sergei K. and Bennion, Ian (2009). Optical communications applications of ultra-long Raman fiber lasers. IN: *International Conference on Optical Communications and Networks (ICOON2009)*. Beijing (CN), 15 – 17 September 2009.
- [34] L. Barker, A. E. El-Taher, M. Alcon-Camas, J. Ania-Castanon, and P. Harper, "42.6Gb/s RZ-ASK transmission over 2500km using quasi-lossless transmission spans," in *CLEO/Europe and EQEC 2009 Conference Digest*, (Optical Society of America, 2009), paper C11\_2.
- [35] [encyclopedia2.thefreedictionary.com](http://encyclopedia2.thefreedictionary.com)
- [36] Amnon Yariv, Dan Fekete, and David M. Pepper, "Compensation for channel dispersion by nonlinear optical phase conjugation," *Opt. Lett.* **4**, 52-54 (1979)
- [37] Paolo Minzioni and Alessandro Schiffrini, "Unifying theory of compensation techniques for intrachannel nonlinear effects," *Opt. Express* **13**, 8460-8468 (2005)

- [38] V. Pusiono et al, "Wavelength Conversion of Real-Time 100-Gb/s POLMUX RZ-DQPSK". OFC 2009.